The influence of drought on *Neochanna apoda* metapopulation persistence under global warming and land-use change

A thesis submitted for the degree of

Doctor of Philosophy in Ecology

by Richard S. A. White

University of Canterbury

2016

Contents

Abstract

Population size is the primary criteria used globally to determine species extinction risk and prioritise conservation risks due to the widely documented positive scaling of population persistence with abundance. However, it is unknown how such scaling is affected by land-use change combined with climate change which, for many populations, is expected to decrease population growth rates and increase population variability. Moreover, it is unknown how such changes to scaling in sub-populations will impact the persistence of larger interconnected metapopulation networks. Using empirically-derived models of *Neochanna apoda* (brown mudfish) metapopulations, I investigated the interactive effects of land-use- (forest clear-felling) and climate-change (extreme drought frequency) on the scaling of population persistence with carrying capacity and quantified how changes in scaling controlled metapopulation persistence. The metapopulation matrix model was parameterised using data from a long-term mark-recapture study of over 70 brown mudfish sub-populations living in forest pools affected by frequent extreme droughts (including a 1/25 year extreme drought), historic clear-felling and wind disturbances. After correcting these data for climate driven uncertainty in capture probability using Cormack-Jolly-Seber models, I found that mudfish survival during droughts was high for populations occupying pools deeper than 139 mm, but declined steeply in shallower pools. This threshold was caused by an interaction between increasing population density and drought magnitude associated with decreasing habitat size, which acted synergistically to increase physiological stress and mortality. Pool depths were lowest in forests affected by historic clear-felling due to the absence of large trees to fall over and excavate deep pools. Consequently, the metapopulation matrix model parameterised by these data showed that the scaling of time-to-extinction with carrying capacity in sub-populations was driven by an interaction between land-use change (forest

clear-felling) and increasing extreme drought frequency with global warming. Population persistence increased exponentially with carrying capacity in large stable habitats, but this relationship was asymptotic at small population sizes in shallow habitats contracted in size by forest logging. Metapopulation persistence in logged forests dropped by over 50 percent due to such asymptotic scaling and lost persistence of large populations. Thus even large populations are likely vulnerable in stochastic environments, with their loss having disproportionately large negative effects on metapopulation persistence in landscapes affected by human disturbances. These results confirm longstanding theory predicting asymptotic population size-persistence thresholds under environmental stochasticity, and by doing so, highlight the keystone role large populations play in mitigating the impacts of global warming and land-use change.

Chapter One:

General Introduction

Global climate change is predicted to increase mean climate (e.g. temperature, precipitation, solar radiation, and wind) but also climate variability, in particular, the frequency and magnitude of extreme climate events, such as droughts and floods (IPCC 2007; Renwick *et al.* 2016). Moreover, such climate changes are likely to coincide with increasing pressures from land-use change, and in particular, rising human demand for water, which could exacerbate drought impacts (Vörösmarty *et al.* 2010; Scheffers *et al.* 2016). While much is known regarding the ecological impacts of increased mean temperature, very little is known about how increasing climate variability will impact ecological communities and populations, and how this will interact with other land-use pressures (Thompson *et al.* 2013). Climate variability is becoming increasingly recognised as a greater threat to ecological persistence than changing mean conditions (Katz & Brown 1992; Ledger *et al.* 2013; Thompson *et al.* 2013). The increased frequency of extreme droughts and floods is predicted to be particularly high in New Zealand (Mullan *et al.* 2005; Clarke *et al.* 2011; Renwick *et al.* 2016). Whilst organisms can evolve adaptations to slow deterministic environmental change, extreme disturbances are sudden, causing high mortality events that increases the statistical probability of extinction irrespective of how well the animal is adapted to their environment (Drake & Griffen 2010). Consequently, understanding the role of environmental stochasticity on population dynamics will likely be important for managing the effects of climate change and other global change drivers on biodiversity.

Anticipating the effects of rising environmental variance on population dynamics requires an understanding of sources of stochasticity affecting population dynamics. In a constant environment, population dynamics are affected by demographic stochasticity, which

refers to chance birth and death events affecting individuals independently of one another, such as accidents, disease or genetic mutations (Lande *et al.* 2003; Desharnais *et al.* 2006; Ovaskainen & Meerson 2010). Because demographic stochasticity operates independently among individuals, it tends to average out in large populations and therefore has greater impact in small populations (Lande *et al.* 2003). For instance, a heart attack affecting a single individual would go largely unnoticed in a large population, but would cause extinction in a population of two. This situation differs substantially in populations subjected to environmental stochasticity, which affects birth and death rates for all individuals simultaneously, and therefore impacts populations of all sizes equally (Leigh 1981; Lande 1993; Foley 1994). For example, populations experiencing droughts of equivalent magnitude will experience the same proportion of mortality regardless of their size. In such cases, all populations, regardless of size, have a significant risk of extinction (Lande *et al.* 2003).

The distinction between environmental and demographic stochasticity is critical because it determines how population persistence scales with carrying capacity under different levels of environmental variability (Ovaskainen & Meerson 2010). Several authors have shown mathematically that in constant environments, time-to-extinction increases exponentially with carrying capacity, K, whereas variation in environmental conditions causes power law scaling (Leigh 1981; Lande 1993; Foley 1994). This scaling of time-to-extinction under different levels of environmental stochasticity can be simplified to the equation K^c, where the slope parameter, c, is quantified as the ratio of the mean population growth rate relative to its variance under environmental variability (Lande 1993) (Figure 1.1). Consequently, decreases in mean population growth or increases in population growth rate variability cause the scaling of time-to-extinction with carrying capacity to flatten from exponential increase ($c>1$), to asymptotic increase ($c<1$) (Lande 1993) (Figure 1.1). This means that increases in extreme climate event frequency under global warming may

significantly increase extinction risk of large populations that are currently considered at low risk of extinction. Moreover, because slope values, *c*, are sensitive to either reduction in mean or increase in variance of population growth rate, changes to the scaling of time-to-extinction with carrying capacity are likely to be greatest in populations affected by combinations of land-use and climate changes which simultaneously depress mean population growth rates and increase variability.

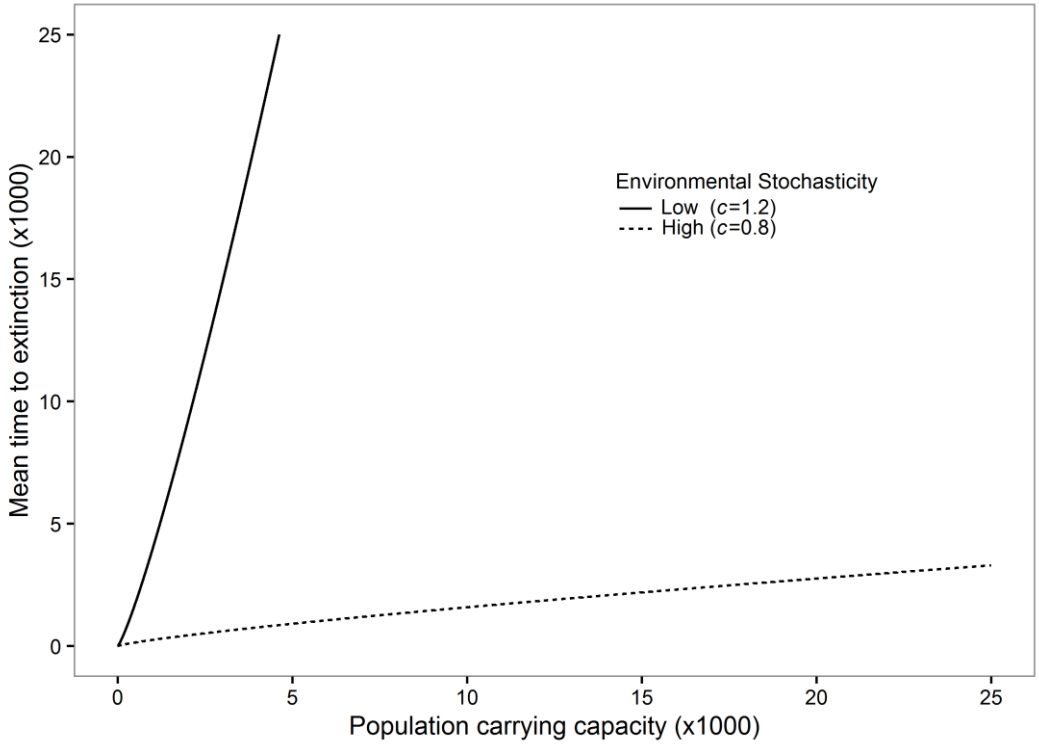

Figure 1.1: The scaling of time-to-extinction with population carrying capacity (*K*), under different levels of environmental stochasticity (line type). All lines were quantified from the equation K^c of Lande (1993), where *c* is the average rate of population growth relative to its variance resulting from environmental stochasticity. Under low environmental stochasticity, variance in population growth rate is low relative to the mean, thus $c>1$, and time-to-extinction increases exponentially with carrying capacity (solid line). Under high environmental stochasticity, variance in population growth rate is high relative to the mean, thus $c<1$, and time-to-extinction increases asymptotically with carrying capacity.

The effects of environmental stochasticity on the scaling of population persistence with carrying capacity (Figure 1.1) have been examined extensively in theoretical contexts, but rarely in empirical studies of actual populations (Ovaskainen & Meerson 2010). Recent research shows the effects of environmental stochasticity on populations are often overestimated relative to other sources of stochasticity, including individual demographic stochasticity (Melbourne & Hastings 2008). Consequently, the amount of environmental variation required to cause asymptotic scaling of population persistence with carrying capacity may be higher than implied by theoretical research. Indeed, species adaptations to environmental disturbances, such as aestivation and dormant life-stages (Chew *et al.* 2004; Urbanski *et al.* 2010), may allow them to maintain surprisingly high population stability in very unstable environments. However, it remains unknown whether the scaling of population persistence with carrying capacity asymptotes under current and future levels of environmental stochasticity in natural populations. Answers to this question have remained elusive because of the near impossibility of quantifying population birth and death rates simultaneously for many populations of varying size, over gradients of environmental stochasticity, and during rare (e.g. < 1 in 100 y) extreme events. It is not sufficient to use simple time series of population abundances due to the difficulties of distinguishing the effects of environmental stochasticity from demographic variance, density dependence and measurement error (Lande *et al.* 2003). Consequently, precise information on the effects of disturbances on birth and death rates are preferred to calculate the variance in population growth rate due to environmental stochasticity (Lande 1993). For many species this is either impractical or very challenging.

The issue of measuring birth and death rates is particularly difficult for species in large open populations where immigration and emigration is high (Pine *et al.* 2003). Mark-recapture techniques are one of the most wide-spread methods used to measure birth and

death rates in natural populations, however, they require high recapture probability for precise accurate estimates (Lebreton *et al.* 1992; Pine *et al.* 2003). High recapture rates are unlikely in populations where marked individuals frequently migrate away from the study area, making it uncertain if they have deceased or are simply not available for recapture (Pradel *et al.* 1997; Pradel *et al.* 2005). Ironically, such populations often inhabit some of the most frequently disturbed environments, such as large flood-prone braided rivers (Scrimgeour *et al.* 1988; Taylor *et al.* 1996; Tockner *et al.* 2006). The issue of low re-capture rate is compounded in situations where the method of census is passive (Pradel & Sanz-Aguilar 2012). Active census techniques, such as electric fishing, are useful if there is relatively high certainty that most animals within a sampling unit were captured, thus ensuring the highest possible capture rates. However, passive techniques, such as trapping, rely on animal behaviour, which is unpredictable, and can itself be correlated with environmental variability (Gordoa *et al.* 2000; Ortega-Garcia *et al.* 2008; Kuparinen *et al.* 2010). Variability in capture rates caused by environmental fluctuation may give the false appearance of a fluctuating population size and would therefore confound estimates of the effects of environmental stochasticity on population dynamics. These sources of measurement error need to be accounted for in order to obtain precise, accurate estimates of environmental stochasticity in natural populations (Lande *et al.* 2003).

Additionally, it will be important to understand how the effects of changes to the scaling of population persistence with carrying capacity alter metapopulation persistence at larger landscape scales. Models of the scaling of time-to-extinction with carrying capacity have typically focussed on single isolated populations that exclude the influence in migration (Ovaskainen & Meerson 2010). However, the assumption of isolation is unrealistic for most populations, which are usually embedded within a much larger metapopulation network connected via dispersal (Hanski 1999). In such cases each sub-population has its own

dynamics controlled by density dependence, and demographic and environmental variability, which may cause the population to have positive or negative growth rate (e.g. sinks versus sources) depending on current conditions (Hanski 1999). However, unlike isolated populations, connections between patches allow sinks to be rescued via immigration from nearby sources following sub-population extinction (Fortuna *et al.* 2006; Abbott 2011; Duncan *et al.* 2015). By allowing migration, connections are thought to increase overall metapopulation stability in a similar way to which species diversity increases community stability (Abbott 2011). The metapopulation framework is becoming an increasingly useful concept due to the rising degree of habitat fragmentation being encountered as a result of land-use change and habitat loss which often breaks populations up into smaller chunks (Bender *et al.* 1998; Fahrig 2002). As each small chunk is prone to extinction due to demographic stochasticity, being connected to large remnant source populations is vital for persistence. The persistence of such large populations within the landscape may therefore have a disproportionate impact on persistence of the overall metapopulation by rescuing smaller populations from extinction. Consequently, by influencing the persistence of large populations, changes to the scaling of population persistence and carrying capacity could have wide-reaching landscape-scale effects on metapopulation persistence under global warming.

Brown mudfish as a model system to examine the influence of environmental stochasticity on population persistence

The question of how changes in the scaling of population persistence with carrying capacity give rise to local and landscape scale persistence under global warming and land-use change is particularly relevant to freshwater fish in New Zealand. A significant proportion of

New Zealand's freshwater fish are considered to be at risk of extinction or decline largely due to land-use change and habitat loss which reduces population carrying capacity and exposes populations to disturbances (McDowall 2006; Goodman *et al.* 2014). Much of this habitat loss is caused by wetland drainage or river water abstraction for irrigation which predisposes populations to extreme droughts (McDowall 2006). Such habitat loss is likely to aggravate future increases in drought frequency and magnitude with global warming. In particular, New Zealand is predicted to experience increases in the frequency of current extreme, 1 in 20 year droughts by 88 percent (i.e. droughts become 1 in 2-3 years) in pessimistic scenarios of the worst hit regions such as the east coast of the North and South Islands, and upper North Island (Mullan *et al.* 2005; Clarke *et al.* 2011; Renwick *et al.* 2016). Consequently, understanding how global warming interacts with other drivers of global change that reduce population size such as habitat loss, will be particularly important in New Zealand.

Brown mudfish (*Neochanna apoda*), in particular, are an excellent organism for examining how changes to the scaling of population persistence with carrying capacity determine metapopulation responses to combinations of global warming and land-use change. Brown mudfish are a threatened freshwater fish endemic to the peat swamp podocarp forests of New Zealand, where they inhabit shallow pools formed by root-wad excavations of fallen trees randomly distributed every 5-10 m throughout the forest floor (Eldon 1968; McDowall 2006; White *et al.* 2015a). The shallow nature of the pools make them very prone to drying, which is exacerbated by unpredictable rainfall patterns can transition from intense rainfall (occasionally exceeding 150-300 mm day^{-1}) followed by days of sunshine (White *et al.* 2015a). In contrast, deeper pools may be completely permanent meaning there are large differences in temporal hydrological variability between pools. Dispersal of *N. apoda* between pools likely occurs during extreme rainfall events which flood the forest matrix and connect the pools. *N. apoda* have also been observed buried within the peaty/mossy matrix

between pools, possibly stranded en-route to open water during a high-water event or dispersing via subsurface pathways (Eldon 1968). Thus, the fish assemblage likely functions as a metapopulation (Levins 1969). The density of small pools and wide range of carrying capacities and permanence make them ideally suited for quantifying environmental stochasticity using mark-recapture data with high replication, accuracy and precision.

That the influence of drought disturbance on *N. apoda* sub-populations is likely mediated by pool depth is important because both natural and human-driven disturbance associated with human disturbance strongly affects this habitat characteristic. Prior to human arrival in New Zealand, catastrophic windthrow and earthquake disturbances were the main drivers of forest dynamics in forests inhabited by *N. apoda* (James 1987; Wells *et al.* 2001; Cullen *et al.* 2003). Recently disturbed mature forest stands likely contained abundant deep, permanent pools formed by tree-fall, containing *N. apoda*. However, historic; logging and burning, usurped and destroyed over 70 percent of indigenous New Zealand forest (Ewers *et al.* 2006), thus preventing such habitat formation. This has likely resulted in large areas of forest re-growth containing only small, shallow pools, which experience greater drought frequencies and magnitudes. Consequently, large populations are likely rare in historically clearfelled forests while the persistence of those that remained are likely undermined by elevated environmental stochasticity which could have detrimental impacts on metapopulation persistence.

Thesis layout

In this thesis I quantified how the scaling of population persistence with carrying capacity was altered by combined land-use and climate change, and how changes to such scaling affected landscape-level *N. apoda* metapopulation persistence. I did this using a metapopulation matrix model parameterised with birth, death and movement rates quantified

from a four year mark-recapture survey of over 70 *N. apoda* populations clustered in different areas of mature and catastrophic windthrow, and clearfelled forest which varied widely in carrying capacity and rates of drying. The period of mark-recapture sampling included an extreme 1 in 25 year drought in New Zealand (Blackham 2013), thus enabling me to quantify the effects of rare extreme climatic events on population dynamics. Each chapter is written in a format suitable for publication with self-contained introduction, methods, results and discussion focussing on the central theme of each chapter. Chapters Two and Three focus on sampling protocol and quantifying accurate and precise estimates of vital rates over time and space for each sub-population to be used in the metapopulation matrix model. This model is then developed and expanded in Chapters Three and Four, respectively, to model the effects of global warming on sub-population and metapopulation persistence in landscapes affected by natural (windthrow) and anthropogenic (clear-felling) disturbances. Finally, I discuss the general implications of my results in the context of the management of wild populations under climate change in Chapter Six. Chapters Two and Three were published prior to thesis submission as White *et al* (2015b) in the *Journal of Fish Biology*, and White *et al* (2016) in *Global Change Biology*, but will be cited as Chapters Two and Three, respectively in this thesis.

Chapter Two

Trap-shyness subsidence is a threshold function of mark-recapture interval in brown mudfish *Neochanna apoda* populations

Abstract

The influence of capture-interval on trap-shyness, and temperature, rainfall and drought on capture probability (*p*) in 827 brown mudfish *Neochanna apoda* was quantified using mark-recapture. In particular, it was hypothesised that the loss of trapping-memory in marked *N. apoda* would lead to a capture-interval threshold required to minimise trap-shyness. *Neochanna apoda* trap-shyness approximated a threshold response to capture-interval, declining rapidly with increasing capture-intervals up to 16.5 days, after which *p* remained constant. Tests for detecting trap-dependent capture probability in Cormack-Jolly-Seber models failed to detect trap-shyness in *N. apoda* capture-histories with capture-intervals averaging 16 days. This confirmed the applicability of the 16-day capture-interval threshold for mark-recapture studies. Instead *N. apoda p* was positively influenced by water temperature and rainfall during capture. These results imply a threshold capture-interval is required to minimise the trade-off between the competing assumptions of population closure and *p* homogeneity between capture occasions in closed mark-recapture models. Moreover, environmental factors that influence behaviour could potentially confound abundance indices, and consequently abundance trends should be interpreted with caution in the face of long-term climate change, such as with global warming.

Introduction

Mark-recapture models are important tools for quantifying population sizes and trends in fish populations (Lebreton *et al.* 1992). However, one does not simply measure fish abundance using mark-recapture models without breaking the assumptions they make about fish capture probability. In particular, mark-recapture models make important assumptions regarding individual and temporal homogeneity of capture probability (*p*) amongst individuals in populations and over time (Lebreton *et al.* 1992; Pine *et al.* 2003). However, these assumptions are often broken due to behavioural responses of fishes to capture-history and environmental effects, which can lead to large biases in abundance estimation if ignored (Lebreton *et al.* 1992). Thus one does not simply measure fish abundance without an understanding of how the data meets the assumptions of mark-recapture models. In particular, previously caught fishes often learn to avoid capture gears resulting in reduced *p* on subsequent capture occasions and positively biased population size estimates (Pradel 1993; Pradel & Sanz-Aguilar 2012). Several studies have shown such "trap-shyness" is learnt gradually in fishes as a result of multiple consecutive capture occasions (Beukema 1970; Beukema & de Vos 1974; Klefoth *et al.* 2013), however evidence for unlearning of trap-shyness behaviour is sparse (Wormald & Steele 2008; Pradel & Sanz-Aguilar 2012). The capture-interval between trapping occasions necessary for trap-shyness to be unlearnt is not known, and is probably gear/species specific, potentially related to variation in memory capacity of each species. Knowledge of this capture-interval would help improve mark-recapture study design and accuracy.

It is possible that a minimum threshold capture-interval is necessary to ensure trapping-memory loss from the total population of marked fishes. For example, individual variation in memory retention and boldness would result in loss of trap-shyness earlier in some individuals than others. Thus *p* would increase with capture-interval up to the interval

that encompasses this variation in memory retention and boldness. Such a threshold capture-interval would be crucial, particularly if using closed population mark-recapture size estimators which require equal detectability of individuals between occasions, and no births, deaths, or migrations between capture occasions (Pine *et al.* 2003). For closed population models, a capture-interval that is too short will break the former assumption, whilst a capture-interval that is too long will increase the likelihood of breaking the later assumption (Pine *et al.* 2003). Identifying a threshold capture-interval necessary to minimise trap-shyness would help manage this trade-off.

Variation in environmental factors over time or space may also influence *p* independently of trapping effects. For instance, animal activity often varies seasonally due to cyclical weather and lunar patterns (Gordoa *et al.* 2000; Ortega-Garcia *et al.* 2008; Kuparinen *et al.* 2010). In ectotherms, particularly salmonids, reduced detectability in winter may result from metabolic responses to colder temperatures or reduced food availability and subsequent declines in activity (Bremset 2000). Such seasonal patterns in *p* may confound population trends if censuses are conducted on an ad-hoc temporal basis. By quantifying these seasonal *p* patterns, it would be possible to time annual censuses on occasions with relatively similar detectability, or incorporate seasonal patterns in *p* into mark-recapture models, to reduce this temporal bias.

Here the effects of capture-interval (trap-shyness) and environmental factors on brown mudfish *Neochanna apoda* Günther 1867 *p* were quantified using Cormack-Jolly-Seber (CJS) mark-recapture models (Cormack 1964; Jolly 1965; Seber 1965). *Neochanna apoda* are endemic to New Zealand and live in silty shallow pools. These pools are impractical to sample using electrofishing equipment, making passive trapping necessary (Eldon 1968; Eldon 1992; O'Brien 2005). *Neochanna apoda* are considered as “declining” and are thus monitored annually using catch-per-unit-effort (CPUE) (Allibone *et al.* 2010).

However, little quantitative information on their capture probability is available. This makes it difficult to determine the accuracy of CPUE-based trends. *Neochanna apoda* often burrow into the pool substrate when pool water levels are low during drought, and pool temperature fluctuates widely (6 – 25 °C) (McDowall 2006; O'Brien 2007; White *et al.* 2015a). Consequently, *N. apoda* detectability is probably lowest during periods of low rainfall and in winter.

First, a field-experiment was conducted to quantify the threshold of capture-interval necessary to minimise trap-shyness behaviour in *N. apoda*. To confirm the applicability of this capture-interval threshold, the presence of trap-dependent capture probability in a CJS model was tested for using *N. apoda* capture-history data with an average capture-interval that was greater than this threshold. It was hypothesised that *N. apoda p* would show a positive threshold response to capture-interval, and that trap-dependent *p* would be absent in capture-histories with interval spacing greater than this threshold. Finally, it was hypothesised that *N. apoda p* would be positively related to pool temperature and rainfall during capture, and positively related to pool depth and drought strength, owing to *N. apoda* metabolic and burrowing responses to climate.

Methods

Study area

The influence of environmental factors and trap-shyness on capture probability of *N. apoda* in Westland National Park, South Island, New Zealand was quantified. The forest studied (43°06’S, 170°23’E) is a 9000 ha temperate peat-swamp-forest dominated by rimu (*Dacrydium cupressinum*), with sections of kahikatea (*Dacrycarpus dacrydioides*) (Adams & Norton 1991) (Fig. 2.1ab). Elevation declines slightly towards the coast, which, combined with the poorly drained peaty soils and high annual rainfall of 3790 mm (Adams & Norton

1991) results in a mossy, waterlogged, forest floor with a high water table and numerous small pools containing high densities of *N. apoda* (White *et al.* 2015a). The pools are usually the remains of tree fall excavations and other depressions caused by tree senescence or wind throw damage. Being shallow (averaging 30 cm deep), these pools are strongly tied to rainfall variation, and can dry within days if it does not rain, sometimes multiple times a month (White *et al.* 2015a).

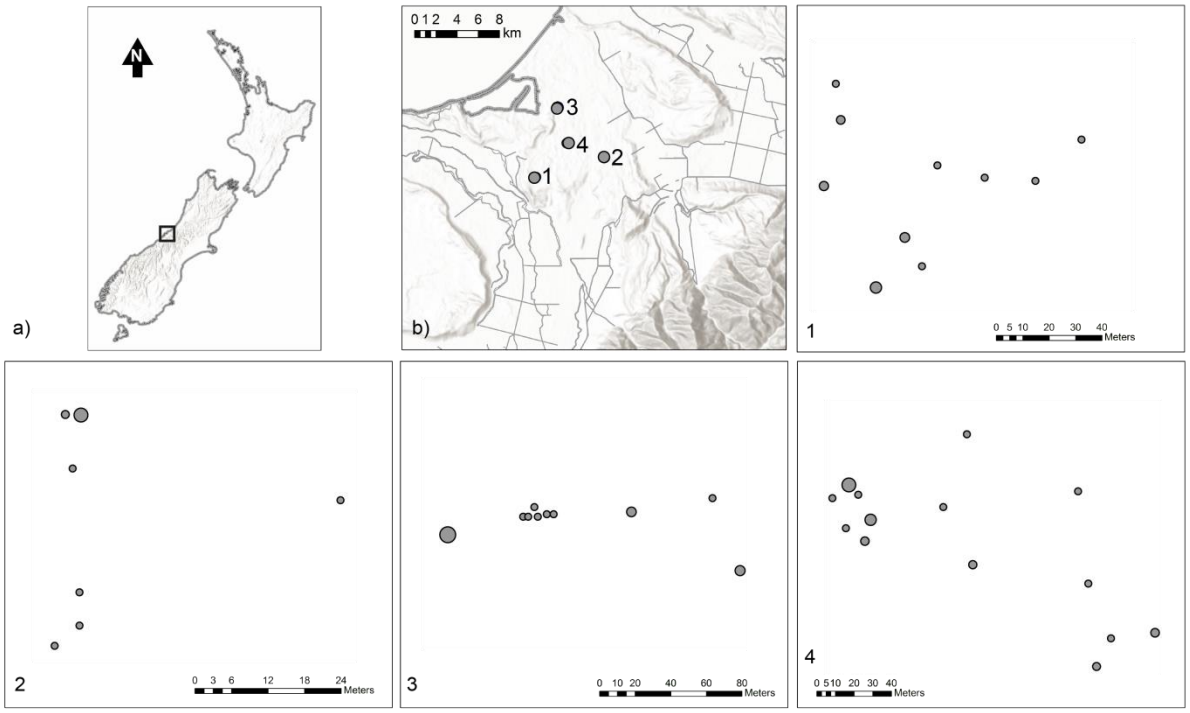

Fig. 2.1: Location of the Southwestland rainforest, where brown mudfish populations were studied within forest pools (a) within the South Island, New Zealand, (b) the location of each transect within the forest, and finally the distribution of pools within each transects one to four (panels 1-4), where circle size gives an approximate relative indicator of population size.

Capture probability survey design

The effects of temperature, rainfall and drought strength environmental variables, and

N. apoda total length (L_T) and pool depth on *N. apoda* capture probability (*p*) from 31 November 2011 to 31 May 2013 were quantified using mark-recapture. Four 100 × 20 m transects positioned on the 100, 80, 60 and 20 m contour lines in the forest were randomly selected (Fig. 2.1), wherein all pools were sampled eight times over this period. This ensured that *p* could be estimated over a wide range of drought, temperature and rainfall conditions, including the largest drought to occur in New Zealand in 25 years (Fig. 2.2a). In total, 41 pools, approximately 10 per transect, were sampled. Transect positions along a contour line were chosen randomly by selecting a grid square from all possible squares containing a road/track intersecting a given contour line resulting in a minimum distance between transects of 2-3 km. This ensured that pools varied greatly in depth (50 – 1584 mm), and thus exposure to drought conditions (Fig. 2.2a). In general, capture occasions were conducted in pairs, with approximately 2-3 weeks separating each occasion within a pair, and 3-6 months separating each pair. However, some capture occasions were conducted singly, and time intervals between capture events ranged between 5 and 182 days (Fig. 2.2a).

Neochanna apoda tagging, environmental and pool variables

On each occasion *N. apoda* were captured using Gee-minnow traps at densities of one trap per m^2 of pool surface area, and the same number of traps, in the same locations within each pool was used on each occasion (White *et al.* 2015a). This ensured a consistent spatio-temporal trapping effort during the entire study. All *N. apoda* greater than 40 mm L_T were uniquely tagged using either visual implant elastomer (VIE) (Northwest Marine Technology, Inc, Shaw Island, Washington, USA, http://www.nmt.us/) for *N. apoda* < 80 mm L_T, or an 8 mm × 1.4 mm FDX-B passive integrated transponder (PIT) tag for *N. apoda* > 80 mm L_T. Before tagging, all *N. apoda* were anaesthetised in a 0.5×10^{-5} g L^{-1} concentration of 2-phenoxyethanol, then weighed using a Scout Pro balance (±0.1 g) (Ohaus, Pine Brook, USA),

and their L_T measured. All PIT-tagged *N. apoda* were also batch marked with a single elastomer tag, and all elastomer-tagged received at least two tags. This allowed the estimation of tag retention rates, should one tag be lost. A preliminary study, whereby 19 *N. apoda* in a single pool were trapped, tagged and held over-night in traps *in-situ* confirmed no initial tag-induced mortality.

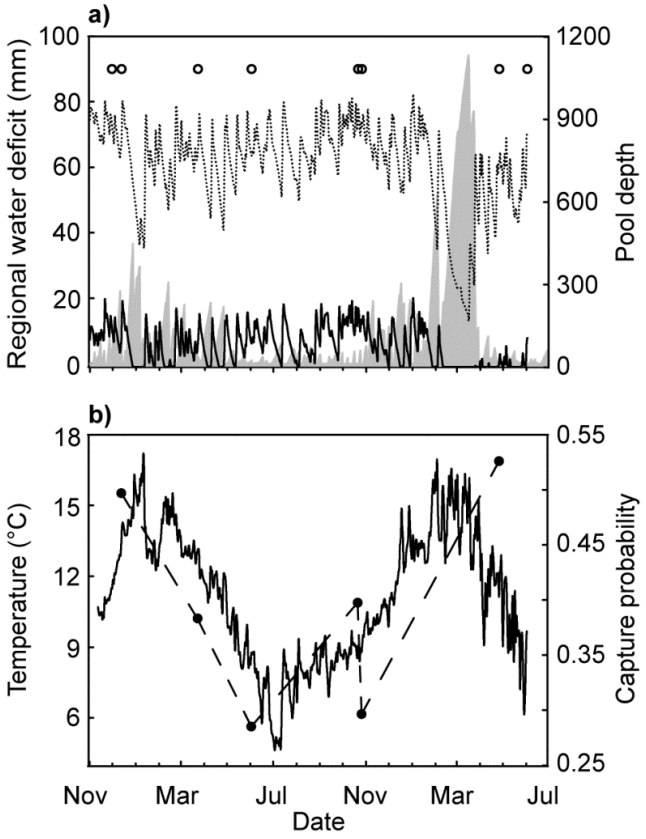

Fig. 2.2: Plots showing (a) capture occasions (open circles), water deficit (grey filled), and pool depth for a representative shallow (solid line) and deep (dotted line) pool, and (b) water temperature in a typical pool (solid line) and capture probability (filled circles with dashed line) estimated from a $\Phi(t)p(t)$ CJS model for each capture occasion, over time.

Twelve pools were randomly selected, stratified by transect, for continuous temperature and depth measurement during the sampling period, using one WT-HR stage/temperature logger (TruTrack, Christchurch, New Zealand, http://www.trutrack.com/) per pool (Fig. 2.2a). Spot depth measures of pools lacking stage height loggers were taken on

each sampling occasion, from a fixed point on a stake embedded in the substrate. To build hydrographs for pools lacking stage height loggers, I fitted least-squares regression equations relating spot depths as a function of the depth recorded at the nearest stage height logger. Continuous pool depth measures could then be predicted for each pool lacking stage-height loggers, using the depth recorded at the nearest stage-height logger. One data logger was randomly selected from which to calculate the average daily pool water temperature over the sampling period for each capture occasion (°C) (Fig. 2.2b). Average daily rainfall (mm) during the sampling period was also calculated from the nearest National Climate Database weather station (agent number 4054) located near the Whataroa River, approximately 5.7 km from the nearest transect. The maximum water deficit (mm) recorded at this station within the time period preceding each capture occasion was used as a measure of drought strength (Fig. 2.2a). Water deficit was calculated using information on soil moisture deficit, potential evapotranspiration and rainfall to estimate a water balance, where increasingly negative water deficits indicated stronger drought conditions.

Trap-shyness

A study was conducted during 6 December 2010 to 2 January 2011 to detect trap-shyness for capture-intervals that were shorter than those used in the capture probability survey described above so that the greatest range of capture-intervals could be analysed for trap-shyness. This involved batch marking (caudal fin-clip) of 50 – 60 % of the population from a subset of four randomly selected pools used in the capture probability survey and determining the proportion of marked *N. apoda* recaptured on two subsequent recapture occasions. The time between occasions one and two was two days, and 22-23 days between occasions one and three. All four of the pools involved in this initial study were continuously sampled as part of the 41 pools used in the main study described above. The data from these

studies were combined, to investigate how trap-shyness behaviour varied with time between capture and release for the greatest range of possible capture-intervals, resulting in trap-shyness data for four pools over fourteen capture-intervals, ranging 2 - 182 days.

Statistical analysis of trap-shyness

Capture probability for the trap-shyness analysis was quantified independently from the CJS models due to the use of batch-marked *N. apoda* for some capture-intervals. Here *p* was quantified as *R*/*M*, where *M* = the total number of marked *N. apoda* on occasion one, and *R* is the number of *M N. apoda* recaptured on occasion two. Capture probability was then regressed against capture-interval. To determine the functional form of this relationship, the fit of four linear and non-linear models was compared using AICc (Akaike's Information Criterion corrected for small sample size) (Burnham & Anderson 2002) and least-squares regression. Three non-linear models were constructed, including, $\log_e$(capture-interval), piecewise regression, and a 2^{nd} order polynomial, as well as a linear model. This was done to determine if the *p*-capture-interval relationship was non-linear, and if so, whether or not such non-linearity was driven by a threshold capture-interval (piecewise-regression) or some positive curve (log model, 2^{nd} order polynomial). The piecewise regression estimated a threshold capture-interval where the slope of the relationship between *p* and capture-interval changes from positive to zero and was constructed using the nls function in the R package "nlme".

Effects of environmental and individual covariates on capture probability

The effect of temperature, rainfall, and drought strength environmental variables, L_T and mean pool depth individual covariates on *N. apoda p* was analysed using Cormack-Jolly-Seber (CJS) models in program MARK (White & Burnham 1999). My analysis strategy

closely followed Lebreton *et al.* (1992). Firstly, the capture histories for all fish caught were built, resulting in an eight digit-long binary string for each individual *N. apoda* encountered, where 1 was an *N. apoda*, *i*, caught on occasion *t*, and 0 was an *N. apoda*, *i*, not caught on occasion *t*.

Goodness-of-fit (GOF) was tested on a fully time-dependent, $\Phi(t)p(t)$, Cormack-Jolly-Seber (CJS) model with these data using the program U-CARE (Choquet *et al.* 2009), where Φ was apparent survival probability, and *p* was capture probability for each capture occasion, t. A fully time-dependent CJS model is one where survival and capture probability parameters are estimated for each occasion separately. The GOF test components are used to determine whether the assumptions of equal catchability and survival inherent to CJS models are satisfied by the data. Test 2 consists of components 2.CT and 2.CL, and evaluates the assumption that all animals alive at a particular date, and which will be trapped again, do not differ in the timing of their re-encounters whether they are currently encountered or not (Pradel *et al.* 1997; Pradel *et al.* 2005). Test 3, consists of components 3.SR and 3.SM, and tests the assumption that all animals released together have the same expected future whatever their past encounter history (Pradel *et al.* 2005). In general, Test 2 is thought to indicate trap-dependent capture probability, and Test 3 is thought to indicate fish transience or tag induced mortality (Pradel *et al.* 2005).

The analysis of the effects of environmental and individual covariates on *p* was carried out in two stages. In stage one, a global model incorporating $\log_e$-transformed environmental parameters temperature (T), rainfall (R_F) and drought strength (D): p = intercept + T + R_F + D was built. Here, T, R_F and D were slope parameters explaining differences in *p* between the eight capture occasions for the average *N. apoda*, i.e. these parameters explained how *p* varied in time due to climate. This model structure was then simplified using a backwards stepwise process similar to that described by Crawley (2005),

by removing parameters in order of their significance based on *p*-values calculated from log-likelihood ratios tests. This simplified model was used for further analysis of individual covariates.

Stage two, for the analysis of L_T and mean pool depth (P_D) individual covariates, started with the global model: p = intercept + environmental variables + $L \times P_D$ for all capture occasions. Here L, P_D and their interaction were slope parameters explaining how each individual *N. apoda* varied in p on each capture occasion (i.e, these parameters explained how p varied in space on each capture occasion). Thus each capture occasion had a separate L, PD and $L \times P_D$ parameter. Environmental variables were the simplified set of variables determined in stage one. This model structure was then simplified using a backwards stepwise process similar to that described by Crawley (2005). Parameters were removed from each capture occasion in-turn by first removing the $L \times P_D$ interaction, followed by the direct effects in order of their significance. For instance, capture occasion one model structure would first be reduced to its simplest form, followed by occasion two and so forth. This process was conducted for a single capture occasion at a time, whilst other occasions were held at the starting $L \times P_D$ structure. This was done to ensure that removal of parameters from one capture occasion did not affect the significance of parameters in other occasions. Parameter significance was tested using log-likelihood ratios of nested models. The model with the lowest QAICc score from the first and second steps was considered the best model explaining variation in p from the entire Cormack-Jolly-Seber model candidate set.

Results

Over the eight capture occasions and 3936 total trapping hours, 827 individual *N. apoda* were uniquely marked and released from the 41 pools. Each *N. apoda* was caught three times on average with 5.71 ± 0.95 (S.E.) *N. apoda* caught per pool, per capture

occasion, ranging from 1 – 32 *N. apoda* per pool, and averaging 234 total *N. apoda* caught per occasion over all pools. *Neochanna apoda* capture probability was 0.38 (95% CI: 0.36 - 0.41) on average throughout the study.

Only 1 % (2/201) of recaptured elastomer tagged *N. apoda* lost tags during sampling, however, 23 % (79/343) of recaptured PIT-tagged *N. apoda* lost their tags. Nevertheless, 54 of the PIT-tag-loss *N. apoda* could be re-identified based on batch mark colour, L_T and capture location (pool ID), thus only 7 % of pit-tagged *N. apoda* could not be re-identified. Therefore only 4.9 % of recaptured marked *N. apoda* were unidentifiable. Amongst PIT-tagged *N. apoda* there was no relationship between tag loss probability and pool depth (type III logistic regression: $\chi^{1,340} = 0.59$, $P > 0.05$). Tag-loss probability did tend to increase slightly with L_T, but there was no significant relationship (type III logistic regression: $\chi^{1,340} = 3.02$, $P > 0.05$). Consequently, tag-loss rate was independent of all the individual covariate variables measured in this study. Therefore, all unidentified tag-loss *N. apoda* were removed from the data set, and no further corrections were made to *p* estimates due to tag-loss. Nevertheless, this finding suggests PIT tags may not be suitable for mark-recapture studies in *N. apoda*.

Trap-shyness

Capture-interval had a large, positive effect on *p* (Fig. 2.3). At the shortest interval, *p* averaged only 0.06 ± 0.03 (S.E.), but increased rapidly beyond this, particularly up to an interval of 18 days, then subsequently tapered off, at a *p* of approximately 0.48, indicating a threshold for dependence of *p* on capture-interval. The $\log_{10}$(capture-interval) model had the lowest AICc score (-18.7), which was slightly lower than that for the threshold model (-17), thus both models had similar support (Table 2.1). The threshold relationship was described by the piecewise function, $p = 0.08 + 0.024 \times$ capture-interval for intervals < 16.5, and $p =$

0.48 for intervals > 16.5. Thus *p* was highest for capture-intervals greater than 16.5 days.

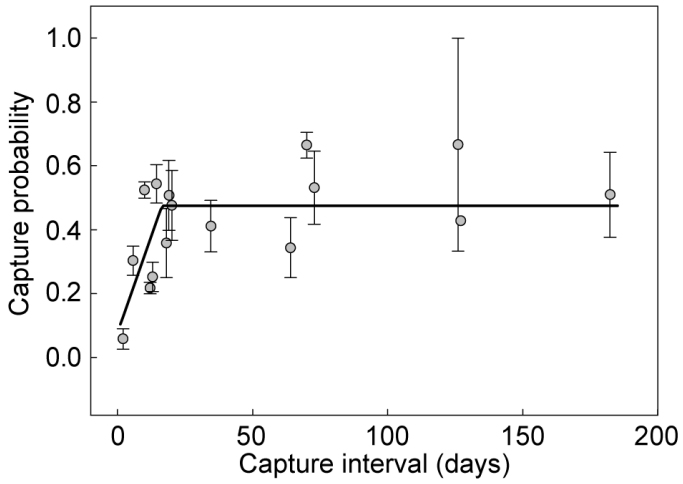

Fig. 2.3: Mean probability of individual *N. apoda* recapture in four forest pools as a function of the interval between initial capture and recapture. The data points are means +/- S.E. of 2-4 independent pools for particular capture intervals. Data points lacking error bars are for capture intervals where only a single pool was measured. The line was plotted using the piecewise regression model, fitted using the raw data, with a threshold of 16.5 days between capture and recapture.

Goodness of fit results

Tests 2.CT and 2.CL were not significant ($\chi^2 = 5.8$, $P > 0.05$ and $\chi^2 = 11.4$, $P > 0.05$, respectively), thus suggesting that *N. apoda* capture-histories used in the Cormack-Jolly-Seber model were not affected by trap-dependent capture probability. The capture-histories used in the CJS model had an average capture-interval of approximately 16 days, and excluded the shortest intervals used in the trap-shyness models in the above section. Thus the lack of detectable trap-dependent capture probability as suggested by tests 2.CT/CL corroborates with the 16 day trap-shyness subsidence threshold determined in the previous section.

Table 2.1: Trap-shyness model selection results, showing the number of model parameters (*K*), and the model coefficient of determination (R^2) and Akaike's Information Criterion corrected for small sample size (AIC_c). The number of data points (*N*) is based on three pools which had *p* estimated for 14 capture intervals, and one pool with *p* estimated for 11 capture intervals.

Model	*N*	*K*	R^2	AIC_c
Log_e(capture interval)	53	2	0.27	-18.7
Threshold	53	3	0.28	-17
Polynomial	53	3	0.21	-13.1
Linear	53	2	0.16	-12.8

Test 3.SM and 3.SR were significant (χ^2 = 23.6, $P < 0.05$ and χ^2 = 96.7, $P < 0.01$ respectively). Thus the data were over-dispersed and did not meet the Cormack-Jolly-Seber model assumption of equal survival probability of marked animals between particular capture occasions. In general, the high χ^2 values in test 3.SR resulted from fewer than expected recaptures of newly marked *N. apoda*, particularly during occasion five. Fitting individual covariates, such as L_T and P_D used in the present study, is normal procedure to correct for such over-dispersion (Lebreton *et al.* 1992). Thus the procedures later taken in the main analyses corrected the over-dispersion in the data. Nevertheless, the over-dispersion was further accounted for by comparing all subsequent model fits using QAICc, which increasingly favours model parsimony as the level of over-dispersion increases. The level of over-dispersion (*c*-hat) used to calculate QAICc scores was estimated using the median-*c* method in program MARK, which estimated *c*-hat to be 1.45. C-hat, a measure of overdispersion, is frequently calculated by dividing the residual deviance by the residual degrees of freedom in maximum-likelihood based statistics, such as binomial or poisson generalized linear models. This value will equal >1 if the data are overdispersed and approximately one, if not.

Effects of environmental and individual covariates on capture probability

The most parsimonious combination of environmental variables explaining variation

in *p* between capture occasions included temperature (T) and rainfall (R_F) (model 4, Table 2.2) The equation for this model was:

$$p = -3.85 + 1.31T + 0.13R_F$$

Both T and R_F were significantly positively related to *p* ($\chi^2 = 12.6$, $P < 0.01$ and $\chi^2 = 5.2$, $P < 0.05$) (Fig. 2.4a,b). In particular, *p* varied strongly with seasonal variation in temperature (Fig. 2.2b) and had a threshold type response to rainfall (Fig. 2.4b). However, the relationship between drought strength (D) and *p* was not significant ($\chi^2 = 0.07$, $P > 0.05$).

Table 2.2: Model selection results for the Cormack-Jolly-Seber models testing for the effects of environmental and individual covariates on *N. apoda p*. Phi (Φ) and *p* are survival and capture probability respectively, with the structure used to model these parameters (param.) shown within brackets hence. A single "t" indicates a model with a single Φ or *p* estimated for each survival or capture period shown in Figure 2.1. Letters T, R_F, L_T and P_D are temperature, rainfall, length and pool depth variables used in a model. The numbers in square brackets indicate the capture occasions where a L_T, P_D or $L_T \times P_D$ interaction parameter was included, with "all" indicating that all occasions had the respective parameter. Thus for model three, differences in *p* between capture occasions were modeled as a function of T and R_F, and variation in *p* between individuals within each capture occasion was modeled as a function of L, P_D and their interaction. Quasi-Akaike's Information Criteria ($QAIC_c$) and the residual quasi-deviance (QDev.) were calculated using a *c*-hat of 1.45.

	Model structure	$QAIC_c$	$\Delta QAIC_c$	Model likelihood	Param	QDev
1	$\Phi(t)p(L_T[2,3,4,5,6,7,8]+P_D[4,5,6,7])$	2976.7	0.0	1.00	19	2938.2
2	$\Phi(t)p(T+R_F+L_T[2,3,4,5,6,7,8]+P_D[4,5,6,7])$	2980.2	3.5	0.17	21	2937.6
3	$\Phi(t)p(T+R_F+L_T[all]+P_D[all]+L_T \times P_D[all])$	2994.1	17.3	<0.01	31	2930.9
4	$\Phi(t)p(T+R_F)$	3042.2	65.4	<0.01	10	3022.1
5	$\Phi(t)p(t)$	3043.3	66.6	<0.01	14	3015.1
6	$\Phi(t)p(T+R_F+D)$	3044.2	67.5	<0.01	11	3022.0
7	$\Phi(t)p(T)$	3045.6	68.9	<0.01	9	3027.5
8	$\Phi(t)p(R_F)$	3056.3	79.6	<0.01	9	3038.2

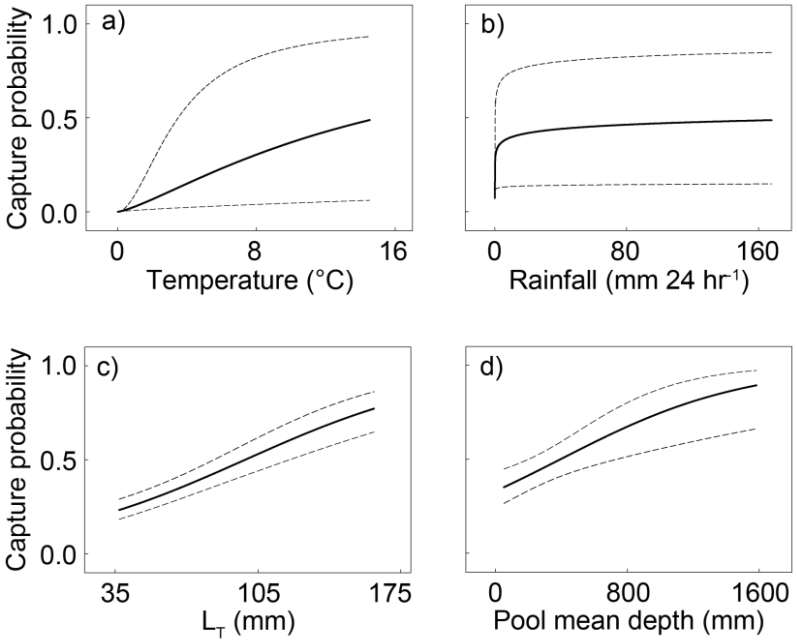

Fig. 2.4: Capture probability of *N. apoda* estimated from 41 pools as a function of (a) temperature (T) and (b) rainfall (RF) from model Φ(t)*p*(T+RF) in Table 2.2, and (c) L_T and (d) mean pool depth (PD) estimated from model Φ(t)*p*(L[2,3,4,5,6,7,8]+PD[4,5,6,7]) in Table 2.2. L_T and pool depth estimates are plotted for capture occasions 2 and 13 respectively when *p* showed the strongest responses to these variables. However, L_T and pool depth slope parameters varied between 0.010 - 0.017 and 0.00016 - 0.00060 respectively for 95% of the capture occasions. Solid and dotted lines are the mean and 95% confidence intervals respectively.

Inclusion of L_T, pool depth (P_D) and $L_T \times P_D$ individual covariates into model for each capture period explained an additional 91.2 units of deviance (models 3 vs 4, Table 2.2). On average, the slopes for L_T and pool depth variables were 0.014 (95% CI: 0.010 - 0.017) and 0.00038 (95% CI: 0.00016 - 0.00060), respectively. However, the $L_T \times P_D$ parameter was not significant for any occasion (Table 2.3). The pool depth parameter was not significant for occasions 2, 3 and 8, but was significant for occasions 4, 5 and 7 (Table 2.3), where the slope was always positive (Fig. 2.4d). Although the P_D parameter was not significant for occasion 6 (Table 2.3), its removal resulted in a QAICc increase of 0.26. This suggests P_D helped explain why marked individuals varied in *p* on occasion 6 and hence helped the data meet the

assumptions of the CJS model. Therefore this parameter was retained in the analysis. L_T was significant for all periods (Table 2.3), where the slope was always positive (Fig. 2.4c). Consequently, the most parsimonious combination of parameters explaining variation in *p* between individuals was pool depth for periods 4, 5, 6 and 7 and L_T for all periods (model 2, Table 2.2).

Table 2.3: Chi-square and *P*-values resulting from log-likelihood ratio tests comparing models of mm *N. apoda* capture probability with and without $L_T \times P_D$, P_D or L_T parameters for specific capture occasions 2-8, where L_T and P_D refer to *N. apoda* total length and pool depth from which it came, respectively. An asterisk (*) designates parameters that were retained in the top model in Table 2.2.

Parameter/capture period		χ^2	*P*
$L_T \times P_D$			
	2	1.2	>0.05
	3	0.07	>0.05
	4	0.07	>0.05
	5	1.2	>0.05
	6	0.74	>0.05
	7	0.97	>0.05
	8	2.1	>0.05
P_D			
	2	1.6	>0.05
	3	0.03	>0.05
	4*	8.8	<0.01
	5*	4.69	<0.05
	6*	2.3	>0.05
	7*	15.12	<0.01
	8	0.24	>0.05
L_T			
	2*	9.7	<0.01
	3*	8.1	<0.01
	4*	3.7	0.05
	5*	12.1	<0.01
	6*	4.7	>0.05
	7*	6.2	<0.01
	8*	20.8	<0.01

Surprisingly, when the L_T and pool depth parameters were included in addition to the environmental parameters (model 3, Table 2.2), both T and R_F become non-significant (χ^2 = 0.07, $P > 0.05$ and $\chi^2 = 0.49$, $P > 0.05$ respectively), despite having strong positive influences on *p* when analysed in the absence of the influence of the individual covariates. Thus the

most parsimonious model overall, included only the individual covariates (model 1, Table 2.2). The equation for this model was:

$$p = -1.9(\text{CI: } -2.31 - 1.62) + 0.01(\text{CI: } 0.01 - 0.02) \times L + 0.0004(\text{CI: } 0.0002 - 0.0006) \times P_D$$

Discussion

This study provides strong confirmation for the potential of trap-shyness subsidence in fishes, for which previous evidence was limited (Wormald & Steele 2008; Pradel & Sanz-Aguilar 2012). The log-capture-interval model had higher other support than other trap-shyness models, suggesting trap-shyness subsidence is gradually continuous. However, the threshold model had close support, and indicated that the greatest loss of trap-shyness had occurred by a threshold capture-interval of 16 days. Despite trap-shyness subsidence being potentially gradual, knowing the capture-interval when this subsidence has mostly occurred will be useful for designing future mark-recapture studies. In particular, such a threshold could help minimise the trade-off between the competing assumptions of population closure and *p* homogeneity between capture occasions, that exist in closed mark-recapture models (Pine *et al.* 2003). This threshold also sets a minimal capture-interval required to maximise *p*, which would increase the strength of inference in open mark-recapture studies (Lebreton *et al.* 1992). The average capture-interval for paired trapping occasions used in the CJS models was 16, and goodness of fit test2.CT, which tests for the influence of trap-dependence (Pradel *et al.* 2005), indicated that trap-shyness did not occur. Thus this study confirms the applicability of the 16-day threshold for use in designing mark-recapture studies of brown mudfish.

Subsidence in trap-shyness may be caused by the gradual loss of trapping memory from marked fishes (Pradel & Sanz-Aguilar 2012). Thus the 16-day threshold point estimated herein may indicate where maximal memory loss has been reached in the population.

Consequently, it is likely that such patterns exist in other fish species. However, the threshold value will likely vary due to interspecific variation in memory capacity, with larger species potentially having higher thresholds, due to the positive relationship between brain size and memory capacity (Paradiso *et al.* 1997). This remains to be tested, however, this study indicates that investigating trap-shyness subsidence thresholds in other species is a worthwhile avenue of future research.

Effects of environmental and individual covariates on capture probability

The average temperature and rainfall that occurred during a trapping occasion both had strong positive relationships with *p*. In particular, seasonal variation in *p* closely followed that of temperature, and was highest for temperatures 14°C or greater, which occurred during mid-January to mid-March (austral summer). This pattern may be driven by reduced metabolic demands or swimming capacity, and thus activity during cold winters, which can occur in ectothermic fishes (Graham *et al.* 1996; Brown *et al.* 2004). However, it is possible that temperature affected *N. apoda* activity *via* indirect means. For instance, activity declines in cold temperatures in salmonids have been attributed to diel behaviour shifts, reduced emergence from concealment and lower food availability during winter (Fraser *et al.* 1993; Griffith & Smith 1993; Bremset 2000), which may be directly or indirectly influenced by temperature. Regardless of the mechanism, it will be important to consider such temperature driven variation in *p* in future studies.

The relationship between *p* and rainfall may be explained by the *N. apoda* burrowing into sediment, which is thought to act as a drought survival mechanism in *N. apoda* (McDowall 2006; O'Brien 2007). Thus during periods with low amounts of rain, *N. apoda* have likely burrowed, are therefore inactive, and not available for trapping. This is supported by the observation that *p* increased rapidly from very low levels of rainfall, and then

plateaued rapidly at approximately 10 mm 24 h^{-1}, which suggests an all-or-nothing effect of rainfall on *p*. This may also explain why *p* was negatively correlated with mean pool depth, because shallower pools were more likely to dry for a given level of drought, and therefore *N. apoda* are more likely to have burrowed in shallow pools. That rainfall became non-significant after the pool depth individual covariate was entered into the model may also be explained by the potentially similar burrowing mechanisms encompassed in rainfall and pool depth variables. Taken together, these results suggest that conducting annual CPUE surveys during the warm January to March months, during wet conditions (>10 mm $24h^{-1}$), and in deep pools, will maximise *p* and increase the accuracy of CPUE as a true approximation of population abundance in *N. apoda*.

Sampling at similar times of year may not, however, prevent long-term changes in climate from obscuring population trends estimated from CPUE. Many studies reporting population responses to climate change utilise long-term CPUE datasets (Winfield *et al.* 2010; Lima & Naya 2011; Zimmerman & Palo 2012). The results reported herein suggest that such responses should be interpreted with caution. For example, potential declines in population size caused by climate change may be undetectable due to the counteracting increase in *p* with temperature. Conversely, population declines caused by increased drought frequency and magnitude may be overestimated using CPUE, due to the reduction in *p* that occurs during low rainfall periods. Similar phenomena have previously led to the unobserved collapse of several fisheries, whereby increases in *p*, and thus CPUE, masked actual population declines (Crecco & Overholtz 1990; Erisman *et al.* 2011). Thus CPUE trends should be interpreted with caution, in the face of long-term trends in climate parameters.

Chapter Three

Drought-survival is a threshold function of habitat size and population density in a fish metapopulation

Abstract

Because smaller habitats dry more frequently and severely during droughts, habitat size is likely a key driver of survival in populations during climate change and associated increased extreme drought frequency. Here I show that survival in populations during droughts is a threshold function of habitat size driven by an interaction with population density in metapopulations of the forest-pool dwelling fish, *Neochanna apoda*. A mark-recapture study involving 830 *N. apoda* individuals during a one-in-seventy year extreme drought revealed that survival during droughts was high for populations occupying pools deeper than 139 mm, but declined steeply in shallower pools. This threshold was caused by an interaction between increasing population density and drought magnitude associated with decreasing habitat size, which acted synergistically to increase physiological stress and mortality. This confirmed two long-held hypotheses, firstly concerning the interactive role of population density and physiological stress, herein driven by habitat size, and secondly, the occurrence of drought-survival thresholds. My results demonstrate how survival in populations during droughts will depend strongly on habitat size, and highlight that minimum habitat size thresholds will likely be required to maximise survival as the frequency and intensity of droughts are projected to increase as a result of global climate change.

Introduction

The predicted increase in frequency and magnitude of extreme climate events is an often-overlooked threat of global warming on populations (IPCC 2007; Ledger *et al.* 2013; Thompson *et al.* 2013; Woodward *et al.* In press). In particular, increasing human water demand, and shifts in rainfall patterns are predicted to cause increased incidences of extreme drought (IPCC 2007), considered to be the final ecological threshold for some freshwater populations (Smol & Douglas 2007). Unlike gradual temperature change, extreme disturbances, such as droughts, cause acute mortality episodes, which do not allow time for adaptation or acclimation, and may thus pose a substantial threat to populations (Covich *et al.* 2003; Lake 2003; McHugh *et al.* 2015). Although populations can recover post-drought through recruitment and immigration (Oliver *et al.* 2013), the immediate influence of drought on populations depends heavily on survival in the population during drought.

Drought-survival in freshwater systems has long been hypothesised to be a threshold response to habitat size, with survival remaining stable during initial habitat shrinkage, then dropping rapidly beyond a habitat size threshold (Boulton 2003). This threshold may occur slightly before or after complete drying, when drought refugia are lost and physiological stressors of desiccation, and poor water quality increase (Acuña *et al.* 2005; Dewson *et al.* 2007; Walters & Post 2011). Other studies indicate a decline in survival prior to drying caused by increased density-dependent competition and predation as habitats compress (Covich *et al.* 2003; Boersma *et al.* 2014). However, few studies have investigated how density-dependent and drying stressors interact during droughts, despite the potential for these forces to operate synergistically and influence survival in non-additive and/or non-linear ways (Christensen *et al.* 2006; Didham *et al.* 2007). For instance, individuals that have undergone increased competition due to higher densities during habitat compression are potentially weaker and less likely to survive the physiological rigours of complete drying.

Consequently, habitat size thresholds of drought-survival in freshwater systems may occur due to the synergistic effect of density-dependent interactions and drying stressors as habitats contract.

Here I investigated how drying and density-dependent stressors interacted to determine habitat size thresholds of drought-survival in metapopulations of the forest-dwelling fish, *Neochanna apoda* (brown mudfish). *Neochanna apoda* are small (~100-160 mm long) freshwater fish inhabiting rainforest pools created by root excavations of fallen trees (tip-up pools), that are subject to frequent intense drying events (Eldon 1968, 1978; White *et al.* 2015a). Areas inhabited by *Neochanna* species in New Zealand are expected to experience increased extreme drought frequencies of up to 45 percent of the current rate by 2080 under global warming (Mullan *et al.* 2005; Clarke *et al.* 2011). Using abundance and survival measures based on fish mark-recapture, I tested the hypothesis that drying stress and population density effects would interact synergistically to decrease drought-survival during intense droughts resulting in a habitat size drought-survival threshold. I predicted that drought-survival would be low for populations in shallow habitats (i.e. pools subjected to the greatest drying stress) with high population density.

Materials and methods

Survival survey design

Neochanna apoda survival was estimated from 41 pools between 31 November 2011 and 31 June 2013 in podocarp forest, of South Westland, New Zealand (Fig. 2.1). The study forest is a low altitude (20 - 100 m ASL) temperate peat-swamp-rainforest with high annual rainfall (3742 mm) containing abundant freshwater habitats (Fig. 2.1a,b). Historic windthrow events cause many pools to form from the root excavations of fallen trees, which can vary greatly in age and depth, and are randomly distributed throughout the forest floor (White *et*

al. 2015a). *N. apoda* dispersal between pools likely occurs during extreme rainfall events, often exceeding 150 - 300 mm h^{-1}, which flood the forest matrix, connect pools and occur several times a year (NIWA National Climate Database). *N. apoda* have also been observed buried within the peaty/mossy matrix between pools, possibly stranded en route to open water during a high-water event or dispersing via subsurface pathways (Eldon 1968). Highly variable rainfall events and a high rate of pool drying in the absence of rain (approximately -10 mm day^{-1} change in depth), result in unpredictable hydroperiods, with shallow pools often drying weekly, for up to 75 consecutive days in the most extreme drought (Chapter 2).

I randomly selected four 100 × 20 m forest patches positioned on the 100, 80, 60 and 20 m contour lines in the forest (Fig. 2.1), and all pools within these patches were trapped on eight separate capture occasions between November 2011 and May 2013 (Fig. 3.1). The minimum distance between forest patches was approximately 2.5 km. Pools within each transect were on average 56 ± 6m apart and had 5.5 ± 0.86 m^2 surface areas (Chapter 2 Fig. 3.1). Eighteen marked fish were observed to move between pools during the study, with movements averaging 21 ± 5 m, but with movements up to 70 m and evidence of permanent *N. apoda* emigration being recorded (Chapter 2). Survival was estimated between capture occasions, and corrected for variation in capture probability between pools, individuals and capture occasions to improve survival probability estimation accuracy (Chapter 2). Time between capture occasions ranged from 2-3 weeks to 3-6 months (Fig. 3.1). Depths of all pools were continuously logged using a combination of stage height loggers and spot measures as described in Chapter Two. On each occasion fish were captured and uniquely marked either using visual implant elastomer (for fish <80 mm T^L) or an 8 mm ×1.4 mm FDX-B passive integrated transponder tag (for fish >80 mm T^L) as described in Chapter 2.

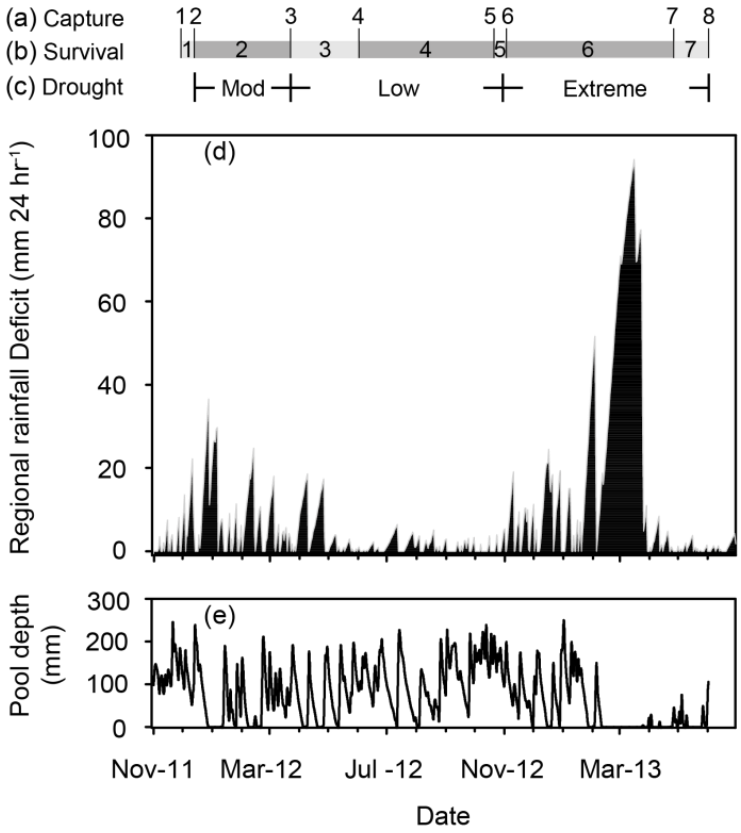

Fig. 3.1: Drought and pool depth conditions in relation to time, capture occasion and survival period in Saltwater Forest, South Westland, New Zealand, during the study of brown mudfish drought resistance. Eight capture occasions (a) were conducted between November 2011 and April 2013, resulting in seven potentially estimable survival periods (b). Survival periods were grouped into three categories based on the maximum drought strength (c) occurring in Saltwater forest based on regional rainfall deficit (d) (e.g. survival was estimated as an average of periods 3-5 for the low drought period). Pool depths to varied widely during these fluctuations in rainfall deficit, as indicated by one single shallow pool (e); deeper pools showed similar variation but did not dry. Because drought survival was only analysed for fish that had been caught at least twice in order to account for data overdispersion, period one was not grouped into any drought category due to the absence of fish that were captured at least twice in this period.

Drought strength was estimated as water deficit, which was the difference between daily rainfall input, and losses from evapotranspiration and runoff measured from the nearest NIWA National Climate Database rain gauge 4054 at the Whataroa River bridge,

approximately 5.7 km from the study location. Drought strength varied strongly during the survey, and could be categorised into three groups of varying drought intensity: low (18 mm regional rainfall deficit), moderate (36 mm regional rainfall deficit) or extreme (94.2 mm regional rainfall deficit) (Fig. 3.1). Survival estimation accuracy within each drought intensity category was maximised by achieving high replication of individual fish (827, each of which was caught an average of 5.71 times over the study) with high recapture probability (0.38 [95% CI: 0.36 - 0.41]) from a large number of pools (41) (Chapter 2), which is considered more important for parameter estimation than replicated time periods in mark-recapture models (Lebreton *et al.* 1992). Moreover, the water deficit for the extreme period coincided with a one-in-seventy year nationwide drought event (which was a 1 in 25 year event in the study forest) (Blackham 2013), making it difficult to achieve highly replicated drought conditions, which are often necessarily measured adjacent in time (Freeman *et al.* 2001; Grantham *et al.* 2012; Katz & Freeman 2015). Drying frequency (the number of days a pool had zero depth per six-month period) and magnitude (the maximum consecutive number of days a pool had zero depth per six month period) were negatively correlated with the average depth of a pool (quasipoisson regression: $\chi^2 = 118.7$, $P < 0.01$ and $\chi^2 = 437$, $P < 0.01$, with overdispersion parameters 2.17 and 3.86, respectively: Fig. 3.2ab). Consequently drying stress for any given pool depth increased with regional drought strength and was highest in shallow pools during the extreme drought strength survival period.

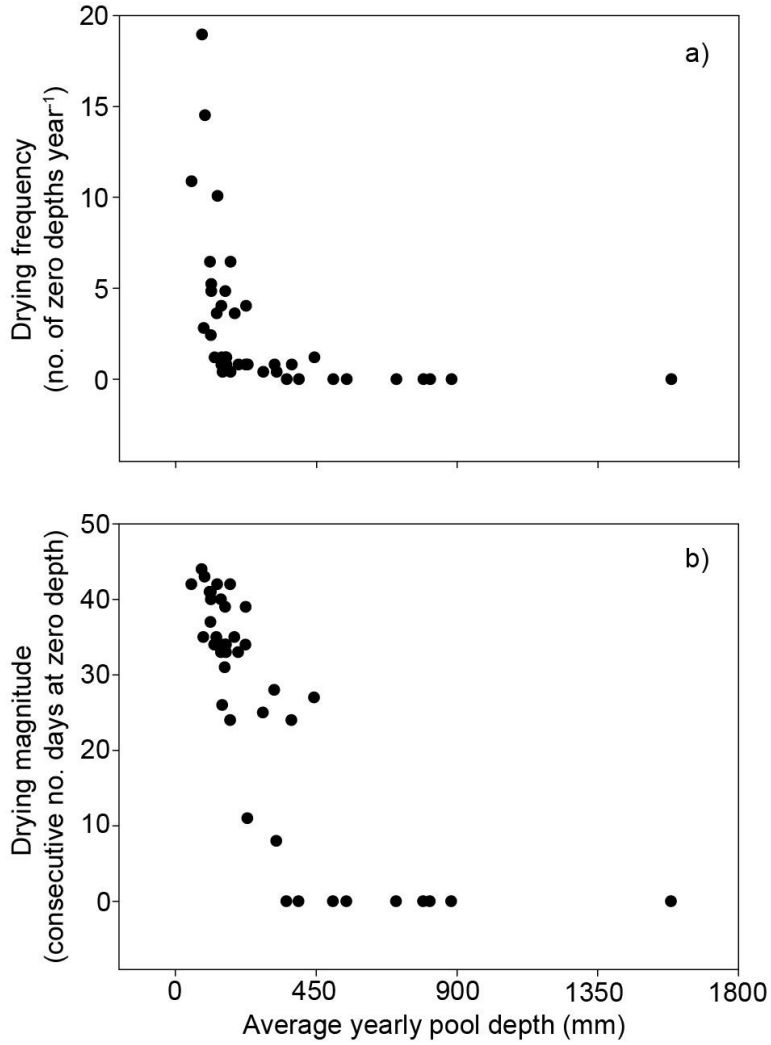

Fig. 3.2: Drought frequency (number of times a pool reaches zero depth a year) a) and magnitude (the maximum consecutive number of days a pool is at zero depth a year), is a negative function of the yearly average pool depth for the pools surveyed in South Westland, New Zealand. All metrics were calculated from continuous measurements of pool depth taken during the length of the study as described in the Methods. An example of such data can be seen for one pool in Fig. 3.1e.

Model selection of factors affecting Cormack-Jolly-Seber population survivorship

For each of the three drought strength periods, survival of individual fish was estimated from a CJS model in Program Mark (White & Burnham 1999) as a function of the interaction between the average depth (i.e. drying stress) and population density of the pool from whence fish came. Monthly survival was calculated in Program Mark by setting time

intervals as the number of 30-day periods between capture occasions to correct for unequal time intervals for each survival probability. Previous goodness-of-fit testing of the mark-recapture data indicated that these data were over-dispersed with an overdispersion parameter of 1.45 (Chapter 2). To correct for this over-dispersion, the fit of all survival models was compared using quasi-AICc, with each model using a time-since-marking survival structure, which estimates survival probability for newly marked fish separately from previously marked fish. Thus survival probabilities reported herein are for previously marked fish only, which are more likely to be permanent pool residents, showing no effects of tagging procedure or emigration, which can otherwise bias survival estimates (Pradel *et al.* 1997). *Neochanna apoda* capture probability was modelled in all CJS models as a logistic function of fish length (T^L: the average length of a fish on first capture) and average pool depth for each *p*, whereby each function had a common intercept, but different slopes for T^L and pool depth depending on the occasion as described previously (Chapter 2).

Population density (fish m^3) was estimated based on abundance and pool volume estimates made at the start of the study period, where abundance was computed using a Lincoln-Petersen mark-recapture estimator with a minimum of 16-days separate between mark and recapture events (Chapter 2). The decision to use initial density versus average density was taken to keep analyses over time consistent, however a regression of initial density as a function of average density (y = 1.01*average density + 5.7, $R^2 = 0.86$), showed the intercept and slope was not significantly different from one or zero ($t^{1,39} = 1.296$, $P = 0.20$, and $t^{1,39} = 0.155$, $P = 0.88$, respectively). Consequently, this decision is unlikely to have altered the conclusions of this study. Average depth was calculated for each pool as the average depth over the entire survey time.

I analysed the effect of T^L and the interaction between average pool depth (P^D) and population density (D) on individual *N. apoda* survival for each drought strength period

separately using a backwards stepwise $QAIC_c$ based model selection procedure similar to the Type III ANOVA described by Crawley (2005). The starting full model included a $\Phi_{ij} = T^L + P^D \times D$ structure for each of the three drought strength periods, where Φ_{ij} = survival probability for fish i during drought strength periods j and T^L is fish total length. I then minimized this model structure for each drought strength period independently by removing variables that decreased $QAIC_c$. The order of parameter removal was determined by the magnitude of resulting $QAIC_c$ decrease, however, interaction parameter removal always preceded removal of their constituent direct effects. Because $QAIC_c$ is particularly sensitive to the number of model parameters, the relative importance of parameters between drought periods, an interest of this study, would be biased by the order in which the drought periods parameter structure was reduced. This would make parameters more likely to be important in the last drought period reduced. This bias was controlled for by reducing drought periods independently, whilst the other drought periods were held at their full $\Phi_{ij} = T^L + P^D \times D$ structure. QAICc values were only reported for variables when they were entered last in the model, thus ensuring that shared deviance between correlated variables was unattributed and only unique deviance of each effect was considered. This was done to account for the correlation between density and pool depth (Pearson correlation coefficient: -0.43).

Results

Overall, the strength of the interaction between pool depth (i.e. level of drying stress) and population density increased markedly as regional drought strength increased (Fig. 3.3a-c). Within the low-drought strength period, removal of the $P^D \times D$ interaction or T^L parameters resulted in $\Delta QAIC_c$'s of -1.6 and 9.7 from the full model, respectively, thus the $P^D \times D$ parameter was removed first (Table 3.1). Removal of T^L, P^D or D from this initial reduced model resulted in $\Delta QAIC_c$'s of 9.4, -1.6 and -2, respectively, thus indicating the D parameter

should be removed second (Table 3.1). Removal of T^L or P^D from this second reduced model resulted in $\Delta QAIC_c$'s of 17.1 and -1.7 respectively, suggesting the P^D parameter should be removed third (Table 3.1). Finally, removal of T^L from this third reduced model resulted in a $\Delta QAIC_c$ of 17, suggesting the minimal model structure for the low drought strength period included only T^L (Table 3.1). Thus *N. apoda* survival during low drought conditions was independent of pool depth and population density (Fig. 3.3a), and dependent only on *N. apoda* length.

Within the moderate drought strength period, removal of the $P^D \times D$ or T^L parameters resulted in $\Delta QAIC_c$'s of 4.6 and -0.4, respectively, indicating the T^L parameter should be removed first (Table 3.1). Removal of the $P^D \times D$ parameter from this initial reduced model resulted in a $\Delta QAIC_c$ of 3.6 suggesting the minimal model structure for the moderate drought strength period included P^D, D and their interaction (Table 3.1). Thus *N. apoda* survival during moderate drought conditions was positively related to pool depth, and negatively related to population density and their interaction (Fig. 3.3b, Table 3.2), but independent of *N. apoda* length.

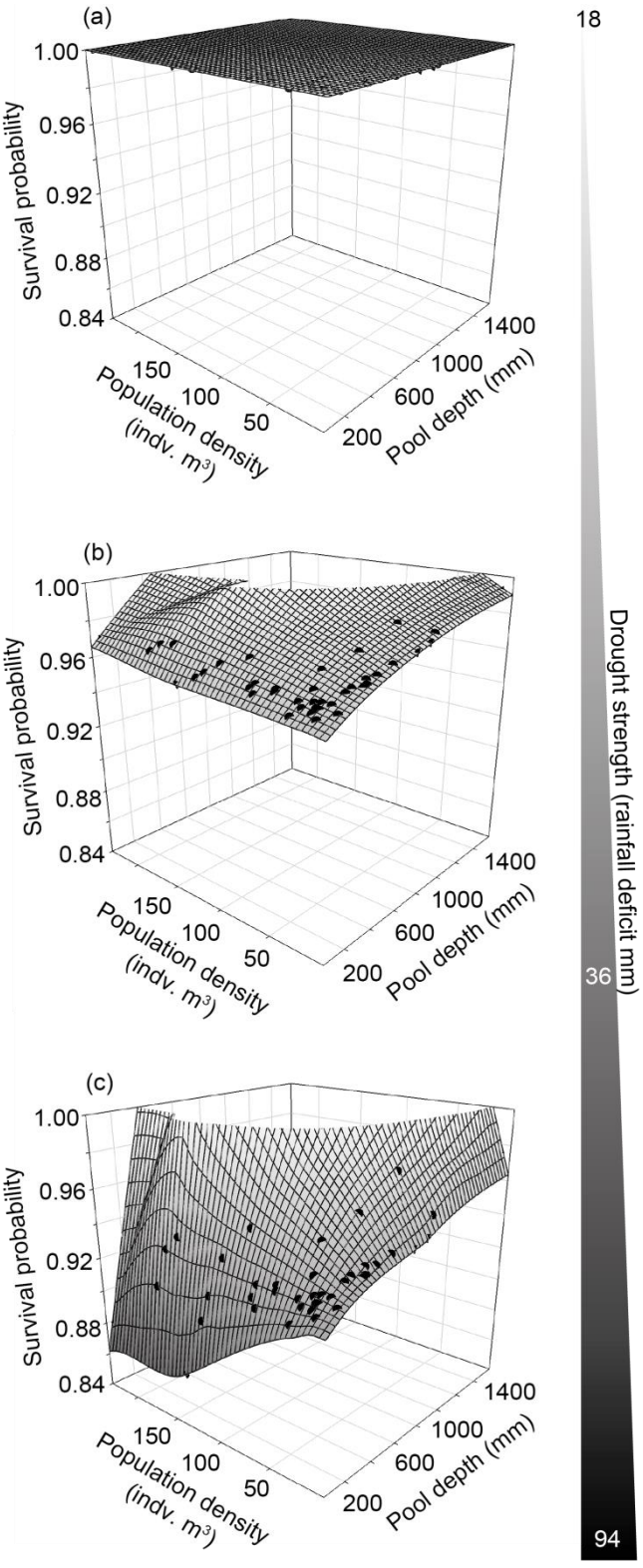

Fig. 3.3: Monthly survival probability of *Neochanna apoda* as a function of population density and pool depth for low (a), moderate (b) and extreme drought strengths (c). Each data point is the average monthly survival probability of individuals in a given pool estimated from model one in Table 3.1, where T^L was calculated as the average length of all individual fish caught.

Table 3.1: Model selection results from the Cormack-Jolly-Seber survival analysis of mark-recapture records of *Neochanna apoda* in South Westland, New Zealand. All models use the most parsimonious *p* structure described previously (Chapter 2), which accounts for variation in spatial, temporal and individual capture probability. Letters T^L, P^D and D are the fish total length, pool depth and population density covariates, respectively used to model how survival probability varied between individual fish during the specific survival periods. Model one was the full model showing the parameter structure used in each drought strength period. Subsequent models show how parameter structure was minimized for each drought strength period separately, whilst the other drought strength periods were held at their full parameterization. The model reduction order shows the sequence of parameter removal within respective drought strength periods, with the removed parameter shown in parentheses. The $\Delta QAIC_c$ values show the change in $QAIC_c$ for each successive model reduction. The minimal model structure best supported by the data for each drought strength period is in bold.

Model no.	Model reduction order	Model structure	$QAIC_c$	$\Delta QAIC_c$	K	QRes. Dev.
		Parameter structure for all periods (full model)				
1	0	$T^L+P^D+D+P^D\times D$	2930.3		34	2860.9
		Parameter structure for the low drought				
2		$P^D+D+P^D\times D$ (T^L)	2940.0	9.7	33	2872.6
3	1	T^L+P^D+D ($P^D\times D$)	2928.7	-1.6	33	2861.3
4		P^D+D (T^L)	2938.1	9.4	32	2872.8
5		$D+T^L$ (P^D)	2927.1	-1.6	32	2861.8
6	2	P^D+T^L (D)	2926.7	-2.0	32	2861.4
7		P^D (T^L)	2943.8	17.1	31	2880.6
8	**3**	**T^L** **(P^D)**	**2925.0**	**-1.7**	**31**	**2861.8**
9		Null (T^L)	2942.0	17.0	30	2880.9
		Parameter structure for the moderate drought				
10	1	T^L+P^D+D ($P^D\times D$)	2934.9	4.6	33	2867.5
11	**2**	**$P^D+D+P^D\times D$** **(T^L)**	**2929.9**	**-0.4**	**33**	**2862.6**
12		P^D+D ($P^D\times D$)	2933.5	3.6	32	2868.2
		Parameter structure for the extreme drought				
14	1	T^L+P^D+D ($P^D\times D$)	2936.6	6.3	33	2869.2
15	**2**	**$P^D+D+P^D\times D$** **(T^L)**	**2926.2**	**-4.1**	**33**	**2860.9**
16		P^D+D ($P^D\times D$)	2928.3	2.1	32	2863.0

Table 3.2: Parameter table for the Cormack-Jolly-Seber model of *N. apoda* survival, that incorporated the minimal parameter structure for each drought strength period reported in Table 3.1. Letters T^L, P^D and D are the fish total length, pool depth and population density covariates, respectively used to model how survival probability varied between individual fish during the specific survival periods. The intercept coefficients for the low and moderate drought periods describe how these intercepts differ from that of the extreme drought period.

Drought period	K	Coeff.	Std. Err.
Low	Int.	-11.98041	5.16156
	T^L	0.24125	0.11153
Moderate	Int.	0.56840	0.82159
	D	-0.00093	0.00890
	P^D	0.00112	0.00140
	P^D×D	-0.00002	0.00006
Extreme	Int.	2.49993	0.32277
	D	-0.00728	0.00318
	P^D	0.00051	0.00072
	P^D×D	0.00006	0.00003

The order of parameter removal for the extreme drought strength period was identical to that of the moderate drought strength period. Removal of the P^D×D or T^L parameters resulted in $\Delta QAIC_c$'s of 6.3 and -4.1, respectively, suggesting the T^L parameter should be removed first (Table 3.1). Removal of the P^D×D parameter from this initial reduced model resulted in a $\Delta QAIC_c$ of 2.1 suggesting the minimal model structure for the extreme drought strength period included P^D, D and their interaction (Table 3.1). Whilst pool depth had a positive influence on survival probability due to lower drying stress in deep pools (model coefficient: 0.00052: Table 3.2, Fig. 3.3c), population density had a negative influence on survival probability (model coefficient: -0.00728: Table 3.2, Fig. 3.3c), probably due to an increase in density-dependent interactions. Moreover, increasing density caused the pool depth slope to steepen (pool depth × population density coefficient: 0.00006; Table 3.2, Fig. 3.3c). Thus the lowest drought-survival occurred where drying stress and density-dependent stressors were highest.

Although the pool depth × population density interaction was important during both moderate and extreme drought strength periods, this only elicited a pool-depth drought-survival threshold during extreme drought conditions (Fig. 3.4a). This threshold occurred at approximately 140 mm pool depth due to the large increase in population density in pools below this depth (Fig. 3.4b), which caused the pool depth – survival slope to steepen, according to the positive pool depth × population density interaction parameter (Table 3.2). In contrast, the pool-depth × population density interaction parameter for the moderate drought period was positive (Table 3.2), which would explain the lack of a clear pool depth threshold during moderate drought conditions (Fig. 3.4a).

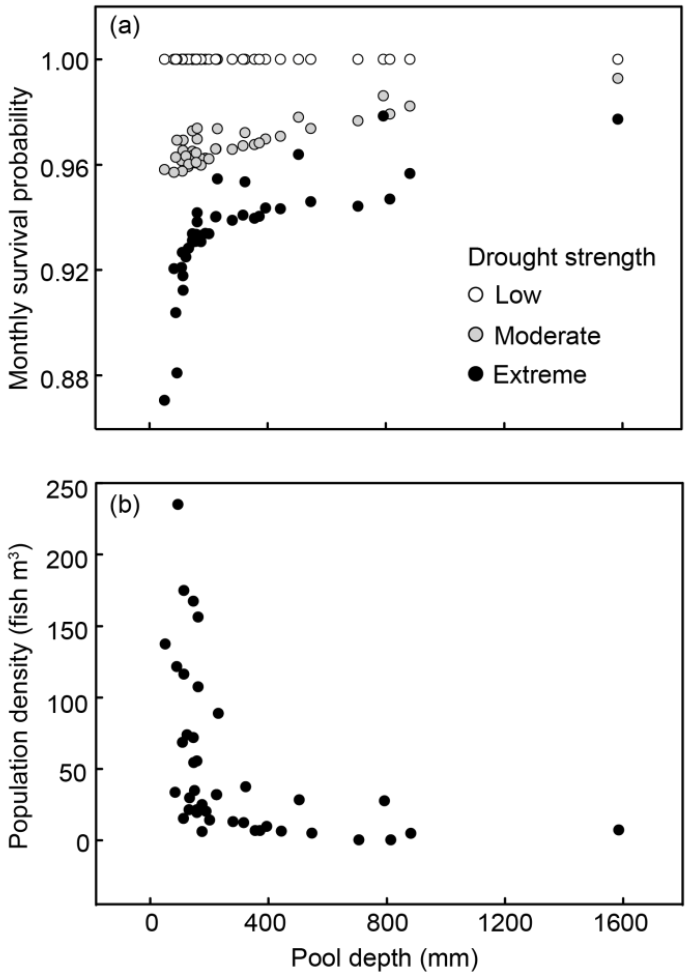

Fig. 3.4: Habitat size thresholds of drought-survival and population density in *Neochanna apoda* living in forest pools. Drought-survival (average monthly survival estimates from Fig. 3.3) dropped abruptly below a threshold pool depth of approximately 140 mm (a) due to the rapid increase in population density in pools below this depth (b) and the strong interaction between depth and density during the extreme drought (Fig. 3.3c). Habitat size drought-survival thresholds were only clearly visible during the extreme drought.

Discussion

Understanding mechanisms of survival in populations during extreme climate events is important for predicting thresholds of population persistence in the face of global warming. I investigated how habitat size and population density interacted to produce thresholds of drought-survival in a freshwater fish metapopulation. As predicted, brown mudfish drought-

survival was positively correlated with habitat-size and negatively correlated with population density. Moreover, habitat-size and population density interacted, with interaction strength increasing with drought intensity. This interaction caused a threshold of habitat-size drought-survival, with survival dropping significantly below approximately 140 mm pool depth, the point at which population density began increasing rapidly with reductions in pool depth. Thus drought-survival was lowest in shallow pools with high densities.

The mechanisms driving the habitat-size and population density interaction effect on drought-survival likely involved an interplay between physiological and density-dependent stressors. Droughts in freshwater ecosystems result in habitat compression, which causes increases in population density with resultant declines in individual fecundity, presumably due to density dependent competition (Covich *et al.* 2003; Boersma *et al.* 2014). Thus upon complete drying, survivors that have sought refuge have already been weakened by competition, and are therefore less likely to be able to resist the physiological stressors of desiccation. In populations with higher pre-drought densities, such crowding effects may be considerably more stressful, and result in further weakening of desiccation tolerance upon complete drying. Thus drought-survival decreases with population density, as found here. Future research could quantify how physiological stress changes as a result of the interplay between reduced water quality, drying and crowding, particularly below the habitat depth threshold. For example, it may be that there were rapid increases in density below the threshold due to the convex/parabolic pool shape which would result in greater volume loss per unit depth. Importantly, these results suggest population sizes may decrease with future increases in extreme drought frequency/intensity due to climate change.

This interaction between drought frequency/magnitude and population density, and the potential compounding of density dependent and physiological stressors driving it, resulted in a habitat-size threshold of drought survival. Drought-survival declined slightly

between pool depths of >1600 mm – 230 mm, and rapidly dropped in pools shallower than 230 mm. This pattern was strongly affected by the relationship between habitat-size and population density, which was similar, but inverse, resembling a power-law, with density increasing significantly below 230 mm pool depth, thus causing survival to plummet below this depth. Similar habitat-size thresholds have driven food-web collapse in stream communities in response to drought, and food-chain length shortening is often attributed to reductions in habitat-size (Sabo *et al.* 2009; McHugh *et al.* 2010; Takimoto & Post 2013; McHugh *et al.* 2015). Thus habitat-size is a key factor driving population/community responses to extreme climate events, and, unsurprisingly, elicited a threshold response in my study organism.

The generality of such habitat-size drought-survival thresholds will likely depend on how population densities in other ecosystems vary with habitat size. Interestingly, a similar habitat size-density power law has been found previously in stream gastropod populations (Foin Jr & Stiven 1970). This is important, because stream populations are less bounded, allowing egress as streams shrink during drought (Lake 2011). In contrast, emigration over land between the isolated pools studied here, would make drought escape difficult, forcing fish to endure drying by burrowing into the moist peat substrate of their pools (O'Brien 2007; White *et al.* 2015a). Thus a habitat size-density power law is more expected in lentic rather than lotic systems, and yet it has been observed in both. Although, such power laws are not found consistently in streams (McHugh *et al.* 2015), there have been few studies investigating the habitat size-density relationship. Clearly there is a need for future studies to investigate the relationship between habitat size and population density, to determine the generality of this pattern which may hugely impact how populations respond to future increases in drought frequency and magnitude with climate change.

Although drought strength periods were temporally adjacent, this is unlikely to have

induced a seasonal effect on survival given that survival was highest in the low drought strength period, which coincided with the austral winter (April – November). Winter survival is often expected to be lower than summer survival (Mitro & Zale 2002; Finstad *et al.* 2004), however, my results add to the growing number of studies that suggest this is not always the case for freshwater fish species (Carlson *et al.* 2008).

The habitat-size drought-survival threshold will have direct implications for setting limits to land-use change affecting freshwater fish populations. *Neochanna sp.* are particularly threatened by forest clearance and wetland drainage (James 1987; McDowall 2006) which significantly reduces habitat size by interfering with catastrophic windthrow and tornado disturbance regimes. These disturbances naturally create large areas with deep drought resistant pools formed by root excavations of fallen trees. Clearfelling prevents windthrow from occurring, thereby reducing average pool depths, making the metapopulations sensitive to increased drought frequencies, which are expected to increase by 75 percent in many *Neochanna* habitats of New Zealand (Mullan *et al.* 2005; Clarke *et al.* 2011). Similar anthropogenic habitat compression is a global issue due to river regulation, irrigation and wetland drainage (Tilman 1999; Brinson & Malvárez 2002; Nilsson *et al.* 2005), and is predicted to intensify as human water demand increases (Vörösmarty *et al.* 2010). By reducing drought-survival, habitat shrinkage may be a mechanism by which land-use and climate-change impacts interact to amplify threats to population persistence. Nevertheless, the type of habitat-size drought-survival threshold found in this study may be useful for setting limits of allowable land-use change so that the combined threats of global warming and land-use change can be managed effectively.

Chapter Four

The scaling of population persistence with carrying capacity does not asymptote in fish populations experiencing extreme climate variability

Abstract

Despite growing concerns regarding increasing climate extremes and imperilled populations, the influence of environmental stochasticity on the relationship between population size and persistence has received little empirical attention. Using empirical estimates of environmental stochasticity in fish metapopulations, I showed that increasing environmental stochasticity resulting from extreme droughts was insufficient to create asymptotic scaling of population persistence with carrying capacity as predicted by theory. Population persistence increased with population size due to declining sensitivity to demographic stochasticity, and the slope of this relationship declined significantly as environmental stochasticity increased. However, recent extreme droughts were insufficient to extirpate large populations. Consequently, large populations may be more resilient to environmental stochasticity than previously thought. Nevertheless, the lack of population size-related asymptotes in persistence under extreme climate variability reveals how small populations affected by habitat loss or overharvesting, may be disproportionately threatened by increases in extreme climate events with global warming.

Introduction

Despite growing concerns about the increasing frequency of extreme climate events caused by global warming, our empirical understanding of this threat to biodiversity is limited (IPCC 2007; Ledger *et al.* 2013; Thompson *et al.* 2013). Moreover, it is unknown how extreme climate events will interact with other impacts that reduce population sizes, such as habitat loss or overharvesting, which are likely to intensify as human populations grow (Dudgeon *et al.* 2006; Vörösmarty *et al.* 2010). As a general rule, small populations are inherently prone to stochastic extinction due to demographic stochasticity (random independent demographic events) (May 1973; Desharnais *et al.* 2006; Griffen & Drake 2008). The effect of small population size on extinction risk will likely be amplified by increased environmental stochasticity (temporal variation in birth and death rates due to environmental perturbations) (Shaffer 1987; Katz & Brown 1992), for example due to increased frequency of extreme droughts. Consequently, the influence of environmental stochasticity on the relationship between population size and persistence will be an important mechanism driving population responses to combined land-use and climate change.

The theoretical effects of environmental stochasticity on slopes of the relationship between population persistence and carrying capacity have been examined extensively, but rarely in empirical studies of actual populations (Ovaskainen & Meerson 2010). From theoretical studies, we know that population persistence asymptotes at low carrying capacities when environmental stochasticity is sufficiently high, in which case large populations are not much more persistent than small ones (Leigh 1981; Lande 1993; Foley 1994). However, more recent research shows the effects of environmental stochasticity on populations are often overestimated relative to other sources of demographic stochasticity (Melbourne & Hastings 2008). Consequently, the impacts of extreme climate events on the relationship between population size and persistence may be less dramatic than previously thought.

Nevertheless, it remains unknown whether population persistence asymptotes at low carrying capacity under current levels of environmental stochasticity in natural populations. Answers to this question have remained elusive because of the near impossibility of quantifying population demographics simultaneously for many populations of varying size, over gradients of environmental stochasticity, and during rare (e.g. <1 in 100 y) extreme events. However, these challenges must be overcome to quantify and anticipate the relative importance of global change drivers. Answers to this question could determine whether all populations, regardless of size, are threatened by extreme events, or whether populations reduced in size by other natural or anthropogenic constraints are disproportionately vulnerable.

I investigated the influence of environmental stochasticity on the relationship between population persistence and carrying capacity in a metapopulation of an endangered wetland fish, *Neochanna apoda* (brown mudfish), in New Zealand. *N. apoda* inhabit forest pools that dry frequently and for long durations that can cause up to 83 percent mortality, as was the case in a recent 1/25 year drought (Chapter 3). Consequently, droughts affecting *N. apoda* populations are an extreme form of environmental stochasticity (*sensu* Lande *et al.* 2003), making this system an excellent model to investigate the influences of environmental stochasticity on the relationship between population persistence and carrying capacity. I quantified the effects of environmental stochasticity due to extreme droughts using a large mark-recapture study of over 1100 *N. apoda* from 41 subpopulations varying widely in size (2–305 fish). Fish survival, recruitment and dispersal were measured across gradients of drought frequency (0-19 yr^{-1}) and magnitude (0-44 days) over three years, including the 1/25 year New Zealand-wide extreme drought (Chapter 2-3). I applied these data to a spatially explicit metapopulation matrix model and classical theoretical models to test the hypothesis that elevated environmental stochasticity due to extreme droughts would create population

size-related asymptotes in persistence.

Methods

Study area and system

Metapopulation dynamics were quantified in a 9000-ha temperate peat-swamp-rainforest within South Westland, Tai Poutini National Park, New Zealand (Fig. 2.1). Freshwater pools formed by root excavations of large fallen trees are randomly distributed every 5-10 m throughout the forest, and most contain *N apoda*. A highly variable climate transitioning from intense rainfall (occasionally exceeding 150-300 mm day^{-1}) followed by days of sunshine cause pools to become dry up to 20 times yr^{-1} for up to 44 consecutive days, with drying frequency and magnitude being negatively correlated with average pool depth (Fig. 4.1a). Dispersal of *N. apoda* between pools likely occurs during extreme rainfall events which flood the forest matrix and connect the pools. Living *N. apoda* have also been observed buried within the peaty/mossy matrix between pools, possibly stranded en-route to open water during a high-water event or dispersing via subsurface pathways (Eldon 1968). Thus, the fish assemblage functions as a metapopulation. The rapid rate of drying, short *N. apoda* life-span, opportunistic reproductive habits of *N. apoda* and often tiny pool sizes, make them ideal to quantify the effects of extreme drying simultaneously on many populations of varying size over short time frames (Chapter 3).

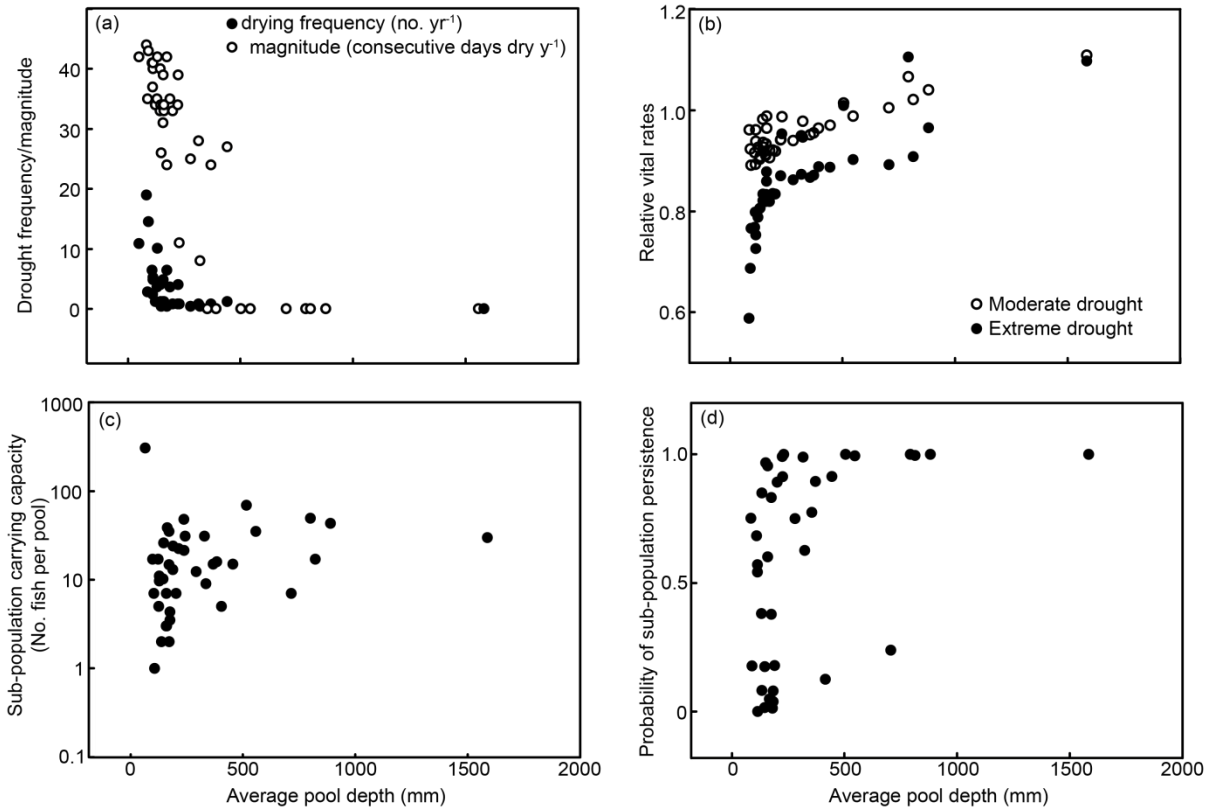

Fig. 4.1: Relationships between pool depth and (a) drying frequency and drought magnitude as measured with stage height loggers, (b) *N. apoda* population vital rates as a proportion of those in a pool of average depth during moderate and extreme droughts, respectively, (c) carrying capacity in populations (log_{10} scale), and (d) population persistence probabilities according to the RAMAS Metapop matrix model. Vital rate change (b) was estimated from a Cormack-Jolly-Seber model as reported previously in Chapter 3, and population carrying capacities were estimated from Lincoln-Peterson abundance models.

A large scale mark-recapture study of *N. apoda* has been ongoing in the study area since 31-November 2011 (Chapter 2-3). Briefly, this work measured *N. apoda* distribution, vital rates, dispersal frequency and abundance in 41 pools, within four 100×20 m forest transects distributed approximately every 2.5 km throughout the forest (Fig. 2.1). Pools within transects were (mean ± SE) 56 ± 6 m apart and had surface areas ranging between 0.13 and 28 m^2 (Fig. 2.1). At commencement of the current study, fish in all pools had been

marked and recaptured every six months using either visual implant elastomer or passive integrated transponder tags until May 2013, a period that included a range of drought intensities including an extreme 1 in 25 yr^{-1} nationwide drought (Chapter 3). Six-monthly survival of *N. apoda* during this time, as estimated by Cormack-Jolly-Seber survival models, was positively related to pool size (average pool depth), particularly during the extreme drought, due to the declining frequency and magnitude of pool drying as pool size increased (Fig 4.2a,b). Thus, all populations were simultaneously impacted by droughts, but the magnitude of this impact varied spatially with pool size.

This present work expanded the mark-recapture study until 31-October-2014, to additionally quantify how *N. apoda* recruitment and dispersal varied during different drought intensities, and to parameterise the projection matrices in the metapopulation model. All protocols were identical to those described in Chapter 2 and 3, with mark-recapture samples being taken every six months from all 41 pools (i.e. two trapping occasions separated by 14 days every 6 months). These data enabled me to make seven population size estimates for each pool using closed Lincoln-Petersen models (i.e. one estimate every 6 months) (Ricker 1975), and to estimate total metapopulation size and recruitment every six months using open Jolly-Seber (POPAN) models (Schwarz & Arnason 1996). All Jolly-Seber models were fitted using maximum-likelihood-estimation incorporating spatial and temporal covariates of fish capture probability described in Chapter 2, which minimised uncertainty in vital rates due to measurement error. Meanwhile, the minimum 14 days between mark and recapture was determined empirically in Chapter 2 to prevent *N. apoda* trap-avoidance behaviour. These procedures enabled me to achieve the high capture probabilities (average 0.38) (Chapter 2), advised for precise, accurate vital rates estimates (Lebreton *et al.* 1992). During each six-month period, the maximum rainfall deficit (difference between evapotranspiration and rainfall in mm) was recorded from the nearest National Climate Database rain gauge (#4054:

http://cliflo.niwa.co.nz/), as a measure of total system drought strength, with high numbers reflecting dryer conditions than usual. These data enabled me to determine how total metapopulation recruitment varied with system dryness over time.

Metapopulation matrix model structure

My spatially explicit matrix model of *N. apoda* metapopulations was constructed using RAMAS Metapop software (Akcakaya 2005). RAMAS Metapop has been widely used to model metapopulation dynamics for applied and research purposes and models the effects of both environmental and demographic stochasticity on population dynamics (Akçakaya *et al.* 2004; Gordon *et al.* 2012; Bond *et al.* 2015). Here I define environmental stochasticity according to Lande (1993) and Lande *et al*. (2003) as temporal fluctuations in birth and death rates caused by environmental perturbations, which can include droughts provided populations are not extuinguished by a single droughts. *N. apoda* survival probability during a 1/25 year drought was measured as at least 17 percent (Chapter 3) which constitutes an extreme form of environmental stochasticity (*sensu* Lande 1993 and Lande *et al* 2003). Demographic stochasticity was defined (*sensu* Lande 1993 and Lande *et al*. 2003) as chance events affecting individual mortality and reproduction.

Environmental stochasticity due to droughts was modelled by randomly drawing one of three projection matrices on each time step characterising vital rates for different metapopulation-wide drought intensities (Fig. 4.2a). The projection matrices reflected mean birth and death rates over six month time periods when maximum drought intensity was either: low (6.4-36 mm rainfall deficit), moderate (36-94 mm rainfall deficit) or extreme (>94 mm rainfall deficit), which occur at probabilities of 0.70, 0.28 and 0.02, respectively according to historic climate data (National Climate Database, NIWA, Appendix 4.1 Fig.

A4.1). The six-month timesteps were chosen to retain the temporal resolution over which survival and recruitment was measured in in Chapter Three and herein. Because survival and recruitment estimated from the mark-recapture data was independent of fish gender, I assumed a 1:1 male to female ratio in each population in the metapopulation model. Uncertainty in vital rates was assumed to be caused by non-drought sources of environmental stochasticity, and this uncertainty was characterised using a standard deviation matrix, which allowed vital rates to vary within each drought category. Because these standard deviations could conceivably be confounded with mark-recapture measurement error, despite my efforts to minimise it in Chapter 2, this assumption was later scrutinised in sensitivity analyses. Spatial variation in environmental stochasticity (Fig. 4.2b) was induced by constraining vital rates as a positive function of pool depth according to drought-specific relationships fitted to the mark-recapture data using maximum-likelihood-estimation in Chapter 3, Table 4.2, and reproduced here in Fig. 4.1b. Consequently, all populations were exposed to the same regional drought events (i.e. low, moderate, or extreme) but sub-population environmental stochasticity was highest in shallow pools. The historic drought time sequence since 1965 showed little evidence of serial autocorrelation (Appendix 4.1 Fig. A4.1), suggesting that modelling drought recurrence serially independent draws adequately captured the system's dynamics.

Recent research showed the effects of environmental stochasticity can be influenced by sources of demographic heterogeneity, such as age-dependent survival and fecundity (Melbourne & Hastings 2008). To account for this, demographic heterogenity was introduced by constraining survival within each projection matrix as a function of age according to *N. apoda* length-survival relationships empirically-derived during each drought in Chapter 3, Table 4.2. Consequently, demographic heterogeneity varied according to drought intensity, with survival increasing with age during a low drought, while being independent of age

during moderate and extreme droughts. Age independent *N. apoda* survival during moderate and extreme droughts implies equivalent drought tolerance across cohorts (Chapter 3). Lengths were converted to ages for the projection matrices using the otolith-based length-age relationship reported for *N. apoda* by Eldon (1978). Within each drought category, recruitment was represented as uniform across ages due to insufficient information on how age-recruitment dependency changed with drought conditions. Consequently, I later investigated the sensitivity of model results to uniform versus positive age-dependent recruitment.

Demographic stochasticity was modelled by selecting the number of survivors and recruits of the *i*th age class from a binomial or poisson distribution, respectively, with the mean survival or fecundity rates, and $N_i(T)$ as parameters (Fig. 4.2c). Consequently, even if average survival probability during a drought, p, was 0.5, there was a probability, $p^{N}i^{(T)}$, that *all* $N_i(T)$ individuals would survive to $i+1$, and a probability $(1-p)^{N}i^{(T)}$ that *none* survive (Akçakaya 1991). This probability is exponentially higher when $N_i(T)$ is small thereby increasing the probability of population extinction, in accordance with the scaling of demographic stochasticity with population size (Shaffer 1987; Akçakaya 1991).

Inter-population dispersal probability (Fig. 4.2d) decayed with distance according to Kitching's (1971) dispersal kernel: $m=a\times e(-D^{g}/b)$, where m was fish movement probability, D was distance (meters) and a, b and g were constants estimated from the mark-recapture data. This dispersal kernal was a pragmatic choice given the lack of further information on the controls of mudfish movement other than the distance between pools. Consequently, inter-pool distance and carrying capacity of the population from which a fish emigrated (as described below) were the two controls determining the probability of fish moving between to given pools. The maximum dispersal distance was represented as 120 m thus allowing fish to disperse between pools within transects, and not between transects. Although *N. apoda*

may disperse distances greater than 120 m over longer time scales, using pools as stepping stones, this would only allow them to move up to 1920 m over their 8 y lifespan, which is less than the minimum distance between transects.

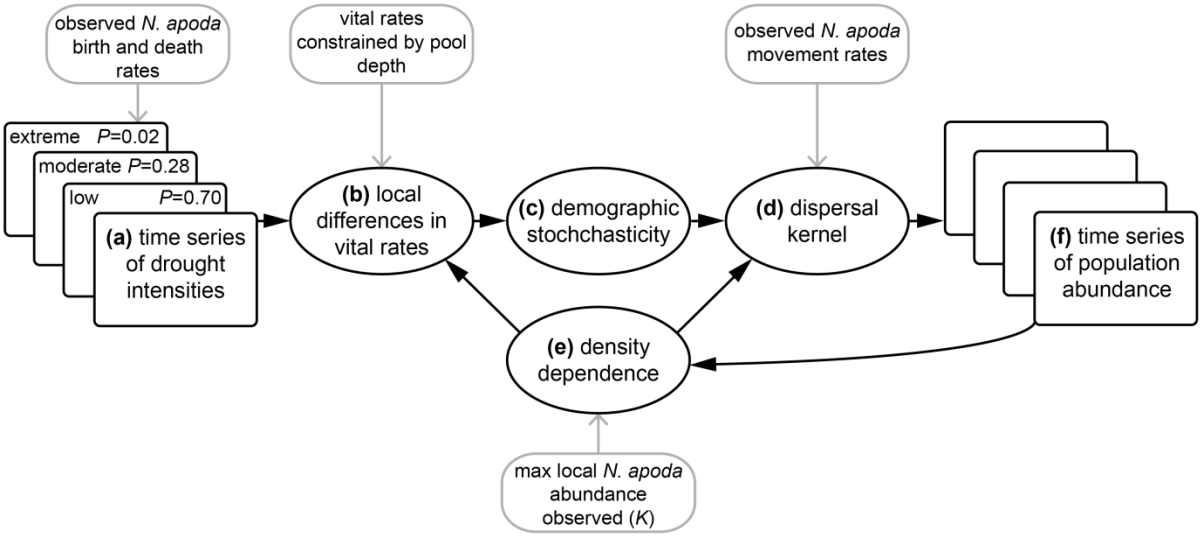

Fig. 4.2: Modelling procedures (black shapes, arrows) in RAMAS Metapop and key inputs (grey shapes, arrows) used to model brown mudfish (*Neochanna apoda*) metapopulations in forest pools affected by drought. Environmental stochasticity (a) was incorporated by generating time series (250 yr, squares) of mudfish vital rates varying according to drought intensities with different likelihoods (*P*). Environmental stochasticity also varied spatially between subpopulations with pool depth (b), being highest in shallow pools which dried more frequently (see Fig. 4.1a-c). Demographic stochasticity (c), affected by subpopulation size, was modelled by a RAMAS algorithm controlling survival or mortality of cohorts. Inter-population dispersal probability (d) decayed with distance according to empirically-derived dispersal measures. Vital rates (b) and dispersal (d) were density-dependent (e), which limited population growth and increased emmigration as subpopulations reached empirically-derived carrying capacities (*K*). Overall, this produced time series of subpopulation abundance (f, squares) affected by environmental and demographic stochasticity, dispersal and density dependence.

Density dependence (Fig. 4.2e) was modelled using the ceiling function in RAMAS.

This allowed exponential growth determined by the projection matrices (Fig. 4.2a and b) until carrying capacity was reached, and negative growth thereafter (Akcakaya 2005). Population carrying capacity, which generally increased with pool depth (Fig. 4.1c), was estimated as the maximum recorded abundance out of seven Lincoln-Petersen mark-recapture estimates taken per population. To check whether using maximum abundance gave undue influence to outliers in the abundance data, I re-ran the model after re-parameterising carrying capacities using the 95th quantile of the relationship between pool surface area and population abundance. Using a high abundance value, less than the observed maximum, recognises the fact that populations occasionally overshoot carrying capacity. Fish in populations closer to carrying capacity were also increasingly likely to emigrate due to linear density dependent dispersal (Fig. 4.2e). Density-dependent emigration slopes are automatically determined by RAMAS for each population separately to ensure positive emigration probabilities for all abundances >1 (Akcakaya 2005).

Matrix model training, validation and sensitivity analyses

The metapopulation matrix model was validated by comparing the relationship between population persistence and carrying capacity predicted by the model, to that observed in the mark-recapture data. To ensure an independent validation, I temporally split the mark-recapture data into training data, used to parameterise the model, and validation data used to evaluate model predictions. Matrix vital rates, population carrying capacities, and dispersal probabilities for training, were estimated using mark-recapture data collected between 30-November 2011 and 2-June 2013. The model trained by these data was run for 1000 repetitions of 500 timesteps (250 yr. at 0.5 yr. time step) and I calculated the probability of persistence for each population, calculated as the average number of timesteps populations

contained >1 fish out of 500. Although this represents a conservative threshold of population persistence, this is in line with the definition of persistence used by Lande (1993). Probability of population persistence in the validation dataset was calculated as the number of sampling occasions fish were encountered in each pool out of the seven total samples taken between 3-June 2013 and 31-October 2014. Using these data, I observed whether there were significant differences in the slope of the relationship of population persistence and carrying capacity by examining the interaction between carrying capacity and data type (i.e. observed versus predicted datasets) in a quasibinomial generalised linear model. One population had to be removed from this analysis due to the lack of any fish captured in the last 1.5 years (population 7.14, transect 7). One fish (tag ID: 8636) was captured in this pool in the first 1.5 years, but disappeared thereafter and was not recaptured in any other pool, indicating it had most likely deceased or emigrated from the study area.

Additional validation procedures involved comparing differences in intercepts and slopes of the relationship between observed and predicted mean population abundance using the training and validation datasets. Observed abundance was calculated as the mean of the Lincoln-Petersen mark-recapture abundances measured during the final 1.5 years of mark-recapture, while predicted abundance was calculated as the mean final population abundance estimated using the metapopulation matrix model. Percent bias (*sensu* Gupta *et al* 1999), the average tendency for predicted values to be larger or smaller than their observed counterparts as a percentage thereof, was also calculated.

Pending model validation, a final metapopulation matrix model was re-parameterised using the entire mark-recapture dataset. Analyses were conducted on this model to determine how sensitive the slope of the relationship between population persistence and carrying capacity was to parameter and structural uncertainty. Thus, I decreased all projection matrix vital rates, individually, to their lower 95 percent confidence limits as quantified using the

mark-recapture models. Sensitivity of results to different carrying capacities was assessed by re-parameterising the model using the predicted 95^{th} quantile of the relationship between pool surface area and abundance (Appendix 4.1 Fig. A4.2). The decision to use uniform recruitment-at-age was scrutinised by comparing results to a model incorporating a positive relationship between age and recruitment estimated from Eldon (1978) (Appendix 4.1 Fig. A4.3). Finally, I examined sensitivity to increases in moderate and extreme drought probability. Sensitivity was quantified using the percentage change in the slope of the relationship between population persistence and carrying capacity before and after parameter/setting adjustment using quasibinomial generalised linear models.

Effects of environmental stochasticity and population size on persistence

I tested the hypothesis that elevated environmental stochasticity due to extreme droughts would create population size-related asymptotes in persistence using both the final metapopulation matrix model and by applying my estimates of environmental stochasticity to a classical population model presented by Lande (1993). Matrix model simulations were run and population persistence was calculated as described for model validation above. Dispersal probability was set to 0 for these simulations so that population persistence was estimated for isolated populations in keeping with classical studies examining the relationship between population size and persistence under environmental stochasticity (Leigh 1981; Lande 1993; Foley 1994). A quasibinomial generalised linear model was used to analyse the effect of population size ($\log_{10}$ carrying capacity), environmental stochasticity, and their interaction, on population persistence. The total number of populations (41) was used as the sample size for the generalised linear model rather than total number of simulations (41000), to avoid inflating the statistical significance of small effect sizes.

For the quasibinomial model, environmental stochasticity was measured for each population as the variance in per-capita population growth rate (r: $\Delta N_{t+1}/N_t$) resulting from the random draws of different drought strength projection matrices. In a typical matrix model run involving consecutive time steps, population growth rate quantified from projection matrices is confounded with population size for a given time step, which varies over time independently of environmental stochasticity (Caswell 1989). To avoid such confounding effects, per-capita population growth rates were quantified from a sample of 10000 independent projection matrices per population, with initial population sizes set at 10000 and carrying capacity set to 20000 (Appendix 4.1 Fig. A4.4). In this manner, my measure of environmental stochasticity was equivalent to the variance in population growth rate caused by the effects of environmental variability on individual fitness *sensu* Lande (1993) and Lande *et al* (2003).

Finally, I applied my estimates of environmental stochasticity, measured above, to a theoretical population model that quantified the form of the relationship between population persistence and carrying capacity at different levels of environmental stochasticity. For different variants of a canonical model, several authors have shown that population persistence scales as a power of carrying capacity (K) proportional to K^c, where c is $2r/V_r$-1, and where r and V_r are the mean and environmental variance in population growth rate, respectively (Leigh 1981; Lande 1993; Foley 1994). The c parameter quantifies the form of the relationship between time-to-extinction, T and carrying capacity, K according to the equation (1) presented by Lande (1993):

$$T = \frac{2}{V_r C}\left(\frac{K^c - 1}{c} - lnK\right) \qquad (1)$$

Thus if environmental variance in growth rate is sufficiently higher than the mean growth rate (i.e. c<1), population persistence asymptotes at decreasingly lower K. Otherwise, persistence

increases exponentially with K (i.e. when $c>1$) (Lande 1993). I used my estimates of r and V_r from the matrix model to quantify c for all populations, and observed the relationship between K and population persistence for the populations with the highest and lowest c.

Results

Metapopulation model training, validation and sensitivity

Using data from the entire duration of the mark-recapture study, the six-monthly per capita recruitment estimates from the Jolly-Seber mark-recapture model averaged 0.37 (+/- 0.06 SD), 0.13 (+/- 0.02 SD), and 0.13 (+/- 0.01 SD), during the low, moderate and extreme drought strengths respectively. Thus, recruitment during moderate and extreme droughts was consistently 35 percent of that during low drought strengths; even moderate drought strengths curtailed recruitment, and this was not worsened by the 1-in-25 year extreme drought. To reduce model complexity, I modelled recruitment in both moderate and extreme droughts as a consistent proportion of recruitment during low droughts. Meanwhile, total metapopulation size, and population carrying capacity averaged 596 (+/- 97 SD) and 25 (range: 1-305), respectively. A total of 97 fish movement events, ranging from 3-112 m were recorded during the entire duration of the mark-recapture study, and all observations were grouped into 3 m distance bins. These bins were multiplied by 1.62 to adjust for unobserved movements due to the probability of fish being undetected, which averaged 0.62 (Chapter 2), thus yielding a total number of non-dispersing fish of 439 (i.e. 596 minus 157). Dispersal probability using this entire data set was a negative function of distance, best fit by the equation: $y=9.68 \times e(-D^{0.18}/0.10)$ (Appendix 4.1 Fig. A4.5). Recruitment, dispersal and population abundance statistics changed only slightly when mark-recapture analyses were restricted to the first 1.5 years for model training and validation purposes (Appendix 4.1 Table A4.1).

When parameterised using vital rates and dispersal data measured during the first 1.5 years of the study, the predicted relationship between population size and persistence closely resembled that observed during the final 1.5 years of study (Appendix 4.1 Fig. A4.6). A quasibinomial regression on these data indicated no significant differences between predicted and observed datasets, in terms of either slopes ($F_{1,78}$=0.16, P=0.69) or intercepts ($F_{1,78}$=12.5, P=0.60). Mean observed abundance was also closely related to predicted abundance according to an intercept and slope of 2.2 and 0.94, neither of which were significantly different from zero ($t_{1,39}$=-0.92, P=0.36) and 1 ($t_{1,39}$=1.77, P=0.09), respectively (Appendix 4.1 Fig. A4.7). Although the intercept was nearly significantly different, predicted abundance values were only negatively biased by 1.47 fish; about 9.99 percent on average, compared to observed values. Consequently, the metapopulation matrix model closely approximated the relationship between population size and persistence I independently observed in real populations, and accurately predicted independently observed abundance. Therefore the final model was parameterised using means and standard deviations reported for the full mark-recapture dataset (Appendix 4.1 Table A4.2).

Sensitivity analysis indicated that the slope of the relationship between population carrying capacity and persistence was sensitive to reductions in low drought period recruitment and survival, moderate drought period survival, and removal of the standard deviation matrix which changed by 28, 20 , 26 and 16 percent, respectively (Appendix 4.1 Table A4.3). However, the changes were only significant for moderate drought survival (Appendix 4.1 Fig. A4.8). Slopes were sensitive to structural alterations including altered population carrying capacities, age-dependent recruitment, and increased moderate drought probability (Appendix 4.1 Table A4.3). However the changes were not significant (Appendix 4.1 Fig. A4.9).

Effects of environmental stochasticity and carrying capacity on population persistence

The relationship between population persistence and carrying capacity was significantly reduced by elevated environmental stochasticity as shown by a significant interaction between population carrying capacity and environmental stochasticity (carrying capacity effect: $F^{(1,37)}$=2285.2 , P<0.001, R^2=0.92, environmental stochasticity effect: $F^{(1,37)}$=53.5, P<0.001, R^2=0.02, interaction effect: $F^{(1,37)}$=22.8, P<0.001, R^2=0.01). This interaction was significant regardless of parameter uncertainty (Appendix 4.1 Table A4.3). Thus population persistence increased with carrying capacity, and elevated environmental stochasticity caused the slope of this relationship to decrease (Fig. 4.3a). However, despite this decrease in slope, even the highest recorded level of environmental stochasticity had surprisingly minor impact on persistence of the largest population (K=305), which, on average went extinct for only 1.4 time steps (out of 500) per model run (Fig. 4.3a). Thus environmental stochasticity had a surprisingly low marginal impact (Fig. 4.3b), with vulnerability to droughts being almost entirely dependent on carrying capacity (Fig. 4.3a). The concerted increase in population carrying capacity and environmental stability as pool depth increased (Fig. 4.1a–c), caused persistence to increase significantly with pool depth (Fig. 4.1d) (quasibinomial regression: $F^{(1,39)}$=7.6, P=0.009, R^2=0.15).

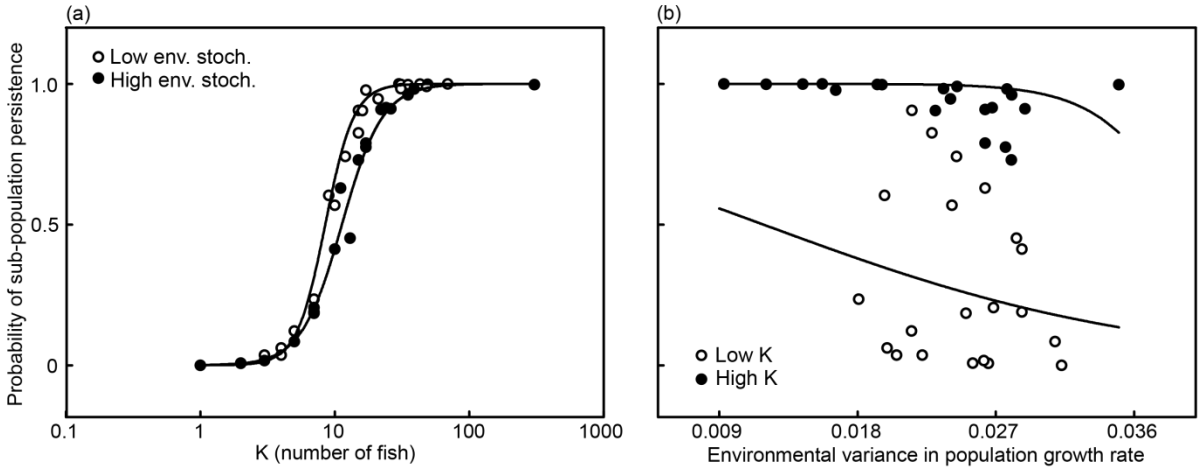

Fig. 4.3: Probability of *N. apoda* population persistence as estimated from the RAMAS Metapop matrix model as a function of the interaction between (a) population carrying capacity ($\log_{10}$ scale) and (b) variance in population growth rate due to environmental stochasticity (normal scale). Symbol types show populations with lower (open) or higher (closed) than median values, of environmental stochasticity or K, respectively.

Mean and environmental variance of per-capita population growth rate (r) in the matrix model ranged between 0.06–0.13, and 0.009–0.035 $\Delta N_{t+1}/N_t$, resulting in c ranging between 2.53 and 26.80. Although, the slope of the population size-persistence relationship declined predictably as environmental stochasticity increased, this was not sufficient to cause the relationship to asymptote at low carrying capacity (Fig. 4.4). This conclusion was robust to model uncertainty as indicated by minimum c values >1 for all model parameters and settings for which sensitivity was investigated (Appendix 4.1 Table A4.3). Thus population persistence increased indefinitely with carrying capacity for all populations, even those experiencing up to 19 complete drying events per year. Consequently, the highest levels of environmental stochasticity measured in this study were insufficient to curtail persistence of large populations.

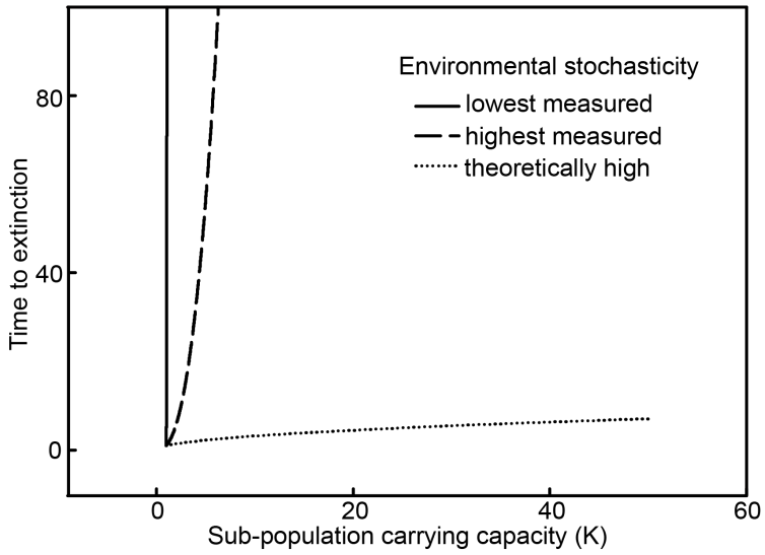

Fig. 4.4: Theoretical time to extinction for *N. apoda* populations under varying levels of environmental stochasticity. All lines were quantified equation (1) in the methods described by Lande (1993). The solid and dashed lines represent predicted persistence time for the populations with the highest and lowest levels of environmental stochasticity measured in this study (c=26.8 and 2.5 respectively), where c is the average rate of population growth relative to its variance resulting from environmental stochasticity. The dotted line represents the level of environmental stochasticity theoretically required to cause population persistence to asymptote at relatively low carrying capacity (c=0.5).

Discussion

Using empirical estimates of environmental stochasticity, this study confirmed long-standing theory that slopes of the relationship between population persistence and carrying capacity decrease as environmental stochasticity increases (Ovaskainen & Meerson 2010). However, I further showed that the decrease in slope caused by environmental stochasticity was far lower than that required to substantially impact large populations. Under sufficiently high levels of environment stochasticity, theory predicts that population persistence asymptotes at relatively low carrying capacities, such that even large populations may go extinct in environmentally variable habitats (Leigh 1981; Lande 1993; Foley 1994). In my

case, population persistence increased with population size, and the slope of this relationship decreased for populations experiencing the highest environmental stochasticity. However, the decrease in slope was not sufficient to cause substantial declines in persistence for the largest populations, despite some pools drying up to 19 times in a year for periods of up to 44 days. This means that large populations may be more resilient to extreme climate event frequency than previously thought.

The lack of population size-persistence asymptotes was surprising given the extreme environmental variability affecting the populations I studied. The largest population (carrying capacity=305) was also the worst impacted by droughts, with mean yearly survival dropping from 0.94 during low drought, to 0.56 and 0.17 during moderate and extreme droughts which occurred on average every 3.5 and 25 years, respectively. However, the mean and variance in population growth rate in this population remained relatively stable at 0.06 and 0.04 $\Delta N_{t+1}/N_t$, respectively, due to rapid recruitment from survivors between droughts. These values were substantially different from those theoretically required to cause asymptotic scaling of population persistence with carrying capacity (Leigh 1981; Lande 1993; Foley 1994). The high population stability in the face of extreme environmental variability I observed is very likely a product of life-history and physiological adaptations, such as cutaneous respiration and burrowing (Urbina *et al.* 2014), which reduces the effects of environmental extremes on birth and death rates in similar emersion-tolerant species (Brauner *et al.* 2004). Importantly, this indicates that even extremely variable environments may be insufficient to cause asymptotic relationships between population size and persistence provided species are well adapted to disturbances. The high environmental stochasticity values used in theoretical studies may therefore apply to species experiencing novel environmental conditions to which they are not adapted, such as land-use changes that expose populations to disturbance (Bond *et al.* 2015).

In my study, the interaction between population size (driven by pool depth) and environmental stochasticity resulted in a non-linear reduction in population persistence as a function of habitat size (which is linearly related to K). As pool depth declined during drought, the drought sensitivity of small pools (< 400 mm) combined with their small population sizes resulted in very low population persistence. This resulted in an apparent threshold relationship between habitat size and population persistence. This pattern is analogous to the way in which population persistence in terrestrial organisms often scales negatively with habitat size due to interactions between reduced survival and small population sizes in small fragmented forest patches (Bender *et al.* 1998; Fahrig 2002). In the terrestrial case, reduced survival is often caused by disturbances which are harsher at patch edges (Fischer & Lindenmayer 2007). For example, populations within small forest fragments may be more exposed to stochastic wind events (Laurance & Curran 2008). The realtively low persistence of *N. apoda* in the shallow pools of my study, like other studies of aquatic species experiencing severe habitat contraction (Griffen & Drake 2008; Bond *et al.* 2015) maps relatively consistently across aquatic and terrestrial metapopulations. Thus, the habitat-size scaling of population persistence via interactions between environmental and demographic stochasticity can be considered general across terrestrial and aquatic ecosystems and for different drivers of environmental stochasticity.

The generality of the habitat size-persistence threshold I observed will depend on how population size and vital rates scale with habitat size. For example, using a similar stage-matrix based modelling approach, Hokit & Branch (2003) showed that sub-population persistence probability in scrub lizards was a positive threshold function of patch size, provided that both vital rates and abundance positively scaled with patch size. When only abundance scaled positively with patch size, the persistence-habitat size relationship was linear (Hokit & Branch 2003). In some cases, particularly for species benefitting from

ecotone habitat, increasing patch size may actually decrease vital rates and abundance, due to the reduction in edge to patch size ratio, thus potentially resulting in negative patch size–persistence relationships (Bender *et al.* 1998; Hokit & Branch 2003). However, approximately fifty percent of taxa considered in studies of plants, mammals, reptiles and amphibians showed positive scaling between demography and habitat size, indicating that positive habitat size-persistence relationships are not uncommon (Bender *et al.* 1998; Hokit & Branch 2003). Nevertheless, in order for such relationships to produce thresholds, both population size and vital rates would likely need to decline, and as my study shows, interact, in concert with habitat contraction.

The role of environmental stochasticity in driving population persistence has been heavily debated (May 1973; Leigh 1981; Lande 1993), leading many authors to emphasise the importance of climate extremes over other global change drivers of species persistence (Katz & Brown 1992; Thompson *et al.* 2013; Kreyling *et al.* 2014). However, recent work shows the effects of environmental stochasticity are often over-estimated relative to other stochastic drivers of population dynamics (Melbourne & Hastings 2008). My research paints a slightly more complicated picture, showing that while the importance of environmental stochasticity may be less than expected, the degree to which this is the case is dependent on population size. The lack of population size persistence asymptotes under extreme climate variability reveals how large populations maybe more resilient to extreme climate variability than previously thought. However, small populations remained highly vulnerable in variable environments. Consequently, the threat of increasing climate extremes likely remains significant, but may be more visible or acute where populations are small or shrinking, such as those constrained by habitat loss and exploitation (Bender *et al.* 1998; Dudgeon *et al.* 2006).

Appendix 4.1

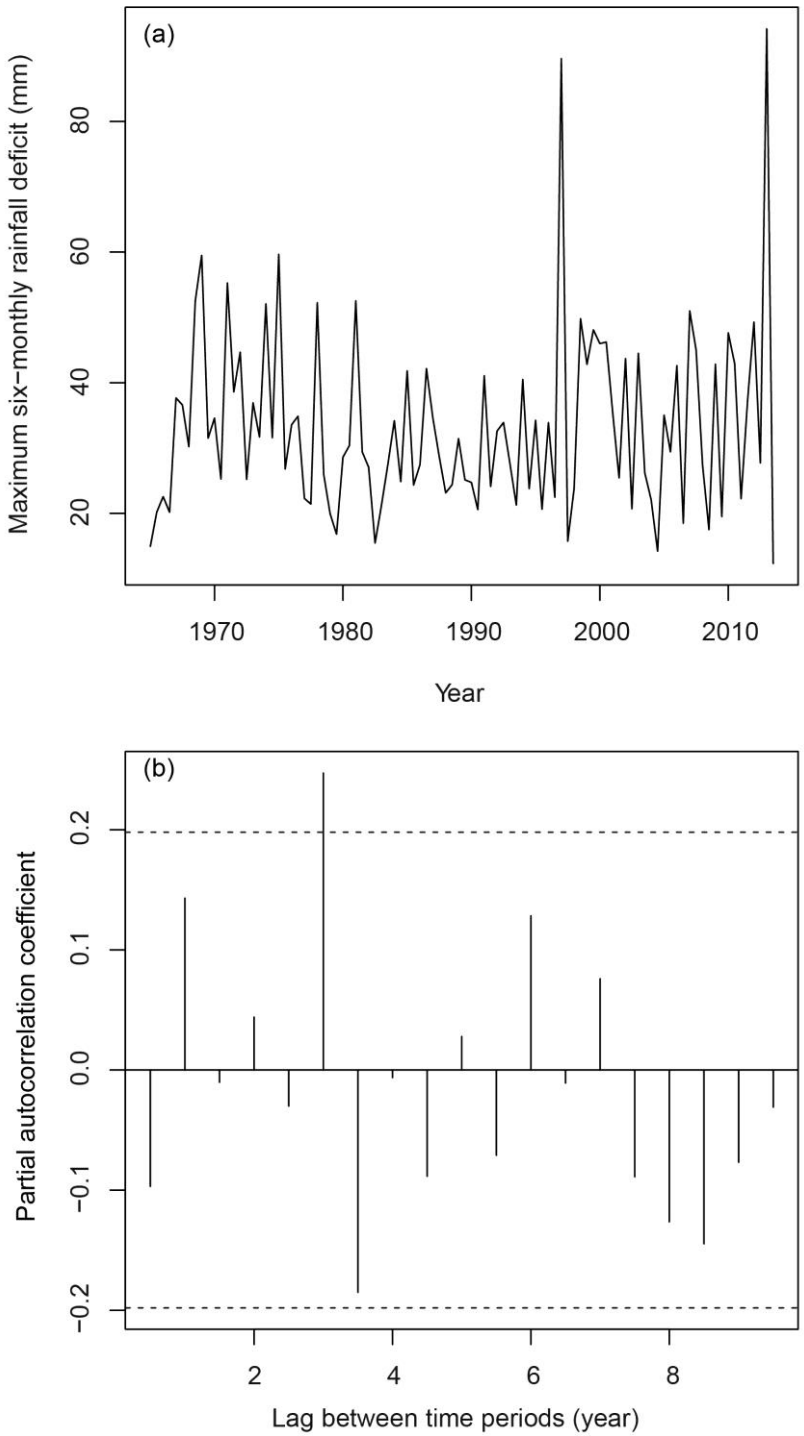

Fig. A4.1: Time series analysis of (a) rainfall deficit recorded near the study region at rainfall gauge 4054 between 1965 and 2013, and (b) the partial autocorrelation coefficients which describe the strength of autocorrelation between rainfall deficits at time *t* and *t+n* (lag between time periods in years). Correlation coefficients above or below the dashed lines are significantly different from 0 at alpha = 0.05.

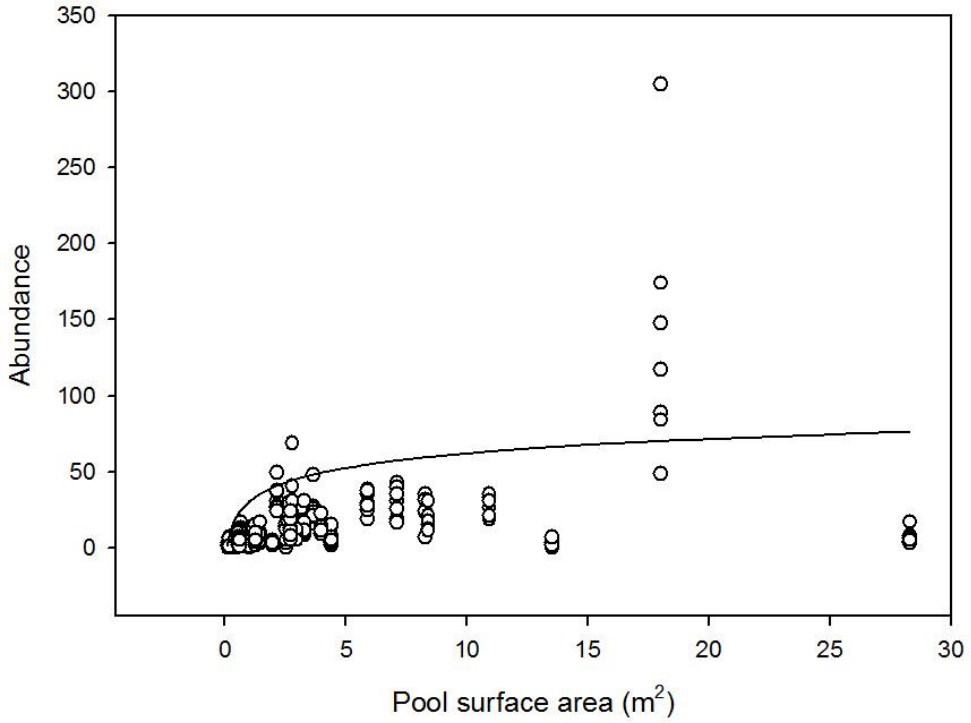

Fig. A4.2: Population abundance of *N*. *apoda* in South Westland forest pools, as a function of pool surface area. The fitted line is the 95th quantile of the relationship when pool surface area is $\log_e$ transformed according to the equation N=30.2+13.8×$\log_e$(pool surface area). This equation was used to parameterise carrying capacity for each population using pool depth to test how sensitive model results were to different carrying capacity parameterisations.

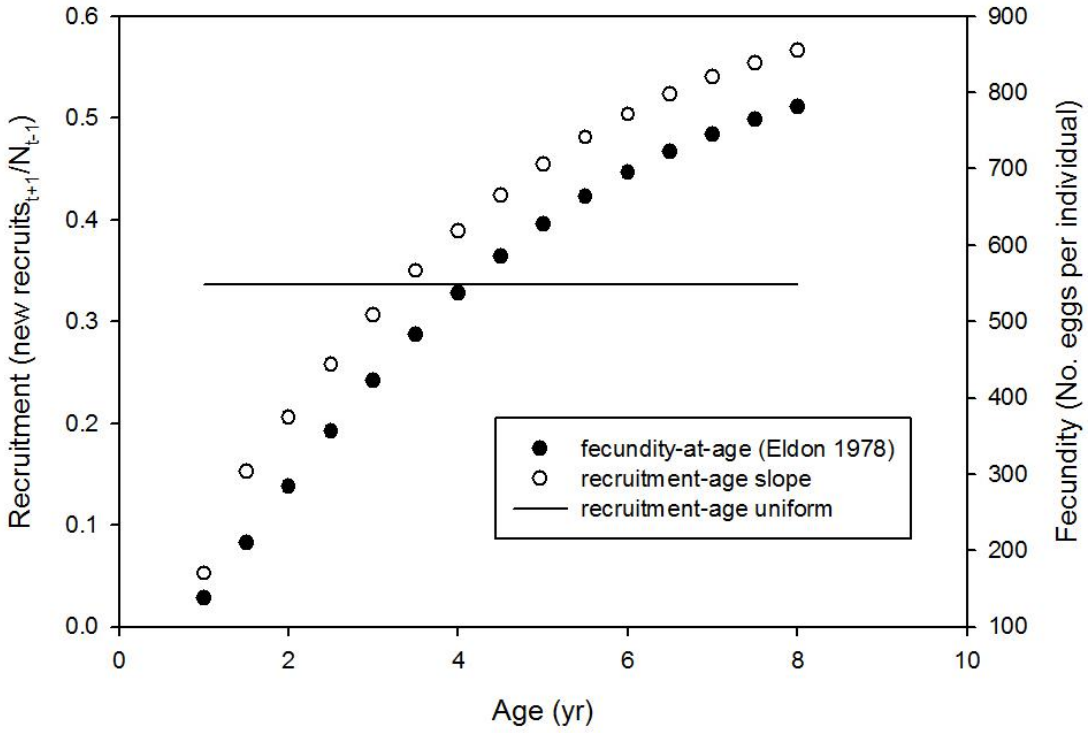

Fig. A4.3: *N. apoda* recruitment and fecundity as a function of age. Filled circles show fecundity (right y-axis) according to the equation 0.011*length$^{2.2}$ presented by Eldon (1978). Length was converted to age for display purposes using the length-age relationship in Eldon (1978). The fecundity equation was used to constrain recruitment for different ages (open circles), while holding mean recruitment across ages at 0.37, which was equivalent to that used in the final metapopulation model that used uniform recruitment across ages (solid line). This enabled me to compare results from a metapopulation model with uniform recruitment, to that with a positive recruitment-age relationship, while holding mean recruitment constant.

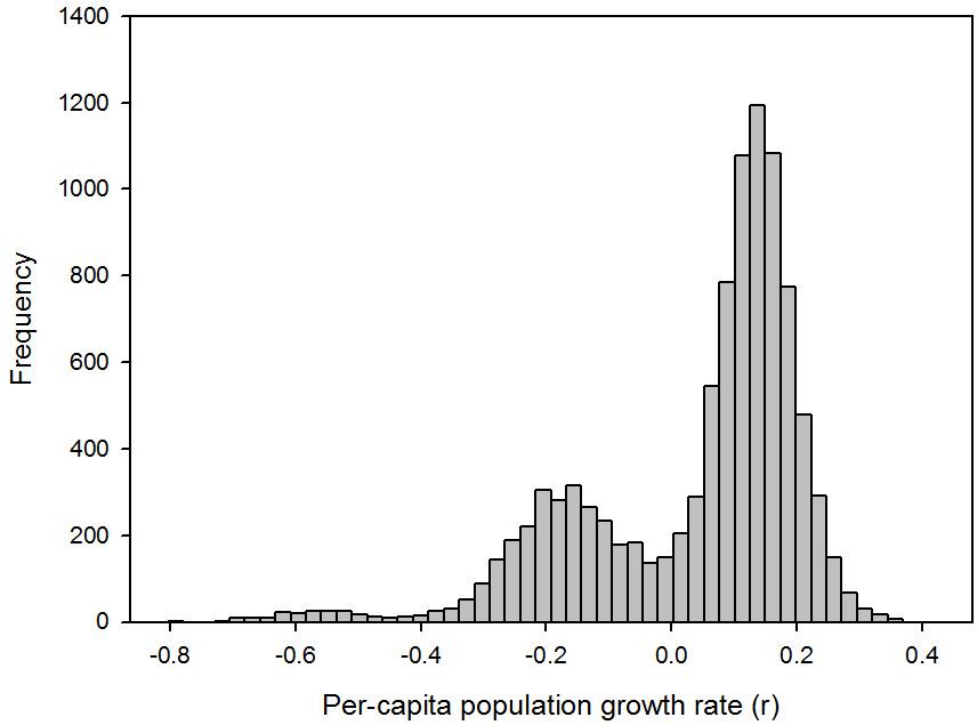

Fig. A4.4: An example of per-capita growth rates resulting from a sample of 10000 independent projection matrices taken for a particular sub-population. The tri-modal distribution reflects the frequency of low, moderate and extreme drought matrices (right, centre and left modes, respectively), each of which have vital rates with a different mean +/- SD, depending on pool depth during a particular drought as shown in Fig 1c in-text.

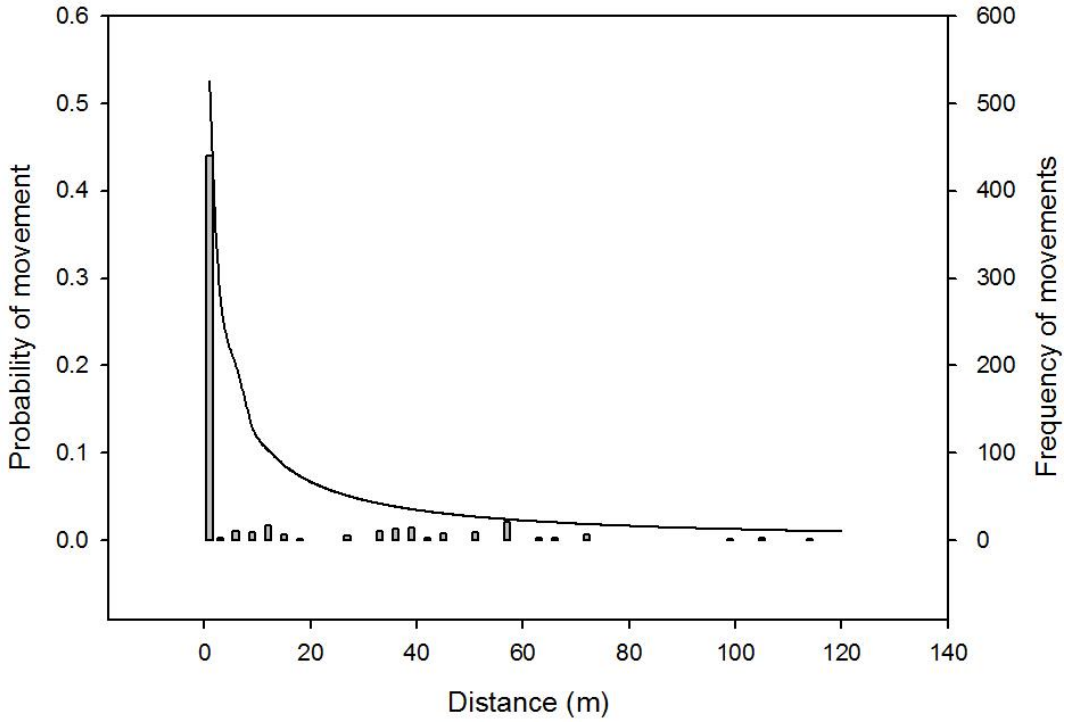

Fig. A4.5: Frequency of observed mudfish movements (right y-axis) between pools of certain inter-pool distances during the mark-recapture study (bars), and the fitted Kitchings Dispersal Kernel (line: left y-axis) indicating the relationship between distance and probability of movement.

Table A4.1: Differences in parameters used in the final metapopulation model relative to that used for model training and validation. The final metapopulation model used parameters estimated using the full duration mark-recapture dataset, whereas model training for validation was limited to the first 1.5 years of mark-recapture to ensure an independent validation. Survival parameters were estimated using the Cormack-Jolly-Seber model reported in Chapter 3, which was fitted using data restricted to the first 1.5 years, and thus did not require temporal splitting to ensure independent validation.

	Full duration		First 1.5 years	
Parameter	Mean	SD/range	Mean	SD/range
Low drought recruitment	0.37	0.06	0.41	0.06
Moderate drought recruitment	0.13	0.02	0.11	0.02
Extreme drought recruitment	0.13	0.01	0.13	0.02
Total metapopulation size	596	97	635	32
Sub-population carrying capacity	25	1-305	23	1-305
Dispersal events	97	3-112m	22	3-72m
Dispersal kernel equation	$y=9.68\times e(-D^{0.18}/0.10)$		$y=10.00\times e(-D^{0.18}/0.10)$	

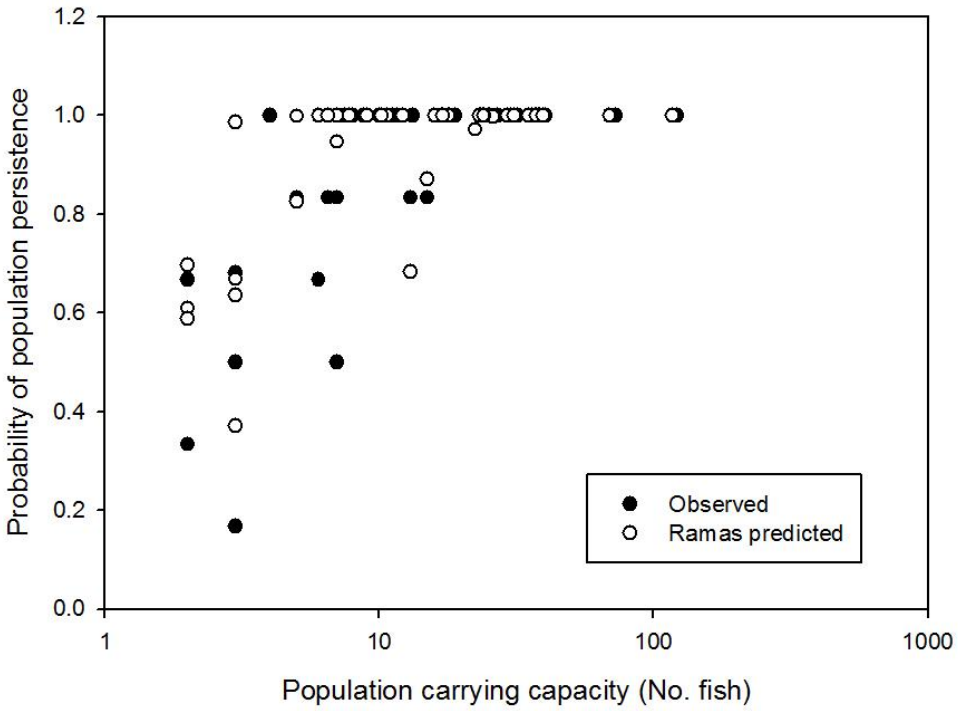

Fig. A4.6: Relationship between the probability of population persistence and population carrying capacity for populations of *N. apoda* in forest pools. Filled circles show observed values, where persistence is calculated as the proportion of sampling occasion's fish were present in pools during the final 1.5 years of the mark-recapture study. Open circles show values predicted by the metapopulation matrix model, whereby persistence is the average proportion of time steps fish are present in a pool.

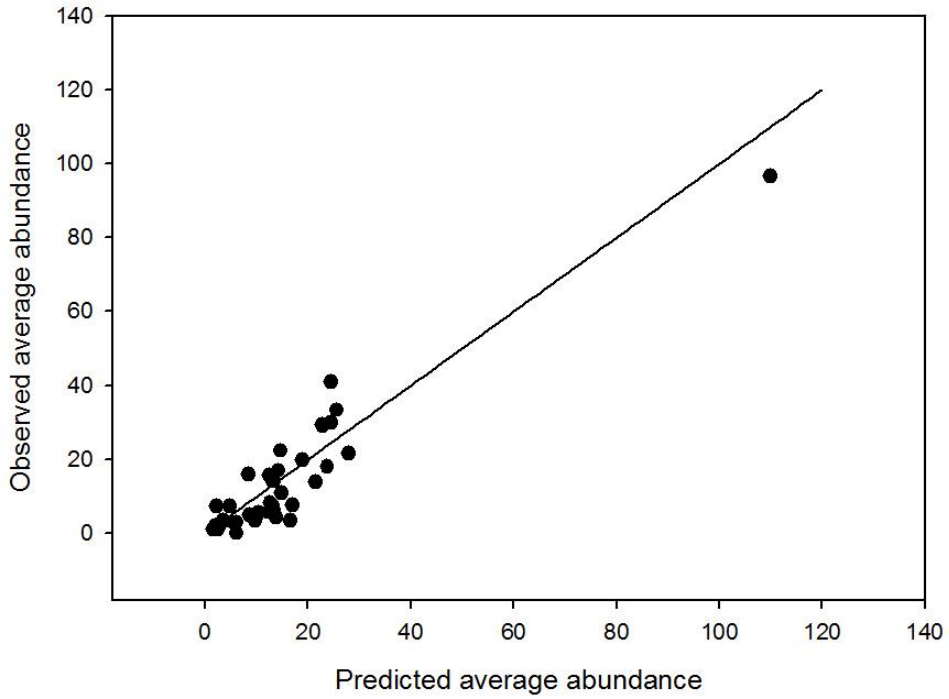

Fig. A4.7: The relationship between observed average abundance during the final 1.5 years of mark-recapture, and that predicted by the metapopulation matrix model for populations of *N. apoda* in forest pools. The solid line shows the 1:1 relationship.

Table A4.2: Stage matrices used for the low, moderate and extreme drought strength timesteps showing vital rates for the average population. Values for the moderate and extreme matrix quantify vital rates as a proportion of those in the low drought matrix.

Stage (year)	0.5	1	1.5	2	2.5	3	3.5	4	4.5	5	5.5	6	6.5	7	7.5	8
Low drought																
0.5		0.37	0.37	0.37	0.37	0.37	0.37	0.37	0.37	0.37	0.37	0.37	0.37	0.37	0.37	0.37
1	0.62															
1.5		0.99														
2			0.99													
2.5				0.99												
3					0.99											
3.5						0.99										
4							0.99									
4.5								0.99								
5									0.99							
5.5										0.99						
6											0.99					
6.5												0.99				
7													0.99			
7.5														0.99		
8															0.99	
Moderate drought																
0.5		0.35	0.35	0.35	0.35	0.35	0.35	0.35	0.35	0.35	0.35	0.35	0.35	0.35	0.35	0.35
1	0.30															
1.5		0.85														
2			0.86													
2.5				0.88												
3					0.89											
3.5						0.90										
4							0.90									
4.5								0.90								
5									0.90							
5.5										0.92						
6											0.92					
6.5												0.92				
7													0.92			
7.5														0.93		
8															0.93	
Extreme drought																
0.5		0.35	0.35	0.35	0.35	0.35	0.35	0.35	0.35	0.35	0.35	0.35	0.35	0.35	0.35	0.35
1	0.24															
1.5		0.79														
2			0.79													
2.5				0.80												
3					0.80											
3.5						0.80										
4							0.82									
4.5								0.82								
5									0.83							
5.5										0.83						
6											0.83					
6.5												0.83				
7													0.83			
7.5														0.83		
8															0.84	

Table A4.3: Sensitivity of slope parameters of the relationship between population size and persistence to adjustments in vital rates and model structural parameters. Percent slope change refers to the change in the slope after parameter adjustment relative to that in the final model (which was 7.49) parameterised by mean values and structured as described and shown in Appendix 1 Figs A8-9. *P*-values of the interaction between environmental stochasticity and carrying capacity (ES-K interaction) after parameter modifications are also shown along with *c* values for the population with the highest environmental stochasticity, where *c* is the average rate of population growth relative to its variance resulting from environmental stochasticity.

Parameter	Final model	Parameter adjustment	% slope change	P-Value ES-K interaction	Minimum *C*
Vital rates	*Mean*	*Lower 95% CI*			
Low drought recruitment	0.37	0.29	-23	<0.001	1.37
Mod/extreme drought recruitment	0.13	0.11	-5	<0.001	2.11
Low drought survival	0.99	0.95	-21	<0.001	1.45
Moderate drought survival	0.90	0.82	-28	<0.001	1.18
Extreme drought survival	0.82	0.79	-4	<0.001	2.38
Structural settings		*Description*			
Standard deviation matrix	on	off	+16	<0.001	3.53
Population carrying capacity	max N	95th quantile	-15	<0.001	2.53
Fecundity-at-age slope	uniform	positive	+19	<0.001	1.53
Moderate drought probability	0.27	0.34	-17	<0.001	1.51
Extreme drought probability	0.02	0.03	-8	<0.001	2.22

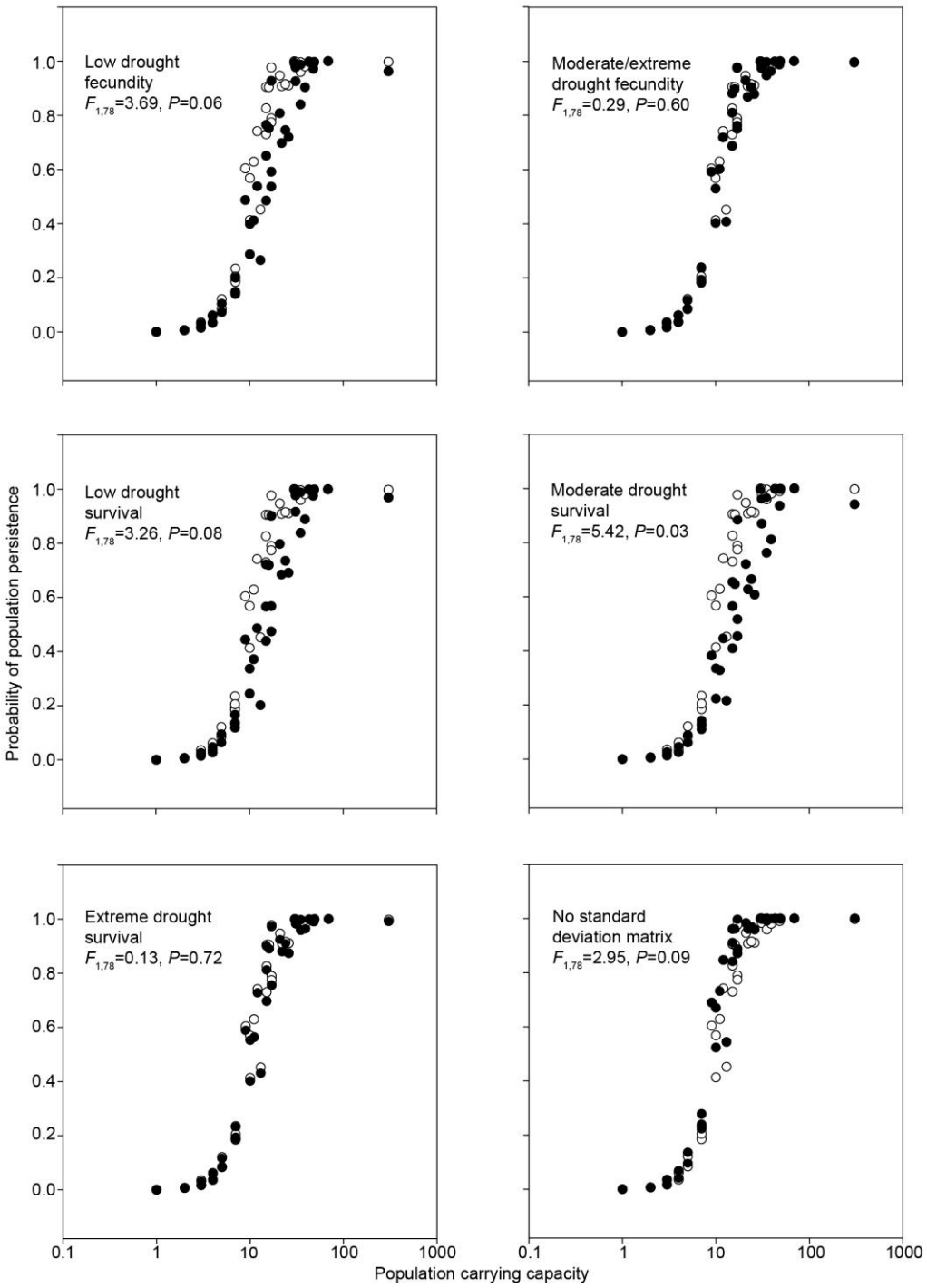

Fig. A4.8: Relationship between population persistence and carrying capacity predicted by the final metapopulation (open circles) and after modification to specific vital rates (closed circles). Each respective vital rate has been reduced to the lower confidence interval reported in Table A4.1. "No standard deviation matrix" refers to model predictions after the standard deviation matrix is removed (closed circles). Differences in slopes between datasets in each panel can be seen in Table A4.1 for which F-ratios and P-values are shown in-figure.

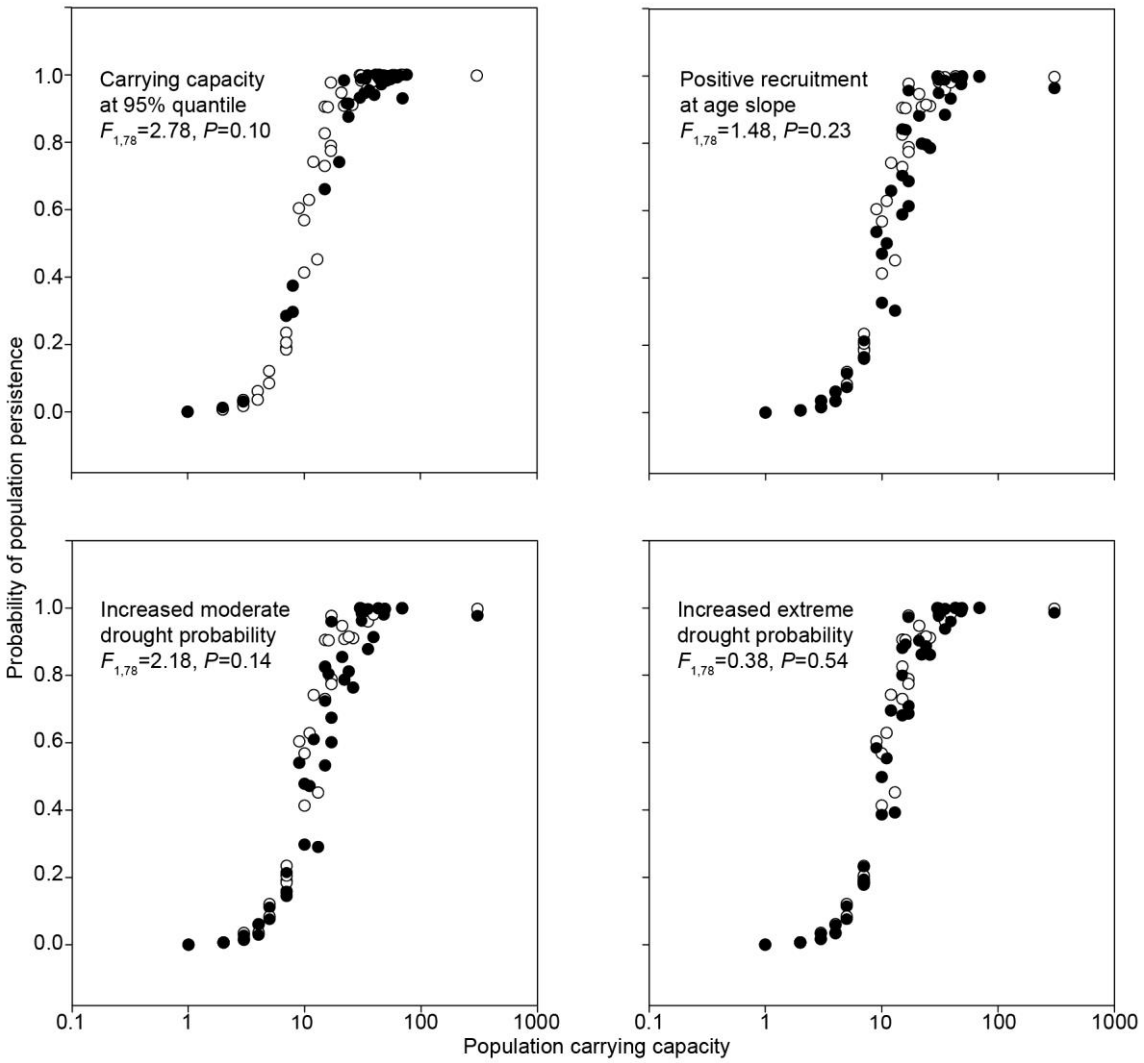

Fig. A4.9: Relationship between population persistence and carrying capacity predicted by the final metapopulation (open circles) and after modification to model structural parameters (closed circles). Each parameter has been adjusted according to the description in Table A4.1 where statistics on differences between datasets in each panel can also be seen. Differences in slopes between datasets in each panel can be seen in Table A4.1 for which F-ratios and P-values are shown in-figure.

Chapter Five

Global warming and land-use change interact to drive changes in population size-based extinction thresholds

Abstract

Population size is the primary criteria used globally to determine species extinction risk and prioritise conservation risks due to the widely documented positive scaling of population persistence with carrying capacity. However, it is unknown how such scaling is affected by land-use change combined with climate change which, for many populations, is expected to decrease population growth rates and increase population variability. Moreover, it is unknown how such changes to scaling in sub-populations will impact the persistence of larger interconnected metapopulation networks. Using empirically-derived models, I show that the scaling of time-to-extinction with carrying capacity in brown mudfish sub-populations is driven by an interaction between land-use change (forest clear-felling) and increasing extreme drought frequency with global warming. Population persistence increased exponentially with carrying capacity in large stable habitats, but this relationship was asymptotic at small population sizes in habitats contracted in size by forest logging. Metapopulation persistence in logged forests dropped by over 50 percent due to such asymptotic scaling and lost persistence of large populations. Thus even large sub-populations are likely vulnerable in stochastic environments, with their loss having disproportionately large negative effects on metapopulation persistence in landscapes affected by human disturbances. My results confirm longstanding theory predicting asymptotic population size-persistence thresholds under environmental stochasticity, and by doing so, highlight the keystone role large populations play in mitigating the impacts of global warming and land-use change.

Introduction

Habitat degradation and loss are currently the major drivers of global biodiversity decline and are likely to be exacerbated by an increasingly variable future climate under global warming (Dudgeon *et al.* 2006; Vörösmarty *et al.* 2010; Scheffers *et al.* 2016). Population size is the primary criteria used globally to determine species extinction risk and prioritise conservation risks (IUCN 2001) due to the widely documented positive scaling of population persistence with carrying capacity (Lande *et al.* 2003; Desharnais *et al.* 2006). However, the theoretical underpinnings of such criteria are based on dynamics of single isolated populations under current climate (Ovaskainen & Meerson 2010). Importantly, it is unknown how the scaling of population persistence with carrying capacity will be altered by the combined effects of on-going global warming and land-use change (Ovaskainen & Meerson 2010), and how such influences will affect persistence of inter-connected metapopulations at landscape scales.

The theoretical effects of environmental stochasticity on the scaling of time-to-extinction with carrying capacity for isolated populations have been examined extensively, but rarely in empirical studies of actual populations (Ovaskainen & Meerson 2010). Mathematical models suggest that in constant environments, time-to-extinction increases exponentially with carrying capacity, K, whereas variation in environmental conditions causes power law scaling with K raised to a slope constant, c (Leigh 1981; Lande 1993; Foley 1994). The slope parameter, c, is quantified as the ratio of the mean population growth rate relative to its variance under environmental variability (Lande 1993). Consequently, decreases in mean population growth or increases in population growth rate variability cause the scaling of time-to-extinction with carrying capacity to flatten from exponential increase ($c>1$), to asymptotic increase ($c<1$) (Lande 1993). Because slope values, c, are sensitive to either reduction in mean or increase in variance of population growth rate, changes to the scaling of time-to-extinction with carrying capacity are likely to be greatest in populations

affected by combinations of land-use and climate changes that simultaneously depress mean population growth rates and increase variability. Moreover, the lost persistence of large sub-populations in such scenarios could have wide reaching impacts on other interconnected, populations whose persistence is bouyed by immigration from large resilient neighbouring populations. Consequently, by influencing the persistence of large populations, changes to the scaling of population persistence with carrying capacity could have wide reaching landscape scale effects on metapopulation persistence under global change.

Based on empirical measures of real populations, I modelled how changes to the scaling of time-to-extinction with carrying capacity under combinations of global warming and land-use affected population persistence at both sub-population and metapopulation scales of an endangered wetland fish, *Neochanna apoda*. *N. apoda* inhabit forest pools formed by fallen trees in New Zealand indigenous forest that dry frequently and for long durations causing up to 83 percent mortality, as was the case in a recent one-in-twenty-five-year drought in 2013 (Chapter 3). The magnitude and frequency of droughts varies spatially with pool depth, being more frequent and severe in shallow pools, which negatively influences the scaling of time-to-extinction with carrying capacity (Chapter 4). Although the increased sub-population variability in shallow, drought prone pools was insufficient to cause asymptotic scaling of time-to-extinction with carrying capacity (Chapter 4), these results suggest shifts towards such scaling will be most likely in shallow habitats under global warming.

That the influence of drought disturbance on *N. apoda* sub-populations is mediated by pool depth is important because both natural and human-driven disturbance strongly affects this habitat characteristic. Prior to human arrival in New Zealand, catastrophic windthrow and earthquake disturbances were the main drivers of forest dynamics in forests inhabited by *N. apoda* (James 1987; Wells *et al.* 2001; Cullen *et al.* 2003). Recently disturbed mature forest

stands likely contained abundant deep, permanent pools formed by tree-fall, containing *N. apoda*. However, historic logging and burning of over 70 percent of indigenous New Zealand forest (Ewers *et al.* 2006) has prevented such on-going habitat formation, likely resulting in large areas of forest re-growth containing only small, shallow pools that experience greater drought frequencies and magnitudes. This implies that changes to the scaling of time-to-extinction with carrying capacity under global warming are likely greatest in *N. apoda* populations affected by historic land-use (clear-felling). I drew upon expansive mark-recapture datasets and metapopulation matrix models (Chapter 2-4) to test the hypothesis that reductions in the slope of the scaling of time-to-extinction under climate change would be greatest in sub-populations affected by land-use change (clear-felling) resulting in significantly reduced persistence at larger metapopulation scales in such habitats.

Methods

Study metapopulations

I modelled metapopulations of *N. apoda* in a 9000 ha temperate peat-swamp-rainforest located within South Westland, Tai Poutini National Park, New Zealand. Freshwater pools formed by root excavations of large fallen trees (tip-up pools) are randomly distributed every 5-10 m throughout the forest floor. Most pools contain abundant *N apoda*, which frequently disperse between pools forming metapopulations (Chapter 4). The study forest has been impacted by a range of natural and human-driven disturbances that have likely impacted pool depths and habitat availability for *N. apdoa* metapopulations. The forest consists predominately of mature indigenous conifer stands containing freshwater pools formed by occasional root excavations of large fallen trees (tip-up pools), with a wide range of depths. Meanwhile, an extensive area of mature forest has recently been disturbed by a large tornado (c. 2011) that generated an approximately 5 x 0.1 km stretch of fresh

windthrow of large mature conifers that likely contains high densities of deep, permanent, pools. Finally, historic logging dating from 1950-1985 has resulted in numerous areas of regenerating clear-fell containing earlier successional shrub and broadleaved forest that likely contains higher densities of shallow, drought-prone pools due to the absence of large trees to form tip-up pools.

I used an empirically-derived metapopulation matrix model (Fig. 4.2) to investigate how sub-population dynamics differed between mature forest, tornado-disturbed and regenerating-clear-fell forests under various climate change scenarios. The metapopulation matrix model was parameterised and validated previously using *N. apoda* birth, death and dispersal data collected from 41 pools in mature forest distributed amongst four 100 x 20m forest transects (Chapters 2-4). The transects were distributed every 2.5 km through the mature forest and were therefore considered as independent metapopulations (Fig. 2.1). The present study expanded the use of the matrix model used for mature forest into three new transects (metapopulations) of regenerating clear-fell, and tornado-disturbed forests, respectively, that were of equivalent size to those in the mature forest. All pools within each transect were located, totalling 44 pools each for regenerating clear-fell and catastrophic windthrow forest types, in addition to the original 41 mature forest pools (129 sub-populations in total). Pool depth and surface areas were continuously recorded all 129 pools between April 2014 and continuing until October 2015 using a combination of stage height loggers and spot depth measurements according to the procedures described in Chapter 2-3.

The key input parameters in the mature forest matrix model were pool carrying capacities and vital rates, which can be predicted for new pools by pool size (pool depth and surface area) based on relationships described for the mature forest. To validate the relationships used to predict pool carrying capacity and vital rates in mature forest for use in all disturbance regimes, I conducted mark-recapture in a subset of 18 regenerating clear-fell

and 18 tornado pools (approximately six in each transect), in addition to the original 41 mature forest pools (77 total). All mark-recapture protocols were identical to those described in previous chapters, with mark-recapture samples being taken every six months from all 75 pools in the mark-recapture pool subset (i.e. two trapping occasions separated by 14 days every six months) commencing April 2014 until October 2015. These data enabled four sub-population size estimates for each pool using closed Lincoln-Petersen models (i.e. one estimate per 6-months^{-1}) (Ricker 1975), and survival and recruitment every six months using open Cormack-Jolly-Seber (CJS) and Jolly-Seber (JS) (POPAN) models (Schwarz & Arnason 1996).

Metapopulation matrix model structure

I used the spatially explicit metapopulation matrix model described in Fig. 4.2, to quantify the interactive effect of extreme drought frequency and land-use change (forest disturbance type) on the scaling of sub-population time-to-extinction with carrying capacity, and how such scaling changes affected metapopulation persistence. The metapopulation model was constructed in RAMAS Metapop, which has been widely used to model metapopulation dynamics for applied and research purposes, and models the effects of environmental and demographic stochasticity, density dependence and dispersal on sub-population dynamics (Akçakaya *et al.* 2004; Gordon *et al.* 2012; Bond *et al.* 2015). Full details of this model as it was applied to *N. apoda* metapopulations, can be seen in Chapter 4. However, I will describe the model structures relevant to it's application in this study.

Environmental stochasticity due to droughts was modelled by randomly drawing one of three projection matrices on each time step characterising vital rates for different metapopulation-wide drought intensities (Fig. 4.2a). The projection matrices reflected mean (± SD) birth and death rates over six month time periods when maximum drought intensity

was either: low (6.4-36 mm rainfall deficit), moderate (36-94 mm rainfall deficit) or extreme (>94 mm rainfall deficit), which occur at probabilities of 0.70, 0.28 and 0.02, respectively, according to historic climate data (National Climate Database, NIWA) (Appendix 4.1, Fig. A4.1). These drought probabilities were manipulated, as described later, to simulate the effects of increasing extreme drought frequency due to climate change.

Spatial variation in environmental stochasticity was induced by constraining vital rates as a positive function of pool depth according to drought-specific relationships fitted to the mark-recapture data collected from mature forest populations using maximum-likelihood-estimation (Fig. 3.4). Consequently, all sub-populations were exposed to the same regional drought events (i.e. low, moderate, or extreme) but sub-population environmental stochasticity was highest in shallow pools. Cormack-Jolly-Seber models fitted to the mark-recapture data collected from the 77 pool subset in this study showed there were no significant differences in survival between forest types after controlling for fish length and the interaction between average pool depth and sub-population density (χ^2=13.16, P=0.51). Consequently, the models fit to the mature forest pools as reported in Chapter 3 are likely valid for pools in all forest types in this study.

Sub-population carrying capacity was estimated for each pool as a function of the interaction between pool surface area and average depth (both on log scales) and forest type using a negative binomial generalized linear model fitted to the mark-recapture data collected from the 77 pool subset. Population abundance for the 77 pools was estimated using Lincoln-Petersen mark-recapture models (Ricker 1975) every six months between April 2014 and October 2015 totalling 4 abundance estimates for each pool. Pool carrying capacity was taken as the maximum of these estimates for each pool, respectively. Carrying capacity was driven by a significant three-way interaction between log surface area and depth and forest type (χ^2=7.8, P=0.008), and thus the model was not simplified further. This three-way interaction,

in addition to all lower order two-way interactions and direct effects, explained 65 percent of the deviance in carrying capacity, predictions from which closely matched actual carrying capacities (Fig. 5.1).

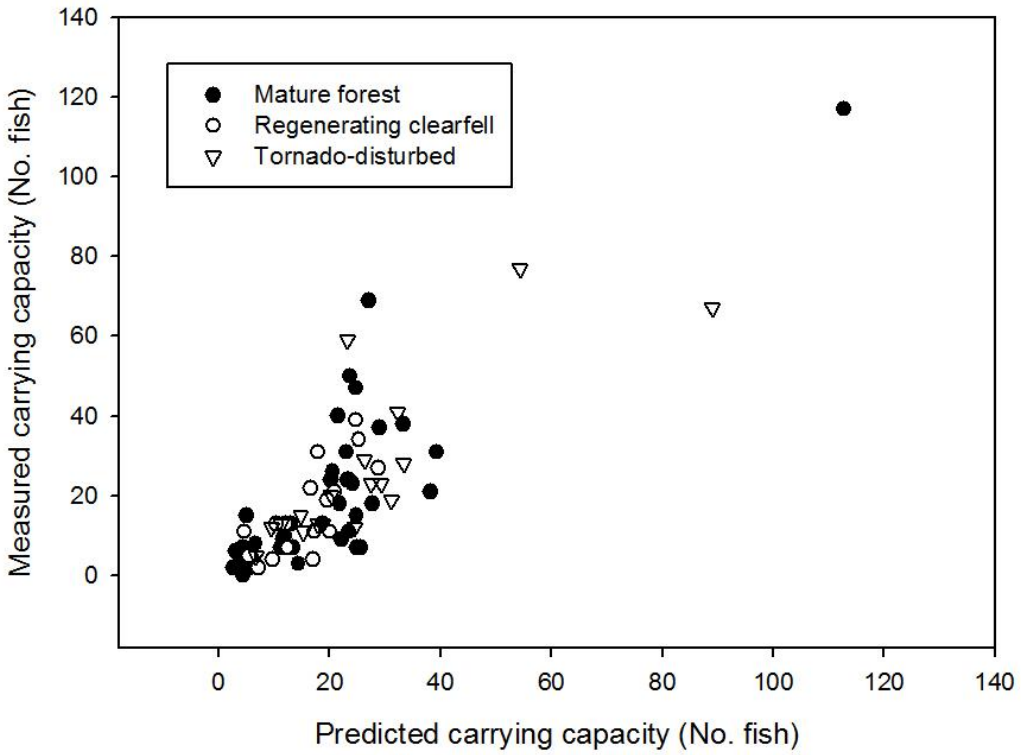

Fig. 5.1: Carrying capacity of sub-populations in different forest-types (symbols) measured from mark-recapture data plotted as a function of that predicted by the negative binomial generalised linear model described in text.

Inter-population dispersal probability decayed with distance according to Kitchings (1971) dispersal kernel: $m=a\times e(-D^g/b)$, where m was fish movement probability, D was distance (m) and a, b and g were constants estimated from the mark-recapture data (Fig. 4.2d). The maximum represented dispersal distance was 120 m, thus allowing fish to disperse between pools within transects, and not between transects. Although *N apoda* may disperse

distances greater than 120 m over longer time scales, using pools as stepping stones, this would only allow them to move up to 1920 m over their 8-y lifespan, which is less than the minimum distance between transects. By altering this equation, I was able to examine how changes to inter-population connectivity affected metapopulation persistence during climate change, as described later.

Interactive effects of climate and land-use change on scaling of sub-population persistence with K

I first used the metapopulation matrix model to quantify the interactive influence of extreme drought frequency and land-use change (forest disturbance type) on the scaling of time-to-extinction and carrying capacity for isolated sub-populations. To this end, I used the metapopulation model to calculate the mean and variance in sub-population growth rate for each sub-population in isolation under eleven different drought frequency scenarios expected for the year 2090. Means and variances in sub-population growth rate were quantified using methods described in Chapter 4, and were used to estimate the scaling parameter, *c*, used in classical population models that quantify the effects of environmental stochasticity on time-to-extinction for isolated populations, whereby *c* is $2r/V_r$-1, and *r* and V_r are the mean and environmental variance in population growth rate, respectively (Leigh 1981; Lande 1993; Foley 1994). The *c* parameter quantifies the form of the relationship between time-to-extinction, *T*, and carrying capacity, *K*, according to the equation (1) presented by Lande (1993):

$$T = \frac{2}{V_r C}\left(\frac{K^c - 1}{c} - lnK\right) \quad (1)$$

According to model (1), if environmental variance in growth rate is sufficiently higher than

the mean growth rate (i.e. $c<1$), population persistence asymptotes at decreasingly lower K. Otherwise, persistence increases exponentially with K (i.e. when $c>1$) (Lande 1993).

The effect of climate change on the mean and variance in sub-population growth rate was simulated by increasing the probability of moderate and extreme drought projection matrices in the matrix model to that expected in New Zealand by 2090 under various IPCC climate change scenarios presented by Mullen *et al.* (2005). Mullen *et al.* (2005) predicted that a 1 in 20 year drought in 2005 would occur up to every 1 in 2.5 years by 2080 in the worst case climate change scenario in New Zealand. This corresponds to a maximum rate of increase in extreme drought probability of approximately 0.001 every 6-months. In my metapopulation model, eleven climate change scenarios were considered ranging from zero rate of change (six-monthly increase in moderate and extreme drought probability = 0) to maximum potential change expected under climate change (six-monthly increase in moderate and extreme drought probability = 0.001). This meant that a current one-in-twenty five-year drought (i.e. the extreme drought) would occur approximately every 25-2.85 years in 2090 in the worst case climate change scenario modelled by Mullen *et al.* (2005). It was assumed that both moderate and extreme drought frequencies would increase in concert. For example, if the probability of moderate drought was increased, the same proportional increase in extreme drought probability was also made for a given scenario.

I then analysed the interactive influence of extreme drought frequency and land-use change (forest disturbance type) on mean sub-population growth rate, variance and slope parameters, c, of the scaling of time-to-extinction and carrying capacity. This was done using linear mixed effects models of each response variable as function of the interaction between extreme drought frequency (no. extreme droughts 25 y^{-1}) and forest disturbance type. Mean and variance in sub-population growth rates were untransformed, however, c values were log(+3) transformed to ensure linearity. Sub-population number (1-129) was used as the

random factor for which I allowed differences in intercepts to control for repeated measures from each sub-population.

Effects of changes to sub-populationl scaling of persistence with abundance on overall metapopulation persistence

I was then interested in determining how changes to the scaling of time-to-extinction with carrying capacity in sub-populations, affected extinction risk in connected metapopulations under combinations of global warming and land-use change. To this end, I ran the metapopulation matrix model for each clear-fell, tornado and mature forest metapopulation (individual transects) separately for 191 consecutive six-month time-steps over for each climate change scenario. The 191 time steps allowed me to quantify metapopulation dynamics between 2015 and 2090, with an initial 20 year burn-in period, which was excluded from analyses.

To investigate the effect of sub-population connectivity on metapopulation persistence during climate change, each climate change scenario was additionally crossed with eight levels of sub-population connectivity (no. connections per pool). I did this by altering the *b* parameter controlling maximum dispersal distance in Kitchings (1971) dispersal equation used to model inter-population dispersal probability on each time step. Maximum dispersal distance, and thus pool connectivity (the number of pools connected to each pool) increases with *b*, where 0 and 10 are minimal and maximal connectivity, respectively. Therefore, *b* determined how many neighbouring sub-populations a given sub-population could exchange fish with. For each climate change scenario, I ran models at eight levels of pool connectivity, with *b* set to 0, 0.8, 1.6, 2, 3, 5, 7 or 10. The total number of models run for each metapopulation (transect) was thus 88 (11 climate change × 8

connectivity scenarios), where each scenario was replicated 1000 times.

I analysed the interactive effects of climate scenario, land-use change (forest disturbance type), and connectivity on the probability of metapopulation persistence using generalized linear mixed models assuming a quasibinomial distribution. Probability of metapopulation persistence was quantified as the proportion of model simulations within connectivity/climate change scenario, where combined abundance within all pools remained >1. For this analysis, transect identity was used as the random factor for which differences in intercepts was considered to control for repeated measures from each transect.

Results

Interactive effects of climate change and forest-disturbance on scaling of sub-population persistence with K

Pool depths, and thus exposure to drought events, varied systematically across each forest disturbance type, being predominately shallow in clear-fell metapopulations and deep in tornado metapopulations (Fig. 5.2). While pool depths in mature growth metapopulations were relatively shallow on average, there was a greater range than in clear-fell metapopulations, including the deepest pool recorded (Fig. 5.2). Consequently, drought exposure was typically highest within clear-fell metapopulations (Fig. 5.2). I hypothesized that the shallow, drought-prone, nature of clear-fell pools would result in greater sensitivity of mean and variance in sub-population growth rates, and thus slopes of the scaling of time-to-extinction with carrying capacity, in response to increased frequency of extreme droughts under climate change. As expected, both mean and variance in sub-population growth rates were driven by a significant interaction between extreme drought frequency and forest

disturbance (mean sub-population growth rate: χ^2=560.8, P<0.001; sub-population growth variance: χ^2=461.9, P<0.001). Thus clear-fell sub-populations were more variable and had lower mean growth rates than in other forest disturbances, and were also more sensitive to changes in extreme drought frequency (Fig. 5.3a-b).

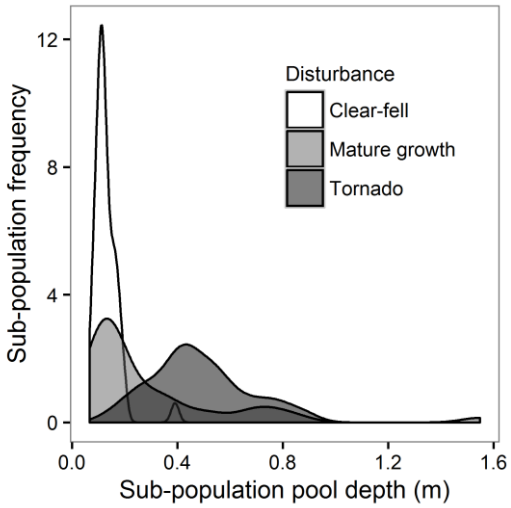

Fig. 2: Frequency distribution of sub-populations inhabiting pools of particular mean depths in *N. apoda* metapopulations affected by different forest disturbances.

As a consequence of the interactive effects of extreme drought frequency and forest disturbance on sub-population growth rate mean and variance, I observed a significant interactive effect of extreme drought frequency and forest disturbance on slope values for the scaling of time-to-extinction with carrying capacity (χ^2=524.7, P<0.001). Thus, slopes of the scaling of time-to-extinction with carrying capacity were lowest in clear-fell sub-populations; slopes declined with increases in extreme drought at a faster rate than in other forest disturbances (Fig. 5.3c). Under current climate conditions of one extreme drought in 25 years, all sub-populations showed exponential scaling of time-to-extinction with carrying capacity, suggesting that sub-populations were relatively resilient to human and natural forest disturbance in isolation (Fig. 5.4a-c, solid lines). However, while scaling remained

exponential on average in mature growth and tornado sub-populations, even under the most extreme climate scenario (Fig. 5.4a,b), only modest increases in extreme drought frequency caused this scaling to asymptote, on average, in clear-fell sub-populations (Fig. 5.4c). Consequently, sub-populations were generally robust to climate change by itself (Fig. 5.4a,b), but not when climate change occurred in concert with existing human-driven disturbances associated with land-use change (Fig. 5.4c).

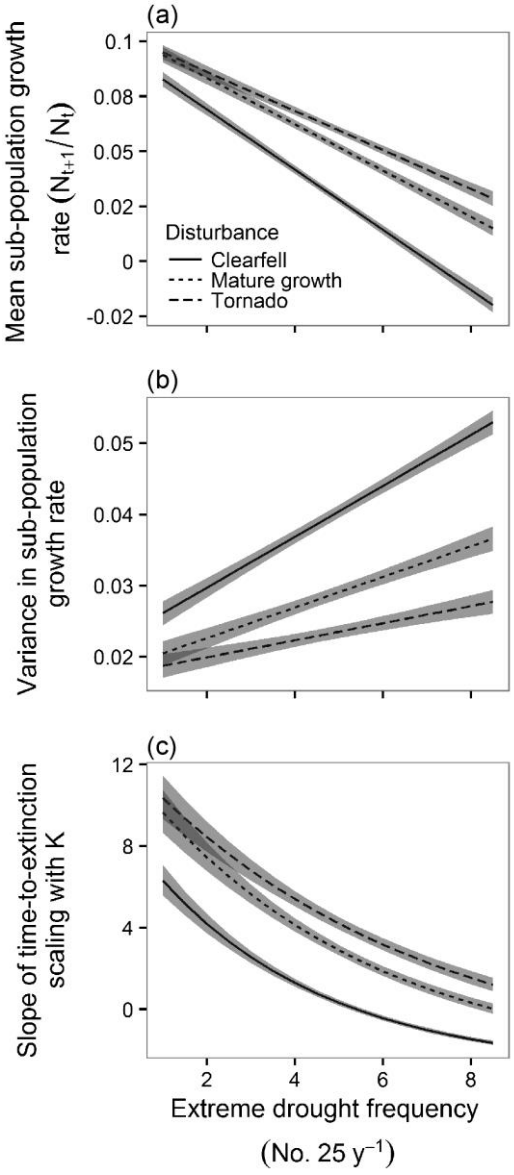

Fig. 5.3: Effects of extreme drought frequency and forest disturbance on mean (a) and variance (b) in sub-population growth rate and slopes of the scaling of sub-population time-to-extinction with carrying capacity (c) for *N*. *apoda* metapopulations in New Zealand. Slopes in (c) are calculated as $2r/V_r$-1, where r and V_r are the mean and variance in population growth rate, respectively, from (a) and (b). All lines and 95 percent confidence intervals (shaded area) were predicted from generalised linear mixed effects models using the interaction between forest-disturbance and extreme drought frequency for each response variable.

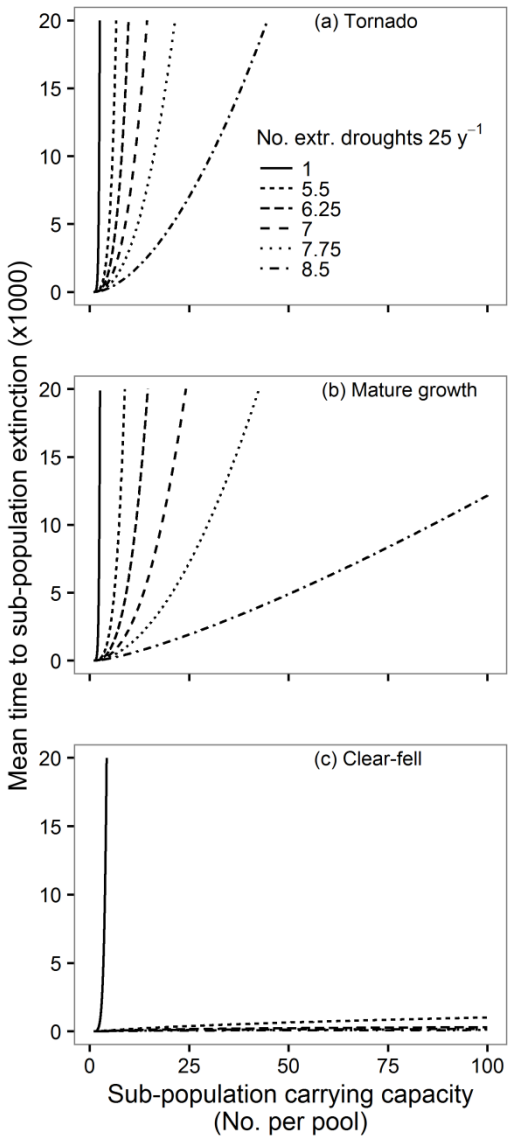

Fig. 5.4: The effects of increasing extreme drought frequency (line style) on the scaling of time-to-extinction with carrying capacity for *N. apoda* sub-populations in (a) tornado, (b) mature growth and (c) clear-fell affected forests. All lines are calculated from eqn. (1) in the methods, parameterised using slope values, *c*, for the average sub-population within each forest-disturbance and drought frequency scenario shown in Fig. 5.3c.

Interactive effects of climate change and forest disturbance on metapopulation persistence

As extreme drought frequency increased, a greater proportion of sub-populations within each metapopulation began showing asymptotic scaling of time-to-extinction with

carrying capacity (Fig. 5.5a-c). However this increase was greatest for clear-fell metapopulations, where almost all sub-populations showed asymptotic scaling under the most extreme climate change scenario (Fig. 5.5c). Differences in persistence of large sub-populations between forest types had a substantial impact on metapopulation persistence, which was driven by a significant two-way interaction between forest type, the frequency of extreme droughts (χ^2=12.6, P=0.002). Thus, metapopulation persistence decreased with increasing extreme drought frequency (Fig. 5.5 d-f), but the rate of decrease was greatest in regenerating clear-fell, where asymptotic scaling of sub-population persistence with carrying capacity was most prominent (Fig. 5.5f). In fact, tornado and old growth metapopulations, which showed exponential scaling of sub-population persistence with carrying capacity in at least 50 percent of sub-populations on average (Fig. 5.5a, b), were generally 100 percent persistent, even when extreme droughts were most frequent (Fig. 5.5d, e). In contrast, clear-fell metapopulations showed marked declines in metapopulation persistence as extreme drought frequency increased (Fig. 5.5f), particularly when asymptotic scaling of persistence with carrying capacity was observed in more than 50 percent of the sub-populations (Fig. 5.5c). Consequently, the lost resilience of large sub-populations at the local scale (Fig. 5.5c) had wider reaching impacts on metapopulation persistence at larger landscape scales (Fig. 5.5f).

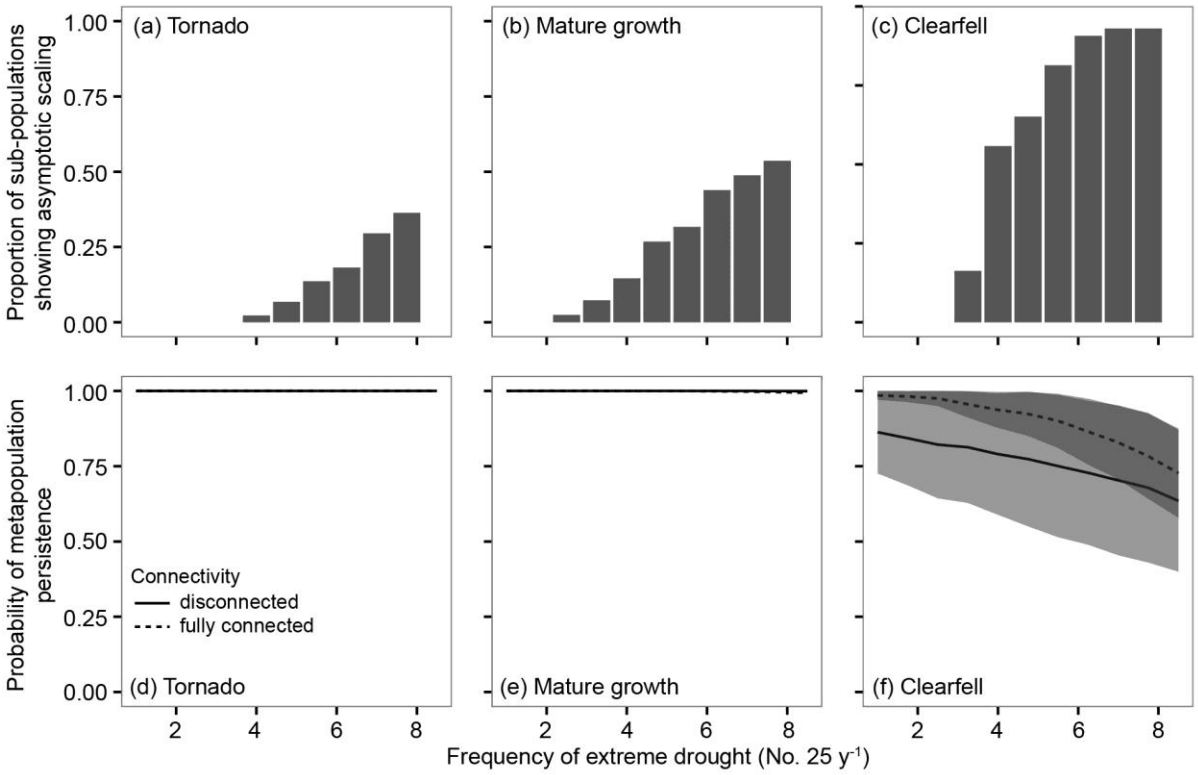

Fig. 5.5: Scaling of sub-population and metapopulation persistence with carrying capacity and extreme drought frequency, respectively, in *N. apoda* metapopulations in tornado (a,d), mature growth (b,e) and clear-fell (c,f) affected forests. The proportion of sub-populations showing asymptotic scaling of time-to-extinction with carrying capacity was calculated as the proportion of sub-populations within each forest-disturbance where slope values were <1 in each climate scenario. Responses of metapopulations are shown when either fully connected (dashed lines: *b*=10, dispersal was possible between all populations in a metapopulation), or disconnected (solid lines: *b*=0, no dispersal occurred).

The effect of extreme drought frequency on metapopulation persistence was dependent on inter-population connectivity owing to a significant interaction between inter-population connectivity and frequency of extreme droughts (χ^2=449.8, P<0.001). In general, increasing inter-population connectivity had a positive effect on metapopulation persistence (direct connectivity effect coefficient=1.85) however, this effect became weaker as extreme

drought frequency increased (connectivity-drought frequency interaction coefficient: -0.00016). Thus, while the most connected metapopulations were the most persistent overall, these metapopulations also showed the greatest rate of decline in persistence as the frequency of extreme droughts increased, particularly in clear-fell forest (Fig. 5.5f). This interaction implied the most connected metapopulations were the most sensitive to increasing drought frequency with global warming. This effect did not differ between forest types as indicated by a non-significant three-way interaction between drought frequency, connectivity, and forest-disturbance (χ^2=0.15, P=0.93).

Discussion

Exponential scaling of time-to-extinction with carrying capacity implies only small populations are at risk of rising environmental stochasticity due to global warming (Ovaskainen & Meerson 2010). However, using empirical estimates of environmental stochasticity, this study has confirmed long standing hypotheses that the scaling of time-to-extinction with carrying capacity asymptotes under extreme environmental stochasticity (Leigh 1981; Lande 1993; Foley 1994). Moreover, the probability of such asymptotes occurring was highest in populations affected by land-use change (clear-felling) which decreases population growth rates and exposes populations to environmental stochasticity. The high proportion of populations showing asymptotic scaling of time-to-extinction with carrying capacity in clear-felled landscapes had a disproportionate impact on persistence of entire metapopulations. Specifically, reduced resilience of large populations, resulted in a more than 50 percent drop in persistence of entire metapopulations affected by asymptotic population size-persistence scaling, compared to those where populations showed predominately exponential scaling. Consequently even large populations were vulnerable to

environmental stochasticity, with their loss being catastrophic for metapopulation persistence.

Population size is the primary indicator of species extinction risk used by conservation practitioners worldwide prompting many managers to prescribe minimum viable population sizes as targets for conservation (IUCN 2001; Reed *et al.* 2003; Traill *et al.* 2010). The reduction in scaling of population persistence with carrying capacity with increasing extreme drought frequency observed herein, however, suggests minimum viable population size prescriptions may need re-evaluating under future climate and land-use change scenarios. In particular, the asymptotic scaling of persistence with carrying capacity observed in some populations means that increasing population sizes will yield diminishing returns on conservation outcomes as opposed to exponential returns currently observed (Lande 1993; IUCN 2001). In such cases, it may be more effective to implement actions that improve habitat stability, especially if such stability led to an exponential rise in time-to extinction with carrying capacity. Consequently, my results suggest climate changes could alter fundamental rules and practices governing conservation decisions.

Here I showed that asymptotic scaling relationships were more likely in the most variable environments, which in this case were controlled by gradients of land-use driven habitat size. Small, shallow habitats in clear-fell forests were the most exposed to extreme droughts during any given climate scenario, which decreased population resilience, relative to those populations in larger, deeper habitats. Such habitat size-mediated disturbance exposure is commonplace in both freshwater and terrestrial ecosystems, and often occurs in conjunction with habitat degradation (McHugh *et al.* 2010). In the terrestrial case, reduced survival in small habitats is often caused by disturbances which are harsher at patch edges (Fischer & Lindenmayer 2007). For example, populations within small forest fragments affected by clear-felling may be more exposed to stochastic wind events (Laurance & Curran 2008). Often such edge effects are linked with reduced forest patch sizes due to deforestation

(Bender *et al.* 1998; Fahrig 2002), which is analogous to the effect clear-felling had on pool size and depth in this study. In both cases, reduced patch/pool size brings populations closer to extinction thresholds. As My study shows, such extinction thresholds may occur due to changes in scaling of persistence with abundance, in addition to reductions in carrying capacity that habitat contraction can cause (Bender *et al.* 1998). Consequently, habitat size gradients may be particularly useful in identifying the most variable habitats and populations at most risk to rising frequency of extreme climate events.

Given that habitat variability is also a key ingredient for species coexistence, biodiversity and ecosystem function (Tews *et al.* 2004; Questad & Foster 2008; Tylianakis *et al.* 2008), managing habitat variability at landscape scales will likely need to consider the requirements of multiple species and their interactions. In freshwater ecosystems, maintaining spatially heterogenous disturbance patterns is a dogmatic conservation paradigm (Poff *et al.* 1997; Lytle & Poff 2004). In this case, increasing local habitat stability maybe necessary for maintaining sub-population persistence in the face of changing climates, however, I also showed this may not be necessary for entire landscapes. I found that metapopulations with the highest spatial heterogeneity in disturbance regimes (mature growth forests), were only marginally less persistence than metapopulations with highly stable, but spatially homogenous regimes (tornado). Metapopulation persistence was only substantially reduced by extreme droughts when more than 50 percent of the sub-populations showed asymptotic scaling of persistence with carrying capacity (clear-fell forests). Consequently, it is not necessary to prioritise disturbance regimes in whole landscapes for a single species, making it possible to maintain diversity in local environmental conditions within the landscape.

In metapopulations where fragmentation reduces population size and persistence, increasing inter-population connectivity can help maintain persistence at larger landscape scales (Fortuna *et al.* 2006; Heard *et al.* 2015). In this case the most connected

metapopulations had the highest probability of persistence under current climate, however they also showed the fastest rate of decline as extreme drought frequency increased. Positive effects of connectivity on metapopulation persistence are most likely if populations undergo asynchronous population dynamics, which decreases the likelihood of synchronised pool extinction (Abbott 2011; Duncan *et al.* 2015). Population asynchrony was unlikely in the system studied herein due to the regional nature in which droughts exposed all pools to the same disturbance events simultaneously. Although drought-specific population growth rates varied spatially between pools, shallow pools were consistently more likely to act as sinks during extreme and moderate droughts, making it unlikely that sources and sinks would swap roles over time. Thus increasing inter-pool connectivity would only have increased the rate at which shallow 'sink' pools leeched fish off deeper 'source' pools. Such an effect would increase as extreme droughts became more frequent thereby reducing metapopulation persistence. This may explain why fully connected metapopulations were the least resilient to climate change, and why metapopulations collapsed once a sufficient number of populations showed asymptotic scaling of persistence with carrying capacity. The effect of inter-pool connectivity is likely to be more important at larger spatial scales where sub-population dynamics are asynchronous owing to spatially heterogeneous weather patterns.

The effect of environmental stochasticity on extinction in populations of different size has been heavily debated over past decades (May 1973; Leigh 1981; Lande 1993), leading many authors to suggest the impacts of climate extremes may outweigh other global change drivers of species persistence (Katz & Brown 1992; Thompson *et al.* 2013; Kreyling *et al.* 2014). Here I found that the impacts due to increasing climate variability under global warming depended on existing land-use changes that exposed populations to extreme droughts. By increasing extreme drought exposure, forest clear-felling significantly reduced population resilience to elevated environmental stochasticity with global warming, even in

large populations that were typically the most robust. Moreover, lost persistence of large populations had a disproportionate impact on entire metapopulation persistence, highlighting the keystone role of large populations in maintaining landscape-scale resilience to rising environmental stochasticity. Consequently, maintaining high carrying capacity in large stable habitats may be the most effective tool for mitigating landscape scale impacts of global warming on populations.

Chapter Six:

General Discussion

Population management under land-use and climate change

Understanding the impacts of extreme climate events on population and community persistence has become increasingly viewed as a priority of climate change research in ecology (IPCC 2007; Ledger *et al.* 2013; Thompson *et al.* 2013; Woodward *et al.* In press). The period January-October 2016 saw the hottest global land and ocean temperatures on record, surpassing records set in immediate years prior (NOAA 2016). In fact, during the writing of this discussion, it was announced on December 13 that 2016 was set to be the warmest year on record in New Zealand (NIWA 2016). Thus it is becoming increasingly clear that the frequency of extreme climate events is rising, and making environments more variable for populations as a result, as has been predicted to result from global warming (IPCC 2007). My study is one of the first to quantify the influence of such increases in the frequency of extreme climate events combined with environmental stochasticity on populations dynamics under global warming. Overall, I showed that *Neochanna apoda* populations have remarkable resilience to increasing environmental variability, but that resilience was undermined by human activities that exposed the populations to extreme events. In particular, metapopulation persistence under the most extreme climate change scenario modelled in Chapter Five, dropped approximately thirty percent in clear-felled forests consisting of shallow, drought-prone pools. However, persistence was largely unaffected in tornado-disturbed and old growth forests consisting of deep, drought-resistant pools. Thus my results suggest that populations of vulnerable species, such as mudfish, may be able to tolerate increasing climate variability under global warming alone, but not in

combination with existing human pressures that push populations beyond the threshold of variability they can withstand.

That impacts of climate variability likely depend on existing human pressures has important implications for population and ecosystem management under climate change. Environmental variability is frequently influenced by human activities (Dudgeon *et al.* 2006; Fischer & Lindenmayer 2007; Laurance & Curran 2008). In freshwater ecosystems, human water abstraction for irrigation purposes alters the natural hydrology in rivers and wetlands, which in many cases, makes environments more drought prone and variable (Dudgeon *et al.* 2006; Vörösmarty *et al.* 2010). My results suggest such actions will undermine population resilience to increasing extreme climate event frequency under climate change. In fact, the persistence of populations affected by land-use in this study was significantly reduced by even the smallest increases in extreme drought frequency under climate change (Fig. 5.3c), but remained relatively unchanged in populations unaffected by clear-felling (Fig. 5.3a,b). Without such additional human pressures, my results suggest many populations could endure increases in extreme climate frequency with global warming. However, human water demand is only likely to increase as human populations grow, droughts increase in frequency and water becomes increasingly scarce (Vörösmarty *et al.* 2010). Thus the interactive effect of land-use and climate change on population persistence reported here-in, is likely to intensify in the future.

Land-use impacts in this study were generally linked to gradients of habitat size. Small, shallow habitats in clear-felled forests were most exposed to extreme droughts during any given climate scenario, which decreased population resilience relative to those populations in larger, deeper habitats. Such habitat size-mediated disturbance exposure is commonplace in both freshwater and terrestrial ecosystems, and often occurs in conjunction with habitat degradation (Fischer & Lindenmayer 2007; Bond *et al.* 2008; McHugh *et al.*

2010). In the terrestrial case, reduced survival in small habitats is often caused by disturbances which are harsher at patch edges (Fischer & Lindenmayer 2007). For example, populations within small forest fragments affected by clear-felling may be more exposed to stochastic wind events (Laurance & Curran 2008). Often such edge effects are linked with reduced forest patch sizes due to deforestation (Bender *et al.* 1998; Fahrig 2002), which is analogous to the effect clear-felling had on pool size and depth in this study. In both cases, reduced patch/pool size brings populations closer to extinction thresholds, and as my study shows, can undermine resilience to increasing extreme climate frequency under global warming. Consequently, focussing on habitat size gradients may be particularly useful in identifying the most variable habitats and populations at most risk to rising frequency of extreme climate events.

Effects of climate and land-use change on the scaling of time-to-extinction with carrying capacity

My study shows that population vulnerability to climate change was strongly tied to changes in population size-based extinction thresholds which were altered by extreme event frequency and land-use. The concept of minimum viable population sizes has long been central to conservation science due to the exponential rise in population persistence as carrying capacity increases (Lande *et al.* 2003). The International Union for Conservation of Nature (IUCN) criteria of extinction risk used worldwide categorises species endangerment as either: 'critical', 'endangered' or 'vulnerable' if global populations are smaller than 250, 2500 or 10000 individuals, respectively (IUCN 2001). However, the IUCN criteria also acknowledge that increases in environmental stochasticity can flatten slopes of the scaling of time-to-extinction with carrying capacity as shown in theoretical models (Leigh 1981; Lande

1993; Foley 1994) (Fig. 1.1), and thus advise extinction risk downgrades for larger populations if they additionally show extreme variability (IUCN 2001). However, it is generally unknown if population variability observed in real populations is sufficient to warrant such treatment, due to the logistical difficulty and uncertainty in quantifying population dynamics of wild populations (Lande *et al.* 2003). In practice, this means that the effects of environmental stochasticity on the scaling of time-to-extinction with carrying capacity generates vast uncertainty in minimum viable population size estimates.

I quantified the influence of environmental stochasticity on the scaling of time-to-extinction with carrying capacity using empirical estimates of demography from real populations of *N. apoda* (Chapter Three). I showed that the scaling of time-to-extinction with carrying capacity was surprisingly insensitive to environmental stochasticity under current climate conditions, but was very sensitive as climate variability increased under global warming scenarios. In particular, all populations showed exponential scaling of time-to-extinction with carrying capacity under current climate conditions, even in populations experiencing drying up to 19 times in a year, for periods of up to 44 days. However, the relationships varied between exponential and asymptotic scaling as extreme climate frequency increased under global warming scenarios. Consequently, this study confirmed long-held theoretical assumptions implicit in population size-based IUCN extinction risk criteria (IUCN 2001). Moreover, the greater variability in scaling relationships under climate change implies that the applicability of such population size-based extinction criteria used world-wide will be subject to increasing uncertainty under future climates.

That the scaling of time-to-extinction with carrying capacity for brown mudfish was relatively insensitive to pool drying under current climate conditions (Chapter Four) was surprising given how often the pools currently dry. Under current climate, all populations showed exponential scaling (Chapter Four), even in shallow, drought-prone pools in clear-fell

forests (Chapter Five). Although, populations in shallow clear-fell pools transitioned to asymptotic scaling with only modest increases in extreme drought frequency (Chapter Five), populations in deeper tornado and old growth forest retained exponential scaling on average. The high population stability in the face of high environmental variability we observed is very likely a product of life-history and physiological adaptations, such as cutaneous respiration and burrowing (Urbina *et al.* 2014), which reduces the effects of environmental extremes on birth and death rates in similar emersion-tolerant species (Brauner *et al.* 2004). Importantly, this indicates that even extremely variable environments may be insufficient to substantially alter the scaling of time-to-extinction with carrying capacity, provided species are well adapted to disturbances. Thus, asymptotic scaling of time-to-extinction with carrying capacity may be most likely in populations experiencing novel levels of environmental variability to which they are not adapted to.

Implications for the conservation of Neochanna sp. *under global warming*

New Zealand is projected to experience increases in extreme drought frequency (defined as a one-in-twenty year drought) from no change, through to 88 percent increase (i.e. a one-in-twenty year drought will increase to occuring every two to three years), depending on location and climate change scenario (Mullan *et al.* 2005; Clarke *et al.* 2011). Although the mudfish populations in this study were located in an area of New Zealand where drought frequency is expected to change very little (South Westland) (Mullan *et al.* 2005; Clarke *et al.* 2011), my results suggest population extinctions under global warming are strongly elevated by clear-felling of podocarp-swamp-forests, which reduces habitat size. Approximately 30-50 percent of indigenous podocarp forest cover, much of which was podocarp-swamp-forest has been lost to clear-felling in South Westland, and only a minor proportion of that has been allowed to regenerate into the type of regenerating clear-fell that

populations in this study were measured in (Ewers *et al.* 2006). My results indicate that even a small increase in drought frequency could cause population extinctions in such habitats. Moreover, the brown mudfish, like most other *Neochanna* species, have populations in areas where change in drought frequency is likely to be highest, including south-east North Island (Eldon 1978), where deforestation has also been the most extensive since European arrival (70-100 percent) (Ewers *et al.* 2006). Consequently, while climate change is unlikely to cause complete *N. apoda* species extinction, sub-population extirpations are increasingly likely if drought frequencies rise as projected under global warming.

The importance of podocarp-swamp-forests and the habitat structure within, such as those investigated here-in for brown mudfish, are unknown for *Neochanna* populations beyond this study. *Neochanna sp.*, including brown mudfish, are found within a large range of habitat types, including roadside ditches, small streams, open pakihi bogs, large open wetland complexes, and swamp-forests consisting of introduced willow, which are often more spatially continuous, with less well-defined sub-populations compared to the patchy array of pools formed by fallen trees in podocarp-swamp-forests I studied (Eldon 1968, 1978; Eldon 1979; Eldon 1992; Hicks & Barrier 1996; Harding *et al.* 2007; O'Brien 2007; O'Brien & Dunn 2007). Nevertheless, this study has highlighted key habitat characteristics important for *Neochanna* population persistence which may be generally applicable across a range of habitats. In particular, we found that deep pools were vital for *N. apoda* survival and population persistence during droughts, simply because deep pools were more permanent, which improved mudfish survival during droughts. It is likely that deep habitats are important for other populations and species of *Neochanna* despite the huge range of habitat types they are found in, simply because such habitats are resistant to drying.

The importance of deep environments to improve survival during droughts presents a paradox for management of *Neochanna* populations under climate change, however. All

Neochanna sp. are well known to be easily extirpated by predators and competitors and rarely coexist with other fish species (Ling & Willis 2005; O'Brien 2005; O'Brien & Dunn 2007; White *et al.* 2015a). The brown mudfish in particular, show a strong allopatric distribution with banded kokopu (*Galaxias fasciatus*) in the study forest I investigated, controlled by pool permanence (White *et al.* 2015a). Drought prone pools favour mudfish presence because banded kokopu are extirpated by drought. Conversely, in permanent habitats, banded kokopu are thought to extirpate mudfish via competition or predation (White *et al.* 2015a). My work in this thesis shows that mudfish populations currently persist within such shallow drought-prone pools under current climate, but may not if drought frequency increases under climate change. Consequently, using drought-prone habitats as refugia from predators is unlikely to be a successful strategy for mudfish under climate change as it has been in the past. Under climate change, mudfish persistence will therefore be determined by the presence of deep, permanent pools that are also inaccessible to predators. In this manner, the role of large falling trees is vital since they are the major mechanism of deep permanent pool creation that are sufficiently distant from rivers, which are the most likely source of predators. The only other deep pools I encountered were within river floodplains which were created via flood scour and contained predatory kokopu (White *et al.* 2015a). These pools contained some mudfish adults, but rarely any juveniles, possibly due to kokopu predation or occasionally high river flows, indicating low overall mudfish recruitment in these pools. Consequently, in cases of clear-felled forests, human intervention may be necessary to create permanent deep, but isolated pools in the absence of large falling trees. Such habitats allow mudfish to exist without predation or drought impacts and achieve maximum population growth rates which I found was essential for their persistence under global warming.

My research also indicates that the presence of such deep, isolated environments may not need to be spatially dense in order to ensure landscape scale metapopulation persistence

under global warming. My metapopulation analyses showed little difference in metapopulation persistence under global warming between tornado and old growth forests, despite there being substantial differences in the abundance of deep pools within these metapopulations. Tornado metapopulations almost entirely consisted of deep permanent pools due to the catastrophic effects of the tornado on tree-fall in those areas, while mean pool depths in old-growth forests were not much deeper than in clear-fell forests (Chapter 5, Fig. 5.2). The metapopulation model indicated that sub-population persistence declined rapidly below approximately 0.2-0.22 m deep (Fig. 4.1d). While there were several pools this deep in all old-growth forest metapopulations, very few existed in clear-fell forests (Fig. 5.2). The loss of only a few deep permanent pools was catastrophic for clear-fell metapopulations undergoing increases in extreme drought frequency under climate change. In-fact, metapopulation persistence appeared to decline once approximately 50 percent of the sub-populations showed asymptotic scaling of time-to-extinction with carrying capacity (Fig. 5.5). Consequently, these results imply that only 50 percent of pools (approximately 4-6 pools per 2 km^2) need to be deeper than 0.2-0.22 m to ensure landscape scale persistence under global warming.

My research also provides additional implications for how *Neochanna* populations should be monitored, particularly if the goal is to detect population decline in response to global warming. The most practical method for measuring population dynamics in mudfish, and many other lentic dwelling species, is to use catch-per-unit-effort (CPUE) (Ling *et al.* 2009). Such methods do not account for variation in capture probability which can confound population dynamics trends over time and space (Lebreton *et al.* 1992; Pine *et al.* 2003). My study showed positive effects of temperature, rainfall, and pool depth on capture probability which could confound trends in population dynamics as climates change due to global warming. Accounting for these relationships was essential in this study to isolate the effect of

climate on population vital rates, which was possible due to individual capture histories of marked fish, but not in CPUE assessments. Conducting CPUE measurements in similar conditions at the same time of year will help reduce the temporal error in CPUE generated by climate driven capture probability. In particular, conducting annual CPUE surveys during the warm January to March months, and wet conditions (>10 mm $24h^{-1}$), in deep pools, will maximise capture probability, and increase the accuracy of CPUE as a true approximation of population abundance in *N. apoda*. Nevertheless, such CPUE measures may still be confounded by long-term changes in climate and should be interpreted with caution in such contexts.

Conclusions

Overall, my results show that populations are capable of persisting despite the increases in frequency and magnitude of extreme climate events that are expected from global warming. My results show that populations can tolerate the increased variability associated with extreme events under global warming, but not when environmental variability is additionally increased by other stressors. The key is to minimise existing environmental variability to ensure high, stable population growth rates, which, in the case of brown mudfish, can be done by improvements to habitat size. Such improvements will need to consider the needs of multiple interacting species. However, my results show that landscape scale metapopulations persistence during climate change can accommodate spatial variability in environmental conditions and thus biodiversity, and that it is not necessary to devote entire landscapes to single species. These conditions are unlikely to be met for many populations, whose population growth rates are depressed and more variable due to existing stressors caused by land-use change and human resource demand. It is fortunate that there are some remaining remnants of suitable habitats (such as forest areas studied in this thesis), that should ensure

brown mudfish continuing persistence, at least for the next 90 years of climate change. However, the outlook maybe less favourable for other species whose entire range coincides within degraded environments and where the greatest changes in climate are expected, for example, Canterbury mudfish, *Neochanna burrowsius* (O'Brien 2005; O'Brien & Dunn 2007). In general, my thesis suggests that many populations, and species of freshwater fish will only persist through the effects of climate variability under global warming if human resource demand, for water in particular, is carefully managed to ensure sustainable, stable population growth rates.

References

Abbott, K.C. (2011). A dispersal-induced paradox: Synchrony and stability in stochastic metapopulations. *Ecol. Lett.*, 14, 1158-1169.

Acuña, V., Muñoz, I., Giorgi, A., Omella, M., Sabater, F. & Sabater, S. (2005). Drought and postdrought recovery cycles in an intermittent Mediterranean stream: structural and functional aspects. *J. North. Am. Benthol. Soc.*, 24, 919-933.

Adams, J.A. & Norton, D.A. (1991). Soil and vegetation characteristics of some tree windthrow features in a South Westland rimu forest. *J. R. Soc. N. Z.*, 21, 33-42.

Akcakaya, H.R. (2005). *RAMAS Metapop: viability analysis for stage-structured metapopulations. Version 6.* Applied Biomathematics, Setauket, New York, USA.

Akçakaya, H.R. (1991). A method for simulating demographic stochasticity. *Ecol. Model.*, 54, 133-136.

Akçakaya, H.R., Burgman, M.A., Kindvall, O., Wood, C.C., Sjogren-Gulve, P., Hatfield, J.S. *et al.* (2004). *Species conservation and management: case studies*. Oxford University Press, New York.

Allibone, R., David, B., Hitchmough, R., Jellyman, D., Ling, N., Ravenscroft, P. *et al.* (2010). Conservation status of New Zealand freshwater fish, 2009. *N. Z. J. Mar. Freshw. Res.*, 44, 271-287.

Bender, D.J., Contreras, T.A. & Fahrig, L. (1998). Habitat loss and population decline: A meta-analysis of the patch size effect. *Ecology*, 79, 517-533.

Beukema, J.J. (1970). Acquired hook-avoidance in the pike *Esox lucius* L. fished with artificial and natural baits. *J. Fish Biol.*, 2, 155-160.

Beukema, J.J. & de Vos, G.J. (1974). Experimental tests of a basic assumption of the capture-recapture method in pond populations of carp *Cyprinus carpio* L. *J. Fish Biol.*, 6, 317-329.

Blackham, M. (2013). Dust bowled. *Water and Atmosphere*, 8, 12-20.

Boersma, K.S., Bogan, M.T., Henrichs, B.A. & Lytle, D.A. (2014). Invertebrate assemblages of pools in arid-land streams have high functional redundancy and are resistant to severe drying. *Freshw. Biol.*, 59, 491-501.

Bond, N.R., Balcombe, S.R., Crook, D.A., Marshall, J.C., Menke, N. & Lobegeiger, J.S. (2015). Fish population persistence in hydrologically variable landscapes. *Ecol. Appl.*, 25, 901-913.

Bond, N.R., Lake, P.S. & Arthington, A.H. (2008). The impacts of drought on freshwater ecosystems: an Australian perspective. *Hydrobiologia*, 600, 3-16.

Boulton, A.J. (2003). Parallels and contrasts in the effects of drought on stream macroinvertebrate assemblages. *Freshw. Biol.*, 48, 1173-1185.

Brauner, C.J., Matey, V., Wilson, J.M., Bernier, N.J. & Val, A.L. (2004). Transition in organ function during the evolution of air-breathing; insights from *Arapaima gigas*, an obligate air-breathing teleost from the Amazon. *J. Exp. Biol.*, 207, 1433-1438.

Bremset, G. (2000). Seasonal and diel changes in behaviour, microhabitat use and preferences by young pool-dwelling Atlantic salmon, *Salmo salar*, and brown trout, *Salmo trutta*. *Environ. Biol. Fishes*, 59, 163-179.

Brinson, M.M. & Malvárez, A.I. (2002). Temperate freshwater wetlands: types, status, and threats. *Environ. Conserv.*, 29, 115-133.

Brown, J.H., Gillooly, J.F., Allen, A.P., Savage, V.M. & West, G.B. (2004). Toward a metabolic theory of ecology. *Ecology*, 85, 1771-1789.

Burnham, K.P. & Anderson, D.R. (2002). *Model Selection and Multimodel Inference: A Practical Information-Theoretic Approach.* 2nd edn. Springer-Verlag Inc, New York.

Carlson, S.M., Olsen, E.M. & Vøllestad, L.A. (2008). Seasonal mortality and the effect of body size: a review and an empirical test using individual data on brown trout. *Funct. Ecol.*, 22, 663-673.

Caswell, H. (1989). *Matrix population models: construction, analysis, and interpretation*. Sinauer Associates.

Chew, S.F., Chan, N.K.Y., Loong, A.M., Hiong, K.C., Tam, W.L. & Ip, Y.K. (2004). Nitrogen metabolism in the African lungfish (*Protopterus dolloi*) aestivating in a mucus cocoon on land. *J. Exp. Biol.*, 207, 777-786.

Choquet, R., Lebreton, J.-D., Gimenez, O., Reboulet, A.-M. & Pradel, R. (2009). U-CARE: Utilities for performing goodness of fit tests and manipulating CApture—REcapture data. *Ecography*, 32, 1071-1074.

Christensen, M.R., Graham, M.D., Vinebrooke, R.D., Findlay, D.L., Paterson, M.J. & Turner, M.A. (2006). Multiple anthropogenic stressors cause ecological surprises in boreal lakes. *Glob. Change Biol.*, 12, 2316-2322.

Clarke, A., Mullan, B. & Porteous, A. (2011). *Scenarios for regional drought under climate change*. NIWA, Wellington, New Zealand.

Cormack, R.M. (1964). Estimates of survival from the sighting of marked animals. *Biometrika*, 51, 429-438.

Covich, A.P., Crowl, T.A. & Scatena, F.N. (2003). Effects of extreme low flows on freshwater shrimps in a perennial tropical stream. *Freshw. Biol.*, 48, 1199-1206.

Crawley, M.J. (2005). *Statistics: An Introduction Using R*. John Wiley & Sons, Inc, Chichester, West Sussex.

Crecco, V. & Overholtz, W.J. (1990). Causes of density-dependent catchability for Georges Bank haddock *Melanogrammus aeglefinus*. *Can. J. Fish. Aquat. Sci.*, 47, 385-394.

Cullen, L.E., Duncan, R.P., Wells, A. & Stewart, G.H. (2003). Floodplain and regional scale variation in earthquake effects on forests, Westland, New Zealand. *J. R. Soc. N. Z.*, 33, 693-701.

Desharnais, R.A., Costantino, R.F., Cushing, J.M., Henson, S.M., Dennis, B. & King, A.A. (2006). Experimental support of the scaling rule for demographic stochasticity. *Ecol. Lett.*, 9, 537-547.

Dewson, Z.S., James, A.B.W. & Death, R.G. (2007). Invertebrate responses to short-term water abstraction in small New Zealand streams. *Freshw. Biol.*, 52, 357-369.

Didham, R.K., Tylianakis, J.M., Gemmell, N.J., Rand, T.A. & Ewers, R.M. (2007). Interactive effects of habitat modification and species invasion on native species decline. *Trends in Ecology and Evolution*, 22, 489-496.

Drake, J.M. & Griffen, B.D. (2010). Early warning signals of extinction in deteriorating environments. *Nature*, 467, 456-459.

Dudgeon, D., Arthington, A.H., Gessner, M.O., Kawabata, Z.-I., Knowler, D.J., Lévêque, C. *et al.* (2006). Freshwater biodiversity: Importance, threats, status and conservation challenges. *Biological Reviews*, 81, 163-182.

Duncan, A.B., Gonzalez, A. & Kaltz, O. (2015). Dispersal, environmental forcing, and parasites combine to affect metapopulation synchrony and stability. *Ecology*, 96, 284-290.

Eldon, G.A. (1968). Notes on the presence of the brown mudfish (*Neochanna apoda* Günther) on the West Coast of the South Island of New Zealand. *N. Z. J. Mar. Freshw. Res.*, 2, 37-48.

Eldon, G.A. (1978). The Life History of *Neochanna apoda* Günther (Pisces: Galaxiidae). *Fisheries Research Bulletin* 19.

Eldon, G.A. (1979). Habitat and interspecific relationships of the Canterbury mudfish,Neochanna burrowsius(Salmoniformes: Galaxiidae). *N. Z. J. Mar. Freshw. Res.*, 13, 111-119.

Eldon, T. (1992). The difficulties of capturing mudfish. *Freshwater Catch*, 48, 16-17.

Erisman, B.E., Allen, L.G., Claisse, J.T., Pondella, D.J., Miller, E.F. & Murray, J.H. (2011). The illusion of plenty: Hyperstability masks collapses in two recreational fisheries that target fish spawning aggregations. *Can. J. Fish. Aquat. Sci.*, 68, 1705-1716.

Ewers, R.M., Kliskey, A.D., Walker, S., Rutledge, D., Harding, J.S. & Didham, R.K. (2006). Past and future trajectories of forest loss in New Zealand. *Biol. Conserv.*, 133, 312-325.

Fahrig, L. (2002). Effect of habitat fragmentation on the extinction threshold: A synthesis. *Ecol. Appl.*, 12, 346-353.

Finstad, A.G., Næsje, T.F. & Forseth, T. (2004). Seasonal variation in the thermal performance of juvenile Atlantic salmon (*Salmo salar*). *Freshw. Biol.*, 49, 1459-1467.

Fischer, J. & Lindenmayer, D.B. (2007). Landscape modification and habitat fragmentation: A synthesis. *Glob. Ecol. Biogeogr.*, 16, 265-280.

Foin Jr, T.C. & Stiven, A.E. (1970). The relationship of environment size and population parameters of *Oxytrema proxima* (say) (Gastropoda: Pleuroceridae). *Oecologia*, 5, 74-84.

Foley, P. (1994). Predicting extinction times from environmental stochasticity and carrying capacity. *Conserv. Biol.*, 8, 124-137.

Fortuna, M.A., Gómez-Rodríguez, C. & Bascompte, J. (2006). Spatial network structure and amphibian persistence in stochastic environments. *P. Roy. Soc. B-Biol. Sci.*, 273, 1429-1434.

Fraser, N.H.C., Metcalfe, N.B. & Thorpe, J.E. (1993). Temperature-dependent switch between diurnal and nocturnal foraging in salmon. *P. Roy. Soc. B-Biol. Sci.*, 252, 135-139.

Freeman, M.C., Bowen, Z.H., Bovee, K.D. & Irwin, E.R. (2001). Flow and habitat effects on juvenile fish abundance in natural and altered flow regimes. *Ecol. Appl.*, 11, 179-190.

Goodman, J.M., Dunn, N.R., Ravenscroft, P.J., Allibone, R.M., Boubee, J.A.T., David, B.O. *et al.* (2014). Conservation status of New Zealand freshwater fish, 2013. Department of Conservation Wellington, pp. 1-16.

Gordoa, A., Masó, M. & Voges, L. (2000). Monthly variability in the catchability of Namibian hake and its relationship with environmental seasonality. *Fish Res.*, 48, 185-195.

Gordon, A., Wintle, B.A., Bekessy, S.A., Pearce, J.L., Venier, L.A. & Wilson, J.N. (2012). The use of dynamic landscape metapopulation models for forest management: A case study of the red-backed salamander. *Can. J. For. Res.*, 42, 1091-1106.

Graham, W.D., Thorpe, J.E. & Metcalfe, N.B. (1996). Seasonal current holding performance of juvenile Atlantic salmon in relation to temperature and smolting. *Can. J. Fish. Aquat. Sci.*, 53, 80-86.

Grantham, T.E., Newburn, D.A., McCarthy, M.A. & Merenlender, A.M. (2012). The role of streamflow and land use in limiting oversummer survival of juvenile steelhead in california streams. *Trans. Am. Fish. Soc.*, 141, 585-598.

Griffen, B.D. & Drake, J.M. (2008). Effects of habitat quality and size on extinction in experimental populations. *P. Roy. Soc. B-Biol. Sci.*, 275, 2251-2256.

Griffith, J.S. & Smith, R.W. (1993). Use of winter concealment cover by juvenile cutthroat and brown trout in the South Fork of the Snake River, Idaho. *N. Am. J. Fish. Manag.*, 13, 823-830.

Gupta, H.V., Sorooshian, S. & Yapo, P.O. (1999). Status of automatic calibration for hydrologic models: Comparison with multilevel expert calibration. *Journal of Hydrologic Engineering*, 4, 135-143.

Hanski, I. (1999). *Metapopulation Ecology*. OUP Oxford.

Harding, J.S., Norton, D.A. & McIntosh, A.R. (2007). Persistence of a significant population of rare Canterbury mudfish (Neochanna burrowsius) in a hydrologically isolated catchment. *N. Z. J. Mar. Freshw. Res.*, 41, 309-316.

Heard, G.W., Thomas, C.D., Hodgson, J.A., Scroggie, M.P., Ramsey, D.S.L. & Clemann, N. (2015). Refugia and connectivity sustain amphibian metapopulations afflicted by disease. *Ecol. Lett.*, 18, 853-863.

Hicks, B.J. & Barrier, R.F.G. (1996). Habitat requirements of black mudfish (*Neochanna diversus*) in the Waikato region, North Island, New Zealand. *N. Z. J. Mar. Freshw. Res.*, 30, 135-151.

Hokit, D.G. & Branch, L.C. (2003). Associations between patch area and vital rates: Consequences for local and regional populations. *Ecol. Appl.*, 13, 1060-1068.

IPCC (2007). *Climate Change 2007: Impacts, Adaptation and Vulnerability. Contribution of Working Group II to the Fourth Assessment Report of the Intergovernmental Panel on Climate Change.* Cambridge University Press, Cambridge, UK.

IUCN (2001). *IUCN Red List categories and criteria, version 3.1, second edition*. International Union for Conservation of Nature, Gland, Switzerland and Cambridge, UK.

James, I.L. (1987). Silvicultural management of the rimu forests of south Westland. *Forest Research Institute Bulletin* 121, 1-33.

Jolly, G.M. (1965). Explicit estimates from capture-recapture data with both death and immigration-stochastic model. *Biometrika*, 52, 225-247.

Katz, R.A. & Freeman, M.C. (2015). Evidence of population resistance to extreme low flows in a fluvial-dependent fish species. *Can. J. Fish. Aquat. Sci.*, 72, 1776-1787.

Katz, R.W. & Brown, B.G. (1992). Extreme events in a changing climate: Variability is more important than averages. *Clim. Change*, 21, 289-302.

Kitching, R. (1971). A simple simulation model of dispersal of animals among units of discrete habitats. *Oecologia*, 7, 95-116.

Klefoth, T., Pieterek, T. & Arlinghaus, R. (2013). Impacts of domestication on angling vulnerability of common carp, *Cyprinus carpio*: The role of learning, foraging behaviour and food preferences. *Fish. Manag. Ecol.*, 20, 174-186.

Kreyling, J., Jentsch, A. & Beier, C. (2014). Beyond realism in climate change experiments: gradient approaches identify thresholds and tipping points. *Ecol. Lett.*, 17, 125-e121.

Kuparinen, A., Klefoth, T. & Arlinghaus, R. (2010). Abiotic and fishing-related correlates of angling catch rates in pike (*Esox lucius*). *Fish Res.*, 105, 111-117.

Lake, P.S. (2003). Ecological effects of perturbation by drought in flowing waters. *Freshw. Biol.*, 48, 1161-1172.

Lake, S.P. (2011). *Drought and Aquatic Ecosystems: Effects and Responses*. Wiley-Blackwell, Oxford, UK.

Lande, R. (1993). Risks of population extinction from demographic and environmental stochasticity and random catastrophes. *Am. Nat.*, 142, 911-927.

Lande, R., Engen, S. & Sæther, B.E. (2003). *Stochastic Population Dynamics in Ecology and Conservation*. Oxford University Press.

Laurance, W.F. & Curran, T.J. (2008). Impacts of wind disturbance on fragmented tropical forests: A review and synthesis. *Austral. Ecol.*, 33, 399-408.

Lebreton, J.D., Burnham, K.P., Clobert, J. & Anderson, D.R. (1992). Modeling survival and testing biological hypotheses using marked animals: a unified approach with case studies. *Ecol. Monogr.*, 62, 67-118.

Ledger, M.E., Brown, L.E., Edwards, F.K., Milner, A.M. & Woodward, G. (2013). Drought alters the structure and functioning of complex food webs. *Nature Clim. Change*, 3, 223-227.

Leigh, E.G. (1981). The average lifetime of a population in a varying environment. *J. Theor. Biol.*, 90, 213-239.

Levins, R. (1969). Some Demographic and Genetic Consequences of Environmental Heterogeneity for Biological Control1. *Bull. Entomol. Soc. Am.*, 15, 237-240.

Lima, M. & Naya, D.E. (2011). Large-scale climatic variability affects the dynamics of tropical skipjack tuna in the Western Pacific Ocean. *Ecography*, 34, 597-605.

Ling, N., O'Brien, L.K., Miller, R. & Lake, M. (2009). Methodology to survey and monitor New Zealand mudfish species. In: *CBER Contract Report 104.* Department of Conservation and University of Waikato Hamilton, p. 60

Ling, N. & Willis, K. (2005). Impacts of mosquitofish, *Gambusia affinis*, on black mudfish, *Neochanna diversus*. *N. Z. J. Mar. Freshw. Res.*, 39, 1215-1223.

Lytle, D.A. & Poff, N.L. (2004). Adaptation to natural flow regimes. *Trends in Ecology and Evolution*, 19, 94-100.

May, R.M.C. (1973). *Stability and Complexity in Model Ecosystems*. Princeton University Press.

McDowall, R. (2006). Crying wolf, crying foul, or crying shame: alien salmonids and a biodiversity crisis in the southern cool-temperate galaxioid fishes? *Rev. Fish Biol. Fish.*, 16, 233-422.

McHugh, P.A., McIntosh, A.R. & Jellyman, P.G. (2010). Dual influences of ecosystem size and disturbance on food chain length in streams. *Ecol. Lett.*, 13, 881-890.

McHugh, P.A., Thompson, R.M., Greig, H.S., Warburton, H.J. & McIntosh, A.R. (2015). Habitat size influences food web structure in drying streams. *Ecography*, 38, 700-712.

Melbourne, B.A. & Hastings, A. (2008). Extinction risk depends strongly on factors contributing to stochasticity. *Nature*, 454, 100-103.

Mitro, M.G. & Zale, A.V. (2002). Seasonal survival, movement, and habitat use of age-0 rainbow trout in the Henrys Fork of the Snake River, Idaho. *Trans. Am. Fish. Soc.*, 131, 271-286.

Mullan, B., Porteous, A., Wratt, D. & Hollis, M. (2005). *Changes in drought risk with climate change*. NIWA, Wellington, New Zealand.

Nilsson, C., Reidy, C.A., Dynesius, M. & Revenga, C. (2005). Fragmentation and flow regulation of the world's large river systems. *Science*, 308, 405-408.

NIWA (2016). National Institute of Water and Atmospheric Research: Online media release. Available at: https://niwa.co.nz/news/2016-set-to-become-new-zealand%E2%80%99s-warmest-on-record Last accessed 13/12/16.

NOAA (2016). National centers for environmental information. State of the climate: Global analysis for October 2016. Available at: http://www.ncdc.noaa.gov/sotc/global/201610 Last accessed 12/12/2016.

O'Brien, L.K. (2005). Conservation ecology of Canterbury mudfish (*Neochanna burrowsius*). *Unpublished PhD thesis, University of Canterbury, Christchurch, New Zealand*.

O'Brien, L.K. (2007). Size-dependant strategies in response to drought by *Neochanna burrowsius*. *N. Z. Nat. Sci.*, 32, 21 - 28.

O'Brien, L.K. & Dunn, N.R. (2007). Mudfish (*Neochanna* Galaxiidae) literature review. *Science for Conservation*, 277, 1-90.

Oliver, T.H., Brereton, T. & Roy, D.B. (2013). Population resilience to an extreme drought is influenced by habitat area and fragmentation in the local landscape. *Ecography*, 36, 579-586.

Ortega-Garcia, S., Ponce-Diaz, G., O'Hara, R. & Merilä, J. (2008). The relative importance of lunar phase and environmental conditions on striped marlin (*Tetrapturus audax*) catches in sport fishing. *Fish Res.*, 93, 190-194.

Ovaskainen, O. & Meerson, B. (2010). Stochastic models of population extinction. *Trends in Ecology and Evolution*, 25, 643-652.

Paradiso, S., Andreasen, N.C., O'Leary, D.S., Arndt, S. & Robinson, R.G. (1997). Cerebellar size and cognition: Correlations with IQ, verbal memory and motor dexterity. *Neuropsy. Neuropsy. BE.*, 10, 1-8.

Pine, W.E., Pollock, K.H., Hightower, J.E., Kwak, T.J. & Rice, J.A. (2003). A review of tagging methods for estimating fish population size and components of mortality. *Fisheries*, 28, 10-23.

Poff, N.L., Allan, J.D., Bain, M.B., Karr, J.R., Prestegaard, K.L., Richter, B.D. *et al.* (1997). The natural flow regime: A paradigm for river conservation and restoration. *Bioscience*, 47, 769-784.

Pradel, R. (1993). Flexibility in survival analysis from recapture data: handling trap dependence. In: *Marked Individuals in the Study of Bird Population* (eds. Lebreton, JD & North, PM). Birkhäuser Velag Basel, pp. 29-37.

Pradel, R., Gimenez, O. & Lebreton, J.D. (2005). Principles and interest of GOF tests for multistate capture-recapture models. *Anim. Biodivers. Conserv.*, 28, 189-204.

Pradel, R., Hines, J.E., Lebreton, J.-D. & Nichols, J.D. (1997). Capture-recapture survival models taking account of transients. *Biometrics*, 53, 60-72.

Pradel, R. & Sanz-Aguilar, A. (2012). Modeling trap-awareness and related phenomena in capture-recapture studies. *PLoS ONE*, 7, 1-4.

Questad, E.J. & Foster, B.L. (2008). Coexistence through spatio-temporal heterogeneity and species sorting in grassland plant communities. *Ecol. Lett.*, 11, 717-726.

Reed, D.H., O'Grady, J.J., Brook, B.W., Ballou, J.D. & Frankham, R. (2003). Estimates of minimum viable population sizes for vertebrates and factors influencing those estimates. *Biol. Conserv.*, 113, 23-34.

Renwick, J., Anderson, B., Greenaway, A., King, D.N., Mikaloff-Fletcher, S., Reisinger, A. *et al.* (2016). Climate change implications for New Zealand. *Royal Society of New Zealand Emerging Issues*, 1-72.

Ricker, W.E. (1975). Computation and interpretation of biological statistics of fish populations. *Fisheries Research Board of Canada Bulletin*, 191.

Sabo, J.L., Finlay, J.C. & Post, D.M. (2009). Food chains in freshwaters. In: *Ann. N. Y. Acad. Sci.*, pp. 187-220.

Scheffers, B.R., De Meester, L., Bridge, T.C.L., Hoffmann, A.A., Pandolfi, J.M., Corlett, R.T. *et al.* (2016). The broad footprint of climate change from genes to biomes to people. *Science*, 354.

Schwarz, C.J. & Arnason, A.N. (1996). A general methodology for the analysis of capture-recapture experiments in open populations. *Biometrics*, 52, 860-873.

Scrimgeour, G.J., Davidson, R.J. & Davidson, J.M. (1988). Recovery of benthic macroinvertebrate and epilithic communities following a large flood, in an unstable, Braided, New Zealand River. *N. Z. J. Mar. Freshw. Res.*, 22, 337-344.

Seber, G.A.F. (1965). A note on the multiple-recapture census. *Biometrika*, 52, 249-259.

Shaffer, M. (1987). Minimum viable populations: coping with uncertainty. In: *Viable populations for conservation* (ed. Soule, ME). Cambridge University Press New York, pp. 69-86.

Smol, J.P. & Douglas, M.S.V. (2007). Crossing the final ecological threshold in high Arctic ponds. *Proc. Natl. Acad. Sci. U. S. A.*, 104, 12395-12397.

Takimoto, G. & Post, D.M. (2013). Environmental determinants of food-chain length: A meta-analysis. *Ecol. Res.*, 28, 675-681.

Taylor, C.M., Winston, M.R. & Matthews, W.J. (1996). Temporal variation in tributary and mainstem fish assemblages in a great plains stream system. *Copeia*, 280-289.

Tews, J., Brose, U., Grimm, V., Tielbörger, K., Wichmann, M.C., Schwager, M. *et al.* (2004). Animal species diversity driven by habitat heterogeneity/diversity: The importance of keystone structures. *J. Biogeogr.*, 31, 79-92.

Thompson, R.M., Beardall, J., Beringer, J., Grace, M. & Sardina, P. (2013). Means and extremes: Building variability into community-level climate change experiments. *Ecol. Lett.*, 16, 799-806.

Tilman, D. (1999). Global environmental impacts of agricultural expansion: The need for sustainable and efficient practices. *Proc. Natl. Acad. Sci. U. S. A.*, 96, 5995-6000.

Tockner, K., Klaus, I., Baumgartner, C. & Ward, J.V. (2006). Amphibian diversity and nestedness in a dynamic floodplain river (Tagliamento, NE-Italy). *Hydrobiologia*, 565, 121-133.

Traill, L.W., Brook, B.W., Frankham, R.R. & Bradshaw, C.J.A. (2010). Pragmatic population viability targets in a rapidly changing world. *Biol. Conserv.*, 143, 28-34.

Tylianakis, J.M., Rand, T.A., Kahmen, A., Klein, A.M., Buchmann, N., Perner, J. *et al.* (2008). Resource heterogeneity moderates the biodiversity-function relationship in real world ecosystems. *PLoS Biol.*, 6, 0947-0956.

Urbanski, J.M., Benoit, J.B., Michaud, M.R., Denlinger, D.L. & Armbruster, P. (2010). The molecular physiology of increased egg desiccation resistance during diapause in the invasive mosquito, Aedes albopictus. *P. Roy. Soc. B-Biol. Sci.*, 277, 2683-2692.

Urbina, M.A., Walsh, P.J., Hill, J.V. & Glover, C.N. (2014). Physiological and biochemical strategies for withstanding emersion in two galaxiid fishes. *Comp. Biochem. Physiol. A Mol. Integr. Physiol.*, 176, 49-58.

Vörösmarty, C.J., McIntyre, P.B., Gessner, M.O., Dudgeon, D., Prusevich, A., Green, P. *et al.* (2010). Global threats to human water security and river biodiversity. *Nature*, 467, 555-561.

Walters, A.W. & Post, D.M. (2011). How low can you go? Impacts of a low-flow disturbance on aquatic insect communities. *Ecol. Appl.*, 21, 163-174.

Wells, A., Duncan, R.P. & Stewart, G.H. (2001). Forest Dynamics in Westland, New Zealand: The Importance of Large, Infrequent Earthquake-Induced Disturbance. *J. Ecol.*, 89, 1006-1018.

White, G.C. & Burnham, K.P. (1999). Program MARK: survival estimation from populations of marked animals. *Bird Study*, 46, 120-139.

White, R.S.A., McHugh, P.A., Glover, C.N. & McIntosh, A.R. (2015a). Multiple environmental stressors increase the realised niche breadth of a forest-dwelling fish. *Ecography*, 38, 154-162.

White, R.S.A., McHugh, P.A., Glover, C.N. & McIntosh, A.R. (2015b). Trap-shyness subsidence is a threshold function of mark-recapture interval in brown mudfish *Neochanna apoda* populations. *J. Fish Biol.*, 87, 967-980.

White, R.S.A., McHugh, P.A. & McIntosh, A.R. (2016). Drought-survival is a threshold function of habitat size and population density in a fish metapopulation. *Glob. Change Biol.*, 22, 3341-3348.

Winfield, I.J., Hateley, J., Fletcher, J.M., James, J.B., Bean, C.W. & Clabburn, P. (2010). Population trends of Arctic charr (*Salvelinus alpinus*) in the UK: Assessing the evidence for a widespread decline in response to climate change. *Hydrobiologia*, 650, 55-65.

Woodward, G., Bonada, N., Feeley, H.B. & Giller, P.S. (In press). Resilience of a stream community to extreme climatic events and long-term recovery from a catastrophic flood. *Freshw. Biol.*

Wormald, C.L. & Steele, M.A. (2008). Testing assumptions of mark-recapture theory in the coral reef fish *Lutjanus apodus*. *J. Fish Biol.*, 73, 498-509.

Zimmerman, J.K.M. & Palo, R.T. (2012). Time series analysis of climate-related factors and their impact on a red-listed noble crayfish population in northern Sweden. *Freshw. Biol.*, 57, 1031-1041.

Acknowledgements

Firstly, I want thank my primary supervisor Angus McIntosh. This thesis is in many ways, a product of his drive to get the very best out of his students and to guide them to achieve their potential. On many occasions, I have sent him manuscripts, and if they were not up to the standards I was capable of, he would say so. He would usually be very blunt about this which was difficult to take at times, especially if I became particularly attached to a piece of writing. But this always inspired me to dig deep, discover more, and help me realise what I can achieve. The often deep discussions we had also helped me develop further as a person. It is very important to have role models in life that can help you realise your potential and encourage you to reach it. I have been very fortunate to have Angus in this role during my time at University and I do not believe I would have made it this far without his leadership and guidance.

Secondly, I owe a great deal of gratitude to my unofficial supervisor and co-mentor *Pete McHugh. Pete was instrumental in helping me set up my initial study of brown mudfish in 2010/11 during my M.Sc. His advice on mark-recapture study design and analysis was very influential in making this thesis possible and I enjoy his down-to-earth outlook on science and life. The way in which he wholeheartedly devotes his time and energy to everyone around him, so selflessly, is something I admire and is such a huge asset to any research group he is involved in. Thank you also for hosting me on my visit to Utah State University and for giving me your socks which I only recently put holes in (but still use for some reason). Oh, and while my brain thanks you for introducing me to hot sauce, my other parts do not.

Acknowledgements

I owe a huge deal of gratitude to my (also unofficial) supervisor, Brendan Wintle at the University of Melbourne. Thank you graciously for always encouraging me to tackle complex model building problems and setting me on the right direction with model structure and for hosting me at Melbourne University. Your guidance helped me realise what I am capable of in quantitative ecology, where my sights are now focussed. I really enjoyed working with you, particularly the way you listened to my problems and gave good practical advice to solve them. Our meetings were always very matter-of-fact, effective and efficient and I always left your office clearly knowing what I had to do next and how to do it. I don't think I have ever learnt so much in such a short time during my brief stint at QAECO (Quantitative and Applied Ecology Research Group), thanks to your guidance.

A special thanks to my unofficial supervisor Doug Booker at Christchurch, NIWA. Your advice on statistical analysis and model validation techniques were very refreshing and greatly enriched my PhD experience. I particularly valued the alternative views you provided on the metapopulation model which helped me realise how it could be improved. In-fact, one of my major 'aha' moments occurred during one of our discussions on that model. I am very grateful to all the time you gave to listen and give advice about my thesis from the very beginning. Thank you also to everyone in the Freshwater Group at Christchurch NIWA, particularly Shannon Crow for providing the big fish database and the R-code you use to analyse it, and to Phil Jellyman for sharing your office.

Also I owe a lot of credit to my official co-supervisor, Chris Glover. Chris was essential in the early stages of this research in gaining initial funding and developing ideas to explore using mudfish. I always appreciated being able to visit him in his office at any time and chew the fat over various topics or concerns I had with my research.

I also wish to thank all other members of QAECO for constructive criticism and advice during my time at QAECO, particularly Amy Whitehead, Natalie Briscoe and Peter Vesk. Thank you, Amy, for introducing me to Brendan and RAMAS, and for looking after me while at QAECO. And also thank you for doing your blue duck research which was one of my inspirations to do population ecology. Thank you also to Natalie Briscoe for providing your R-scripts for streamlining the RAMAS parameterisation and analysis process. These scripts really saved my, ah….life in the last few weeks of the thesis.

I also wish to extend a warm thank you to all past and present members of FERG (Freshwater Ecology Research Group) and other colleagues in the School of Biological Sciences. I am particularly grateful to Helen Warburton, Simon Howard and Olivia Burge, who on many occasions selflessly offered vital R-advice that got me through. Helens R-loop scripts were particularly loopy and saved me hours of manual button clicking labour. Thank you also to Tom Swan for being inspirationally down-to-earth and positive and for being my experimental mentee. Thank you also to all the wonderful technical staff in the School of Biological Sciences, particularly Alan Wood, Linda Morris, and Matt Walters, who do a huge amount of work to make student experiences in the School are the highest quality possible.

Thank you also to all members of the Fluvial Habitat Center and the Institute of Applied Ecology at Utah State University and University of Canberra during my visits. I am very grateful to Nick Bouwes, Richard Duncan and Ross Thompson for hosting me during my visits to their research groups. I am particularly grateful to Richard Duncan, Wendy Ruscoe and Jon Bray for allowing me to stay with them for two days during my visit to Canberra.

I owe a great deal of gratitude to all the people who offered their valuable time to me in the field. In particular, thank you to Simon Howard, Nixie Boddy, Jack McMack (even

though that's not your real name), Rachel Paterson, Rachel Harley, Kevin Fraley, Mark Gelatoswitch, Jon Bray and Roseanna Gamlen-Greene and Alan Lilley. Thank you for tolerating the wet muddy conditions with me. In particular, I will always remember being marooned inside the tilting fieldstation with Rachel Paterson during 150 kph winds of cyclone Ita, with no water or electricity. Thank you for being so resourceful and cooking dinner on the open fire that night.

On that note, this research was made so much more practical, enjoyable and memorable due to the Hari Hari fieldstation (or as it is affectionately known as the Green Elephant by locals). In a part of the country that gets over 7000 mm of rainfall a year, it is important to have a warm, dry place to retreat to at night and dry clothes, gear and cook food. I became particularly fond of the Green Elephant over the last few years, and offer my warmest thanks to Jack van Berkel and Jenny Ladley for managing this fantastic facility. I will greatly miss the exfoliating backwashes provided by the most powerful shower in human history at this field station.

This research was made possible by generous funding from the NIWA Sustainable Water Allocation Program, the Brian Mason Scientific and Technical Trust, the Department of Conservation, and the University of Canterbury Roper Scholarship in Science. A generous donation of elastomer tags was also provided by Northwest Marine Technology. I am also grateful to the Claude McCarthy Fellowship, British Ecological Society and School of Biological Sciences at UC for international travel and research scholarships. It has been a huge privilege to receive this financial support. Thank you also to the Department of Conservation, New Zealand for permitting access to Saltwater Forest (permit no. 48005-RES) and to the University of Canterbury animal ethics committee from which all procedures pertaining to mudfish sampling was granted under permits 2010/23R and 2013/27R

Acknowledgements

I owe a great deal of gratitude to my parents and to my good friend Alan Lilley. Thank you mum and dad for giving me a solid foundation in life from which to develop and for all your support over the last few years. Finally, a special thanks to Alan Lilley. Alan in particular spent many many weeks with me in the field over the course of this study, and kept my field kits organised. I'm certain this research would have been significantly harder, if not impossible, without his support and friendship.